Title: Analiza udziału białek ściany komórkowej w odpowiedzi na stres temperaturowy u modelowego gatunku trawy *Brachypodium distachyon*

Author: Artur Piński

UNIWERSYTET ŚLĄSKI
W KATOWICACH

Wydział Nauk Przyrodniczych

Instytut Biologii, Biotechnologii i Ochrony Środowiska

Zespół Cytogenetyki i Biologii Molekularnej Roślin

ARTUR PIŃSKI

Praca doktorska

Analiza udziału białek ściany komórkowej w odpowiedzi na stres temperaturowy u modelowego gatunku trawy *Brachypodium distachyon*

Promotor:
Prof. dr hab. Robert Hasterok
Uniwersytet Śląski w Katowicach
Promotor pomocniczy:
Dr hab. Alexander Betekhtin, prof. UŚ
Uniwersytet Śląski w Katowicach

Praca została sfinansowana ze środków Narodowego Centrum Nauki przyznanych na podstawie decyzji numer: DEC-2014/14/M/NZ2/00519 i DEC-2018/31/N/NZ1/01418.

Katowice 2021

Podziękowania

Składam serdecznie podziękowania Promotorowi prof. dr hab. Robertowi Hasterokowi za opiekę naukową podczas postawania tej pracy.

Chciałbym podziękować Promotorowi Pomocniczemu dr hab. Alexandrowi Betekhtinowi prof. UŚ za konsultacje naukowe, cenne uwagi i wskazówki.

Składam również podziękowania współautorom publikacji naukowych, kolegom i koleżankom z Zespołu Cytogenetyki i Biologii Molekularnej Roślin za pomoc naukową.

Wielkie podziękowania dla mojej żony dr Joanny Żur-Pińskiej za pomoc i cierpliwość wykazaną w trakcie powstawania tej pracy.

Spis treści

ROZDZIAŁ I AUTOREFERAT ROZPRAWY

Rozdział I.1 Wprowadzenie

Nasilające się zmiany klimatyczne z jednej strony powodują wzrost średniej temperatury powierzchni Ziemi, z drugiej - zwiększają częstość występowania ekstremalnych zjawisk pogodowych, które są zagrożeniem dla produkcji żywności (Debaeke i in., 2017). Metaanalizy wskazują, że wzrost średniej temperatury na świecie o każdy stopień Celsjusza będzie miał negatywny wpływ na plony czterech głównych upraw: kukurydzy, pszenicy, ryżu i soi, co będzie skutkowało niedoborami żywności. Należy jednak zauważyć, że wyniki badań są bardzo niejednorodne pod względem obszarów geograficznych i rodzajów upraw, paradoksalnie sugerując pozytywny wpływ rosnącej temperatury w niektórych rejonach Ziemi (Zhao i in., 2017). Równocześnie, powiększająca się populacja ludzi i zmniejszająca się powierzchnia gruntów nadających się pod uprawę wymusza wzrost produktywności roślin (Jansson i in., 2018). By przeciwdziałać negatywnym skutkom zmian klimatycznych i sprostać wzrastającemu zapotrzebowaniu na żywność, istnieje pilna potrzeba opracowania nowych upraw przyjaznych dla klimatu (ang. *climate-smart crops*), które wpisują się w podejście rolnictwa inteligentnego dla klimatu (Taylor, 2017, Jansson i in., 2018, De Pinto i in., 2020). Rozwój takich upraw możliwy jest dzięki inżynierii genetycznej i hodowli nowych odmian (Pushpalatha i Gangadharan, 2020, Varotto i in., 2020), co wymaga szczegółowej wiedzy na temat mechanizmów molekularnych leżących u podstaw różnych reakcji na stresy, w szczególności stres temperaturowy (Le Gall i in., 2015, Acosta-Motos i in., 2017, Niu i Xiang, 2018, Yamauchi i in., 2021).

Stres temperaturowy, który indukowany jest zarówno przez niskie, jak i wysokie temperatury, prowadzi u roślin do złożonych zmian w wydajności fotosyntezy, produkcji reaktywnych form tlenu, zaburzeń potencjału redoks, rearanżacji cytoszkieletu i przebudowy ścian komórkowych (Bita i Gerats, 2013, Janmohammadi i in., 2015). Wysoka temperatura zmienia również ekspresję genów kodujących białka zaangażowane w produkcję osmoprotektantów, enzymów odtruwających, transporterów, białek regulatorowych i opiekuńczych (Tiwari i in., 2020). Liczne badania wykazały różnorodne zmiany w architekturze ściany komórkowej, które dotyczą głównie biosyntezy celulozy i hemiceluloz, jak też modyfikacji pektyn. Zmiany w ścianie komórkowej są rozleglejsze w korzeniach, gdyż są one bardziej wrażliwe na stres temperaturowy, niż nadziemne części rośliny. Niemniej, niekorzystny wpływ stresu temperaturowego na liście bezpośrednio wpływa na produktywność roślin (Le Gall i in., 2015, Mareri i in., 2018).

Badania wpływu stresu temperaturowego na białka ściany komórkowej w tej rozprawie doktorskiej skupiały się na *Brachypodium distachyon* ze względu na jego status modelowego gatunku dla traw, m.in. zbóż i roślin energetycznych takich jak miskant i rózgacznik (Draper i in., 2001). *B. distachyon* jest blisko spokrewniony z najważniejszymi pod względem ekonomicznym zbożami strefy klimatu umiarkowanego: pszenicą, jęczmieniem oraz owsem, co czyni go ważnym obiektem modelowym. Rośliny tego gatunku charakteryzują się niewielkim rozmiarem, krótkim cyklem życiowym, niewielkimi wymaganiami siedliskowymi, a także małym, jak na trawę, genomem jądrowym (~310 Mpz/1C) (Wolny i Hasterok, 2009). *B. distachyon* posiada także zsekwencjonowany genom referencyjny cechujący się wysoką jakością złożenia odczytów i adnotacji (International Brachypodium Initiative, 2010). Niedawne prace badawcze dostarczyły danych z całogenomowego sekwencjonowania licznych genotypów *B. distachyon* zebranych m.in. w Hiszpanii czy Turcji (Gordon i in., 2017, Skalska i in., 2020). Wiele lat badań nad tą rośliną modelową umożliwiło rozwój różnorodnych narzędzi eksperymentalnych, w tym kluczowego dla dalszych analiz molekularnych systemu transformacji kalusa embriogennego z wykorzystaniem *Agrobacterium tumefaciens* (Alves i in., 2009, Hus i in., 2020). Skuteczna transformacja kalusa embriogennego wraz z rozwojem mutagenezy ukierunkowanej z wykorzystaniem systemu CRISPR/Cas9 pozwoliła na precyzyjne modyfikacje genomu wybranych gatunków *Brachypodium*, w tym „programowaną" inaktywację poszczególnych genów (Hus i in., 2020). Względna łatwość aplikacji systemu CRISPR/Cas9 umożliwiła znaczny postęp w badaniach nad wzrostem i rozwojem *B. distachyon*, jak też odpowiedzią tej rośliny na określone stresy biotyczne i abiotyczne (Betekhtin i in., 2020). Szczególnie interesujące i obiecujące są badania nad wtórną ścianą komórkową, ze względu na liczne różnice w budowie ściany komórkowej traw w aspekcie głównych polisacharydów strukturalnych, ich połączeń, obecności związków fenolowych, białek i pektyn (Vogel, 2008). Obiecująco zapowiadają się badania w dziedzinie biosyntezy lignin, identyfikacji nowych substratów i enzymów zaangażowanych w polimeryzację lignin i ich modyfikacje (Coomey i in., 2020). Złożona struktura ściany komórkowej, która zbudowana jest z polimerów takich jak celuloza, hemiceluloza i pektyny, ulega modyfikacjom i remodelowaniu przez białka ściany komórkowej, które stanowią także rusztowanie dla budujących ją polisacharydów. Choć białka ściany komórkowej zwykle nie stanowią więcej niż 10% suchej masy u roślin dwuliściennych i 1% u jednoliściennych, są niezwykle istotne dla rozwoju rośliny, jak też jej odpowiedzi na stresy biotyczne i abiotyczne (Vogel, 2008, Le Gall i in., 2015, Novakovic i in.,

2018). Intensywne badania skupiające się na białkach ściany komórkowej pozwoliły na eksperymentalne potwierdzenie 754 takich białek u *Arabidopsis thaliana* i 739 u *B. distachyon* (http://www.polebio.lrsv.ups-tlse.fr/WallProtDB/) (San Clemente i Jamet, 2015, Pinski i in., 2021b). W celu łatwiejszej analizy funkcji białek ściany komórkowej, zostały one podzielone na dziewięć klas: białka działające na węglowodany, oksydoreduktazy, proteazy, białka związane z metabolizmem lipidów, białka zaangażowane w przekazywanie sygnałów, białka z domenami interakcji, białka o zróżnicowanych funkcjach, białka strukturalne i białka o nieznanej funkcji (Albenne i in., 2009, Albenne i in., 2014, San Clemente i Jamet, 2015).

Wśród białek ściany komórkowej szczególnie interesujące są białka bogate w hydroksyprolinę (ang. *hydroxyproline-rich glycoprotein*), których część to białka strukturalne a część zaangażowana jest w przekazywanie sygnałów. Białka bogate w hydroksyprolinę zwykle dzielone są na trzy rodziny: białka arabinogalaktanowe (AGP, ang. *arabinogalactan proteins*), ekstensyny i białka bogate w prolinę (Johnson i in., 2017). AGP to glikoproteiny wyróżniające się białkowym rdzeniem, który stanowi 2–10% ich masy i składa się głównie z proliny, hydroksyproliny, alaniny, glicyny, seryny i treoniny. Pozostałą część AGP stanowi rozbudowana część węglowodanowa, która składa się z łańcuchów galaktozy połączonych wiązaniami β-1→3 i β-1→6, a także reszt arabinozy, ramnozy, fruktozy i kwasu glukuronowego (Nothnagel, 1997). AGP dzielone są na podrodziny: klasyczne AGP, bogate w lizynę AGP, peptydy arabinogalaktanowe i AGP typu Fasciclin (FLA, ang. *fasciclin-like arabinogalactan protein*) (Pereira i in., 2015). Ostatnia podrodzina charakteryzuje się obecnością domeny Fasciclin, która jest domeną adhezji komórkowej wspólną dla roślin i zwierząt. FLA biorą udział m.in. w formowaniu wtórnej ściany komórkowej, rozwoju męskich gametofitów i odpowiedzi na stresy biotyczne i abiotyczne, w szczególności na stres solny (Griffiths i in., 2014, Seifert, 2018). Z kolei ekstensyny wyróżniają się obecnością motywu składającego się z aminokwasu seryny, po którym następuje ciąg od trzech do pięciu reszt prolin. Ekstensyny, jako białka strukturalne, zaangażowane są we wzmacnianie ściany komórkowej poprzez tworzenie wiązań poprzecznych, które wymagają odpowiedniej glikozylacji i konformacji strukturalnej glikoproteiny. Rosnąca liczba doniesień naukowych wskazuje także na rolę ekstensyn w obronie przed fitopatogenami i interakcji z bakteriami endofitycznymi (Liu i in., 2016, Pinski i in., 2019a, Castilleux i in., 2021).

Rozdział I.2 Cel pracy doktorskiej

Ze względu na globalne ocieplenie i związany z nim stres temperaturowy zagrażający roślinom ze szczególnym uwzględnieniem roślin uprawnych, niezwykle istotnym jest poznanie mechanizmów odpowiedzi roślin na warunki stresu temperaturowego. W szczególności słabo poznanym aspektem tej odpowiedzi jest udział białek ściany komórkowej. W związku z powyższym w pracy podjęto próbę scharakteryzowania zmian w obecności białek ściany komórkowej u modelu dla traw, jakim jest *Brachypodium distachyon* w odpowiedzi na stres abiotyczny wywołany inkubowaniem roślin w obniżonej (4 °C) i podwyższonej (40 °C) względem optymalnej (ok. 21 °C) temperaturze.

Głównymi celami badawczymi pracy doktorskiej było:

1. Określenie rozmieszczenia epitopów AGP i ekstensyn w liściach *B. distachyon* – genotypu referencyjnego Bd21.
2. Analiza zmian w intensywności i rozmieszczeniu epitopów AGP i ekstensyn w liściach *B. distachyon* Bd21 w odpowiedzi na stres temperaturowy: 4 °C i 40 °C.
3. Określenie zmian w profilu ekspresji wybranych genów kodujących AGP i ekstensyn w odpowiedzi na stres temperaturowy jak wyżej.
4. Określenie zmian w obecności białek ściany komórkowej w odpowiedzi na stres wysokiej temperatury.
5. Uzyskanie mutantów *B. distachyon* Bd21 z inaktywowanymi genami kodującymi białka ściany komórkowej: białko arabinogalaktanowe typu Fasciclin (*Bradi3g39740*) i metyloesteraza pektynowa (*Bradi3g24750*).

Rozdział I.3 Materiały i metody

Materiał badawczy

W prowadzonych badania wykorzystano *Brachypodium distachyon* genotyp Bd21 (numer akcesyjny: PI 254867). Nasiona pozyskane zostały z kolekcji National Plant Germplasm System prowadzonej przez bank nasion USDA (ang. *United States Department of Agriculture*). Nasiona wysiewane były do doniczek wypełnionych ziemią wymieszaną z wermikulitem w stosunku 3:1, a następnie hodowane w szklarni w stałych warunkach temperatury 21±1 °C w warunkach fotoperiodu: 16 godz. światła i 8 godz. ciemności. Rośliny oświetlane były lampami emitującymi światło białe o strumieniu fotonów 150 µmol m^{-2} s^{-1}. W szklarni utrzymywano względną wilgotność na poziomie około 50%. Do dalszych analiz wpływu stresu temperaturowego wykorzystywano rośliny w czwartym stadium wzrostu według systemu zaproponowanego przez Hong i in. (2011). W celu poddania roślin stresowi temperaturowemu przenoszono je do fitotronów i inkubowano 24 godz. w temperaturze 40 °C lub 4 °C. Do dalszych analiz profilu ekspresji genów, immunocytochemii i proteomiki ściany komórkowej pobierano liście flagowe.

Utrwalenie materiału i immunocytochemia

Fragmenty środkowej części liścia utrwalano w mieszaninie paraformaldehydu (4%, w/v) i glutaraldehydu (1%, w/v) w buforowanej fosforanem soli fizjologicznej (PBS, pH 7). W celu usunięcia powietrza, materiał poddano infiltracji (pięć razy po 15 min.). Próbki inkubowano przez 12 godz. w 4 °C, po czym przepłukiwano materiał buforem PBS (trzykrotnie po 15 min.) i odwadniano w szeregu etanolowym (10, 30, 50, 70, 90 i 100% etanolu; każde stężenie etanolu dwukrotnie po 30 min.). Materiał zatopiono w wosku Steedmana (Sala i in., 2017). Przekroje poprzecznie liścia o grubości 7 µm wykonano na mikrotomie rotacyjnym HYRAX M40 (Zeiss) i zbierano na szkiełkach mikroskopowych pokrytych poli-L-lizyną (Menzel Gläser). Materiał na szkiełkach odwoskowano i uwadniano w szeregu etanolowym (100, 90 i 50% etanolu, każde stężenie etanolu 10 min.), a następnie jednokrotnie w PBS (10 min.). Na preparaty nakropiono roztwór blokujący składający się z 2% (w/v) płodowej surowicy cielęcej i 2% (w/v) albuminy surowicy bydlęcej rozpuszczonych w PBS (pH 7,2). Następnie na preparaty naniesiono pierwszorzędowe przeciwciała monoklonalne rozpuszczone w roztworze blokującym i inkubowano przez 1,5 godz. Do analiz wykorzystano przeciwciała specyficzne względem AGP (przeciwciała JIM8, JIM13, JIM16, LM2, MAC207), pektyn/AGP (LM6) i ekstensyn (JIM11,

JIM12 i JIM20) (Plant Probes). Preparaty zostały przepłukane i przeciwciało drugorzędowe AlexaFluor 488 goat anti-rat IgG (Jackson ImmunoResearch Laboratories) zostało naniesione na preparat. Kilkukrotnie przepłukane roztworem blokującym preparaty wybarwiono 0,01% (w/v) fluorescent brightener 28 (Sigma-Aldrich) w PBS przez 5 min. Na wysuszone preparaty nakrapiano fluoromount (Sigma-Aldrich) w celu ich zabezpieczenia (Betekhtin i in., 2016). Zdjęcia preparatów wykonano wykorzystując mikroskop epifluorescencyjny Zeiss Axio Imager Z2 wyposażony w kamerę monochromatyczną AxioCam Mrm (Zeiss).

Analiza profilu ekspresji genów

Analizę profilu ekspresji genów przeprowadzono z wykorzystaniem techniki odwrotnej transkrypcji ilościowego PCR (RT-qPCR) (Betekhtin i in., 2016). Całkowity RNA wyizolowano wykorzystując Trizol (Invitrogen) i zestaw RNeasy Mini Kit (Qiagen) zgodnie z instrukcją producenta. Pozostałości DNA z próbek usunięto DNazą (Qiagen), a następnie próbki oczyszczono na kolumnach RNeasy MiniElute (Qiagen). Stężenie i jakość wyizolowanego RNA oceniano na podstawie odczytów ze spektrofotometru NanoDrop (Thermo Scientific), a integralność na podstawie obserwacji rozkładu prążków na 1% (w/v) żelu agarozowym. Syntezę pierwszej nici cDNA przeprowadzono z wykorzystaniem zestawu do syntezy cDNA (Thermo Fisher Scientific). Odwrotnej transkrypcji poddano 1000 ng oczyszczonego RNA z wykorzystaniem starterów oligo$(dT)_{18}$. Do dalszych analiz cDNA rozcieńczano pięciokrotnie i wykorzystywano bezpośrednio do reakcji RT-qPCR lub przechowywano w -20 °C. Regiony kodujące analizowanych genów (CDS, ang. *coding DNA sequence*) pozyskano z bazy Phytozome (https://phytozome.jgi.doe.gov/pz/portal.html). Oligonukleotydy do amplifikacji CDS zaprojektowano używając oprogramowania PrimerQuest Tool (https://eu.idtdna.com/PrimerQuest/Home/Index). Analizy profilu ekspresji przeprowadzono z wykorzystaniem aparatu LightCycler 480 Real-Time PCR System (Roche). Jako gen referencyjny do obliczeń metodą $2^{-\Delta\Delta CT}$ wykorzystano gen kodujący poliubikwitynę (*Bradi1g32860*), która wykazuje stabilny profil ekspresji w warunkach stresu temperaturowego (Pfaffl, 2001). Statystycznie istotne różnie między kontrolą (21 °C) a roślinami poddanymi stresowi termicznemu w 4 °C lub 40 °C obliczano wykorzystując test t-studenta (STATISTICA wersja 13).

Analiza proteomu ściany komórkowej

W celu analizy proteomu ściany komórkowej wyizolowano ściany komórkowe z liści roślin kontrolnych i tych poddanych stresowi wysokiej temperatury (Feiz i in., 2006, Douché i in., 2013). W tym celu około 3 g liści przemyto wodą destylowaną i zmielono w blenderze w 5 mM buforze octanowym (pH 4,6) z dodatkiem 0,4 M sacharozy (Chempur) oraz mieszaniny zawierającej inhibitory proteinaz (P9599, Merck) i poliwinylopirolidonu (Merck). Ściany komórkowe zostały odseparowane od płynów cytoplazmatycznych poprzez wirowanie przez 15 min. przy wartości siły 3000 g w 4 °C (Eppendorf). Supernatant został delikatnie odrzucony a osad przemyty schłodzonym 5 mM buforem octanowym (pH 4,6) z dodatkiem 0,6 M sacharozy i ponownie wirowany jak opisano powyżej. Proces oczyszczania powtórzono z 5 mM buforem octanowym (pH 4,6) z dodatkiem 1 M sacharozy. Tak oczyszczone ściany komórkowe przeniesiono na nylonową siatkę o średnicy porów 25 µm, a następnie obficie przemywano 5 mM buforem octanowym (pH 4,6) w celu usunięcia sacharozy. Ściany komórkowe zamrożono w temperaturze -80 °C, a następnie utarto tłuczkiem w moździerzu w ciekłym azocie. Próbki liofilizowano przez dwa dni w liofilizatorze (Christ). Z wysuszonych ścian komórkowych izolowano białka wykorzystując roztwory soli, zaczynając od 0,2 M roztworu $CaCl_2$ w 5 mM buforze octanowym (pH 4,6) z dodatkiem mieszaniny zawierającej inhibitory proteinaz (P9599, Merck). Próbki były worteksowane przez 30 min. w 4 °C, a następnie wirowane przez 15 min. przy wartości siły 5000 g w 4 °C (Eppendorf). Supernatant zbierano do osobnej probówki. Izolację białek powtórzono ponownie z wykorzystaniem 0,2 M roztworu $CaCl_2$ w 5 mM buforze octanowym (pH 4.6), a następnie dwukrotnie z 1 M roztworem LiCl w 5 mM buforze octanowym (pH 4,6). Zebrany supernatant odsolono z wykorzystaniem kolumn Econo-Pac 10 DG (Bio-Rad) kondycjonowanych 0,1 M roztworem soli amonowej kwasu mrówkowego (Merck). Próbki zostały poddane liofilizacji i rozpuszczone w wodzie. Stężenie białek zostało zmierzone zestawem Pierce BCA Protein Assay Kit (Thermo Fisher Scientific). Z każdej próbki pobrano 200 µg białek, które poddano ponownej liofilizacji, a następnie analizie w Małopolskim Centrum Biotechnologii w Krakowie celem oznaczenia białek. W celu wizualizacji wyizolowanych białek, 60 µg otrzymanych próbek nakropiono na żel poliakrylamidowy (12% żel separacyjny, 7% żel zagęszczający) w warunkach denaturujących i poddano elektroforezie. Białka wybarwiono odczynnikiem EZBlue Gel Staining Reagent (Merck), a następnie płukano w wodzie destylowanej. W celu identyfikacji białek wykorzystano wysokoprzepustową technikę chromatografii cieczowej z tandemową spektrometrią

mas (LC-MS/MS). Próbki do analizy przygotowano zgodnie z protokołem FASP (Wisniewski i in., 2009), a następnie białka poddano fragmentacji z wykorzystaniem trypsyny. Oczyszczone peptydy wykorzystano do analizy LC-MS/MS. Szczegółowy opis analizy proteomicznej zamieszony jest w pracy **Pinski i in. (2021a)** zamieszczonej w **rozdziale II.2**. Uzyskane dane LC-MS/MS analizowano z wykorzystaniem oprogramowania MaxQuant (wersja 1.5.8.3). Sekwencje referencyjne dla *B. distachyon* Bd21 pozyskano z bazy danych Phytozome (wersja adnotacji 3.2, liczba białek 56 847). Podczas identyfikacji peptydów wzięto pod uwagę następujące modyfikacje: oksydacja metioniny, acetylacja końca N-terminalnego i oksydacja proliny. Współczynnik fałszywych wykryć (FDR *ang. false discovery rate*) został ustalony na poziomie 1%. Uzyskane wyniki analizowano z wykorzystaniem platformy Perseus (Tyanova i in., 2016). Białka nie pochodzące z *B. distachyon* usunięto i dane poddano transformacji logarytmicznej. Celem identyfikacji białek różnicujących traktowania wykorzystano test t-studenta z wartością FDR wynoszącą 1%. Pod uwagę wzięto tylko białka z co najmniej dwoma unikatowymi peptydami i progiem wartości zmiany powyżej 1,5. Ze względu na obecność zanieczyszczeń białkowych pochodzących z cytoplazmy, białka ściany komórkowej zostały zidentyfikowane z wykorzystaniem narzędzi bioinformatycznych (TargetP, SignalP, LocTree3, Phobius, Predotar, TMHMM i Aramemnon) implementowanych w bazie WallProtDB (San Clemente i Jamet, 2015).

Ukierunkowana mutageneza z wykorzystaniem systemu CRISPR/Cas9

W celu inaktywacji dwóch genów kodujących domniemane białka ściany komórkowej wykorzystano system CRISPR/Cas9. Skupiono się na genie kodującym FLA (*Bradi3g39740*) i genie kodującym metyloesterazę pektynową (PME, *Bradi3g24750*). Ze względu na precyzję i specyficzność białka Cas9 pracę rozpoczęto od amplifikacji CDS wybranych genów z wykorzystaniem cDNA pochodzącego z liści i ich porównania do sekwencji zawartych w bazie Phytozome. Na podstawie wyników sekwencjonowania zaprojektowano jedną 20-nukleotydową sekwencję RNA (ang. *guide RNA*, gRNA) dla genu FLA (*FLA_BbsI*) i dwie sekwencje gRNA dla genu PME (*PME_BsrGI* i *PME_AccI*) korzystając z programu Geneious Prime (Biomatters). Sekwencje gRNA dobrano w taki sposób by enzym restrykcyjny obejmował sekwencję między trzecim i czwartym nukleotydem powyżej sekwencji PAM. Taki dobór enzymu restrykcyjnego umożliwia łatwiejsze poszukiwanie zmutowanych sekwencji w teście protoplastów jak też w przypadku uzyskanych roślin. Sekwencja gRNA *FLA_BbsI* została wklonowana do uprzednio

pociętego enzymem restrykcyjnym *BsaI* (New England Biolabs) wektora pENTRsgRNA z wykorzystaniem ligazy T4 PNK (New England Biolabs). Następnie wektor ze wstawioną sekwencją gRNA *FLA_BbsI* wykorzystano jako donor kasety w reakcji rekombinacji typu Gateway z wektorem pOsCas9, co umożliwiło przygotowanie finalnego wektora do ukierunkowanej mutagenezy. Z kolei wektor z dwoma sekwencjami gRNA dla genu PME (*PME_BsrGI* i *PME_AccI*) przygotowano zgodnie z protokołem opisanym przez Lowder i in. (2015). W celu wykonania testu efektywności przygotowanych wektorów do edycji genomu *B. distachyon* przeprowadzono test protoplastów. Izolację protoplastów i ich transfekcję przeprowadzono zgodnie z protokołem opisanym przez Jung i in. (2015). Protoplasty wyizolowano z liści *B. distachyon* wykorzystując roztwór enzymów: 2% (w/v) celulaza "Onozuka" R-10 (Serva), 0,5% (w/v) drizelaza (Sigma) i 0,4% (w/v) macerozym R-10 (Duchefa). Materiał inkubowano w temperaturze 26 ºC przez 3 godz. z wytrząsaniem z prędkością 30 obr./min, którą zwiększano do 50 obr./min. i wytrząsano przez dodatkowe 30 min. Materiał filtrowano przez filtr nylonowy i zawieszano w buforze W5. Następnie, po usunięciu buforu W5, protoplasty zawieszano w buforze MMG tak by otrzymać koncentrację wynoszącą ok. 10 mln protoplastów w 1 mL buforu. W celu transfekcji do każdej z probówek dodawano ok. 1 mln protoplastów, 10 µg DNA wektora i roztwór glikolu polietylenowego. Mieszaninę inkubowano przez 7 min., po czym transfekcję zatrzymywano poprzez dodanie buforu W5. Zawiesinę protoplastów inkubowano przez dwa dni w ciemności w temperaturze 25 ºC. Następnie z protoplastów izolowano DNA korzystając z metody z wykorzystaniem bromku cetylotrimetyloamoniowego i cięto materiał genetyczny z wykorzystaniem enzymu restrykcyjnego dobranego względem użytego gRNA. Sekwencję dla wybranego genu amplifikowano i klonowano do wektora pGEM-T Vector (Promega), po czym dla każdego z genów sekwencjonowano po kilkanaście wektorów.

Przygotowane finalne wektory wprowadzono do bakterii *Agrobacterium tumefaciens* szczepu AGL1 poprzez elektroporację. By uzyskać kalus embriogenny zbierano nasiona z 7-9-tygodniowych roślin *B. distachyon*. Z wysterylizowanych w 70% etanolu (2 min.) i 5% (w/v) roztworze podchlorynu wapnia (10 min.) nasion izolowano zarodki (0,3-0,7 mm) i przenoszono je na pożywkę indukującą tworzenie kalusa. Szczegółowy skład pożywek i całej procedury indukcji kalusa i jego transformacji znajdują się w pracy Alves i in. (2009). Wyindukowany kalus embriogenny pasażowano trzykrotnie, po 21 dniach, 14 dniach i 7 dniach, a następnie poddawano

transformacji komórkami bakteryjnymi *A. tumefaciens* AGL1 posiadającymi odpowiednie wektory. Komórki *A. tumefaciens* AGL1 wysiewano na pożywkę stałą zawierającą odpowiednie antybiotyki selekcyjne i acetosyringon, który zwiększa efektywność procesu transformacji. Przed transformacją zbierano skalpelem warstwę komórek i wytrząsano w pożywce BdAMG celem rozbicia agregatów komórkowych. Gęstość optyczną hodowli ustalono na poziomie OD_{600} równym 1. Uprzednio przygotowany kalus zalewano hodowlą bakteryjną i inkubowano przez 5 min, a następnie starannie usuwano płyn pozostawiając kalus do wyschnięcia w komorze z przepływem laminarnym na 7 min. Kalus po transformacji przenoszono na pożywkę BdCCM, po czym płytki inkubowano w fitotronie przez 48 godz. w ciemności w temp. 25 °C. Po inkubacji kalus przenoszono na pożywkę selekcyjną, która zawierała higromycynę. Po trzech tygodniach przenoszono kalus na świeżą pożywkę selekcyjną, a następnie po upływie kolejnych trzech tygodni na pożywkę regeneracyjną, którą inkubowano w fitotronie w temperaturze 25 °C w warunkach fotoperiodu: 16 godz. światła i 8 godz. ciemności. Pojawiające się rośliny (o długości ok. 2 cm) przenoszono na bieżąco do pożywki indukującej rozwój korzeni. Ze zregenerowanych roślin pobierano fragment liścia (ok. 1 cm) i izolowano z niego DNA, po czym sprawdzano obecność transformującego DNA (T-DNA) poprzez amplifikację unikalnego fragmentu T-DNA. Rośliny w których stwierdzono obecność T-DNA przenoszono do doniczek wypełnionych ziemią wymieszaną z wermikulitem w stosunku 3:1. Następnie sprawdzano modyfikacje w docelowym genie poprzez jego amplifikację i restrykcję z uprzednio wybranym enzymem restrykcyjnym, który tnie w obrębie rejonu ciętego przez białko Cas9. Brak restrykcji sugerował zmiany w sekwencji genu, co następnie potwierdzano poprzez sekwencjonowanie. Transformowane i modyfikowane rośliny hodowano w celu uzyskania nasion.

Rozdział I.4 Wyniki i dyskusja

Analizę rozmieszczenia epitopów AGP (przeciwciała monoklonalne: JIM8, JIM13, JIM16, LM2 i MAC207), pektyn/AGP (LM6) i ekstensyn (JIM11, JIM12 i JIM20) w liściach *B. distachyon* wykonano dla roślin rosnących w warunkach kontrolnych. Występowanie epitopów AGP związane było głównie z wiązką przewodzącą. Epitopy AGP dla wszystkich badanych przeciwciał obserwowano we floemie, jak też, z wyjątkiem epitopów przeciwciał MAC207 i LM6, w wewnętrznej pochwie okołowiązkowej. Sygnał w zewnętrznej pochwie okołowiązkowej obserwowano tylko dla przeciwciał JIM16 i LM2. Z kolei we włoskach kłujących sygnał obserwowano dla przeciwciała JIM13, a w epidermie dla przeciwciała LM2. Epitopy ekstensyn dla trzech badanych przeciwciał (JIM11, JIM12 i JIM20) obserwowano w mezofilu, a w przypadku przeciwciał JIM12 i JIM20 w zewnętrznej pochwie okołowiązkowej i naczyniach drewna. Sygnał dla przeciwciała JIM20 obserwowano także we floemie. Wyniki analizy rozmieszczenia epitopów posłużyły jako punkt odniesienia do dalszych analiz zmian w intensywności sygnału i rozmieszczenia epitopów w odpowiedzi na stres temperaturowy: 4 °C i 40 °C. Rośliny poddane były tym stresom przez 24 godziny. Dokładna analiza intensywności i rozmieszczenia sygnału dla badanych przeciwciał ujawniła brak zmian w przypadków przeciwciał, które rozpoznają epitopy ekstensyn. Brak różnic wynikać może z użycia tylko trzech przeciwciał swoistych dla epitopów ekstensyn. Niemniej wyniki te są interesujące ze względu na to, że niewiele jest badań poświęconych roli ekstensyn w stresie abiotycznym, a zwłaszcza stresie temperaturowym (Casero i in., 1998, Zhang i in., 2008, Xu i in., 2011, Wu i in., 2017). Natomiast, dla czterech przeciwciał, JIM8, JIM16, LM2 i LM6, u *B. distachyon* zaobserwowano znaczące różnice w obecności i intensywności sygnału. Epitop rozpoznawany przez przeciwciało JIM8 był mniej reprezentowany we floemie w liściach roślin inkubowanych w niskiej temperaturze. W liściach poddanych działaniu wysokiej temperatury zaobserwowano wzrost intensywności sygnału fluorescencyjnego w ścianach komórek łyka w porównaniu z liśćmi rosnącymi w niskiej temperaturze. Dla porównania, w liściach bananowca, sygnał dla przeciwciała JIM8 stawał się bardziej intensywny w odpowiedzi na niską temperaturę (Yan i in., 2015). Może to sugerować, że zmiany składu chemicznego ścian komórkowych w odpowiedzi na stres temperaturowy są specyficzne gatunkowo. Epitop rozpoznawany przez przeciwciało JIM16 w kontroli roślin *B. distachyon* był obecny w niewielkiej ilości w przedziałach międzykomórkowych w komórkach wewnętrznej i zewnętrznej pochwy okołowiązkowej, w łyku,

a także w miękiszu ksylemu. Epitop ten nie został wykryty w miękiszu ksylemu w 40 °C, dodatkowo, w 4 °C nie wykryto obecności tego epitopu z wyjątkiem pojedynczych sygnałów w pochwie okołowiązkowej. Wykazana w liściach bananowca obecność epitopu JIM16 wyższa u odmiany tolerancyjnej w odpowiedzi na niską temperaturę, sugeruje, że u tego gatunku opisywany epitop może brać udział w tolerancji na stres termiczny (Yan i in., 2015). Kolejny z epitopów, rozpoznawany przez przeciwciało LM2, obserwowano w przedziałach komórkowych pochwy okołowiązkowej, łyku i miękiszu ksylemu. W przypadku roślin inkubowanych w warunkach podwyższonej temperatury w porównaniu do kontroli, epitop ten był bardziej obfity. Dodatkowo LM2 wykryto w przedziałach międzykomórkowych i/lub ścianach epidermy oraz w komórkach zawiasowych liści roślin poddanych działaniu wysokiej temperatury. Sygnał w komórkach mezofilu wykryto tylko w liściach roślin, które były inkubowane w 40 °C. Epitop LM6 wykryto w łyku, miękiszu ksylemu i w mniejszych ilościach w przedziałach komórkowych i/lub ścianach zewnętrznej pochwy okołowiązkowej. Sygnał fluorescencji tego epitopu w miękiszu ksylemu był intensywniejszy w przypadku roślin inkubowanych w temperaturze 40 °C w porównaniu do kontroli. Poza wiązką naczyniową, sygnał dla przeciwciała LM6 był obecny w ścianach komórkowych i/lub w przedziałach międzykomórkowych mezofilu. Funkcja łańcuchów bocznych arabinanu nie jest dobrze poznana i postuluje się, że ich rola polega na zaangażowaniu w rehydratację i zwiększenie elastyczności ściany komórkowej (Ha i in., 2005, Larsen i in., 2011, Moore i in., 2014, Tenhaken, 2014). Większa obecność składników ściany rozpoznawanych przez przeciwciało LM6, szczególnie w przedziałach cytoplazmatycznych, może wskazywać, że liście reagują na stres temperaturowy poprzez syntezę i depozycję (1-5)-α-L-arabinanów w ścianie komórkowej (https://plantcellwalls.leeds.ac.uk/plantprobes/).

Biorąc pod uwagę zmiany w intensywności i rozmieszczeniu dla czterech przeciwciał rozpoznających AGP zbadano profil ekspresji kilku wybranych genów kodujących te białka jak też ekstensyny. Geny wybrano bazując na wynikach wcześniejszych analiz bioinformatycznych i wcześniejszych analizach udziału białek bogatych w hydroksyprolinę w starzeniu się kultur kalusa *B. distachyon* (Liu i in., 2016, Betekhtin i in., 2018). Jak wykazano w poprzednich badaniach, analizy rozmieszczenia i zmian w intensywności sygnału epitopów można porównać z profilami ekspresji genów kodujących białka, na które te przeciwciała są ukierunkowane (Betekhtin i in., 2018, Betekhtin i in., 2019). Zbadano profil ekspresji pięciu różnych genów kodujących FLA (*Bradi4g34420*, *Bradi2g00220*, *Bradi5g18950*, *Bradi3g39740* i *Bradi2g60270*).

Poziomy akumulacji transkryptu genów *Bradi4g34420* i *Bradi2g00220* wzrosły w obu eksperymentalnych reżimach temperaturowych w porównaniu z warunkami kontrolnymi. W przypadku genu *Bradi5g18950* ekspresja w liściach inkubowanych w 4 °C nie różniła się statystycznie od kontroli, podczas gdy jego ekspresja w 40 °C była sześciokrotnie wyższa. Podobny wzór zaobserwowano dla genu *Bradi3g39740*, chociaż nastąpił tylko niewielki (1,7-krotny) wzrost jego ekspresji w temperaturze 4 °C. Ekspresja genu *Bradi2g60270* była wykrywalna tylko w liściach roślin inkubowanych w 40 °C. Stres temperaturowy powodował wzrost poziomu ekspresji genów kodujących FLA, chociaż wzrost ten był bardziej wyraźny w 40 °C. Udział AGP w odpowiedzi na stres temperaturowy liści jest dotychczas słabo opisany (Mareri i in., 2018). U pszenicy zaobserwowano przejściowe pojawienie się dwóch białek AGP w odpowiedzi na niską temperaturę (Garaeva i in., 2006, Mareri i in., 2018). Z kolei, w roślinach transgenicznych *A. thaliana* nieklasyczne AGP poprawiały tolerancję siewek na przemarzanie (Gong i in., 2012). U pszenicy cztery geny kodujące FLA wykazywały obniżony poziom ekspresji w odpowiedzi na stres niskotemperaturowy (Faik i in., 2006). Podobnie dwa inne geny FLA (*OsFLA1* i *OsFLA4*) wykazywały obniżony poziom ekspresji w odpowiedzi na niską temperaturę u ryżu (Ma i Zhao, 2010). Może to odzwierciedlać wewnętrzne różnice między analizowanymi gatunkami lub być wynikiem fragmentaryczności przeprowadzonych eksperymentów, które skupiają się jedynie na kilku z licznych genów *FLA* obecnych w genomach roślin okrytozalążkowych. Stresy temperaturowe wywołane niskimi lub wysokimi temperaturami hamują pobieranie wody, co natychmiast prowadzi do spowolnienia wzrostu liści. Obserwacja ta była skorelowana z utratą turgoru w komórkach liści i regulacją osmotyczną, która umożliwia komórkom odzyskanie turgoru (Nahar i in., 2015). AGP są dobrze znane ze swoich właściwości zatrzymywania wody (Ellis i in., 2010). Na przykład w roślinach rezurekcyjnych (np. *Anastatica hierochuntica*) boczne łańcuchy pektyny są silnie wzbogacone w polimery bogate w arabinozę, w tym AGP. Ich obecność może zapobiec utracie wody podczas osuszania (Gechev i in., 2014, Le Gall i in., 2015). Postawiona została hipoteza, że organy podatne na utratę wody, takie jak liście, zwiększają grubość ścian komórkowych poprzez produkcję specyficznych cząsteczek, takich jak AGP, które ograniczają w ten sposób wysychanie. Hipoteza ta wspierana jest przez wyniki uzyskane dla liści *B. distachyon* (Mareri i in., 2018, Pinski i in., 2019b).

Określono również poziom akumulacji transkryptów dziewięciu różnych genów kodujących kinazy receptorowe ekstensyn i białek podobnych do ekstensyn (*Bradi1g22980*,

Bradi3g59780, Bradi4g03720, Bradi4g11250, Bradi3g12902, Bradi2g00900, Bradi2g49240, Bradi1g07019 i *Bradi3g31967*). Statystycznie istotny wyższy poziom ekspresji *Bradi3g59780* i *Bradi4g03720* wykazano tylko dla 40 °C. Z kolei poziom akumulacji transkryptu *Bradi4g11250* wzrósł znacząco w 4 °C. Większą akumulację transkryptu genu *Bradi2g00900* stwierdzono w 4 ° C, natomiast większy poziom akumulacji transkryptu genu *Bradi2g49240* w 4 °C i 40 °C. Co ciekawe, ekspresję drugiego genu *Bradi3g31967* zaobserwowano jedynie w liściach poddanych stresowi temperaturowemu. Zmiany w ekspresji genów kodujących ekstensyny w dużym stopniu zależą od ich klasy, jak wykazano w przypadku roślin *A. thaliana* poddanych stresowi niskotemperaturowemu (Seki i in., 2002). Inna analiza transkryptomiczna odpowiedzi *A. thaliana* na stres związany z niską temperaturą wykazała obniżoną ekspresję jednego z genów kodujących kinazę receptorową bogatą w prolinę podobną do ekstensyn (Kreps i in., 2002). Dane pokazujące zmiany w rozmieszczeniu poszczególnych składników ściany komórkowej, w szczególności AGP, w powiązaniu ze stresem temperaturowym, są szczególnie ważne, ponieważ wyniki te mogą być wykorzystane w inżynierii genetycznej do zwiększania tolerancji roślin na stres (Wang i in., 2003). Omówione powyżej wyniki zostały zaprezentowane w pracy **Pinski i in. (2019b)** zamieszczonej w **rozdziale II.1**.

Biorąc pod uwagę, że również inne białka ściany komórkowej, poza białkami bogatymi w hydroksyprolinę, biorą udział w odpowiedzi na stres temperaturowy podjęto się charakterystyki ogólnych zmian w proteomie ściany komórkowej. Wyizolowane białka, które rozdzielono za pomocą elektroforezy 1D, wykazywały powtarzalny wzór prążków we wszystkich czterech powtórzeniach biologicznych. Co więcej, żadna z próbek nie wykazała widocznych wzorów degradacji białek. Wzory elektroforetyczne były inne dla białek izolowanych z roślin poddanych stresowi w 40 °C i roślin kontrolnych. Analiza białek z wykorzystaniem chromatografii LC-MS/MS umożliwiła identyfikację 1533 unikalnych białek, z których 338 oznaczonych zostało jako białka ściany komórkowej, co stanowiło 22% wszystkich białek. Proteom ściany komórkowej zawiera nie tylko białka ściany komórkowej, ale także wiele białek pochodzących z cytoplazmy, które w dalszej analizie traktowane są jako zanieczyszczenia (Albenne i in., 2014). Wśród 338 białek, 39 okazało się nowo zidentyfikowanymi białkami ściany komórkowej, wzbogacając tym samym listę białek znajdującą się w bazie danych *WallProtDB* dla *B. distachyon* do 738 białek ściany komórkowej (San Clemente i Jamet, 2015, Pinski i in., 2021b). Przewidywane masy cząsteczkowe białek zwykle mieściły się w zakresie 20-60 kDa, ale udało się zidentyfikować

również białka o masie do 120 kDa, co sugeruje dobrą reprezentację białek. Dla większości białek zaobserwowano wysokie pokrycie sekwencji białkowej zidentyfikowanymi peptydami; dla 80% białek zaobserwowano pokrycie sekwencji powyżej 20%. Liczba zidentyfikowanych białek ściany komórkowej wynosiła w kontroli 311 białek, a w 40 °C 253 białek. Analiza głównych składowych PCA (ang. *principal component analysis*) wykazała znaczne różnice w próbkach izolowanych z roślin inkubowanych w 40 °C. W istocie, dalsza analiza jakościowa wykazała brak 60 białek ściany komórkowej w 40 °C, które były obecne w kontroli. Zidentyfikowano 46 białek ściany komórkowej o zróżnicowanej obecności między kontrolą a 40 °C. Spośród nich cztery białka charakteryzowały się zwiększoną obecnością w 40 °C, a 42 zmniejszoną. Po przyporządkowaniu tych białek do klas funkcjonalnych analiza wykazała zmiany w obecności białek w siedmiu klasach. Największe zmiany dotyczyły klasy białek działających na polisacharydy ściany komórkowej z dwoma białkami o zwiększonej obecności i 12 o zmniejszonej. Biorąc pod uwagę rodziny białek, większość białek o zróżnicowanej obecności została sklasyfikowana jako hydrolazy glikozydowe (11 białek), proteazy asparaginowe (6), peroksydazy klasy III (4) i lipazy GDSL (4). Różnice w obecności mieściły się w zakresie od 23,2-krotnego wzrostu w temperaturze 40 °C dla białka Bradi4g09430 (inhibitor ksylanazy/chitynaza klasy II z rodziny hydrolaz glikozydowych GH18 według bazy danych CAZy, ang. *Carbohydrate-Active enZYmes*, http://www.cazy.org/) do 15,8-krotnego spadku dla białka Bradi1g52050 (poligalakturonaza z rodziny hydrolazy glikozydowe GH28) w porównaniu z kontrolą. W celu korelacji wyników analiz proteomicznych, porównano je z wynikami analizy profilu ekspresji uzyskanych wykorzystując technikę RT-qPCR dla sześciu genów (*Bradi1g52050*, *Bradi1g38780*, *Bradi1g25517*, *Bradi1g58997*, *Bradi4g09417* i *Bradi4g09430*). Relatywny poziom ekspresji pięciu z sześciu analizowanych genów w 40 °C wykazywał podobny trend zmian jak w przypadku analizy proteomicznej. Warto zauważyć, że analiza proteomiczna wykazała zmiany w obfitości białek, które ulegały kumulacji lub degradacji podczas całego okresu inkubacji (24 godz.), podczas gdy analiza ekspresji informuje o poziomie ekspresji genów w określonym punkcie czasowym, czyli po 24 godz. traktowania. Co więcej, zależność między poziomem ekspresji danego genu a biosyntezą kodowanego przez nie białka jest złożona i podlega różnym poziomom regulacji, co sprawia, że analiza proteomiczna jest bardziej informatywna w odniesieniu do faktycznych zmian w proteomie ściany komórkowej. Rozbieżności w wynikach prezentowanych przez analizy poziomu transkrypcji i akumulacji białek są znaczne i wynikają z regulacji potranskrypcyjnej, jak

też różnic w średnim czasie półtrwania matrycowego RNA i białka, które jest od niego znacznie trwalsze (Haider i Pal, 2013, Bathke i in., 2019, Wang i in., 2019).

Zaobserwowane zmiany w proteomie ściany komórkowej liści w temperaturze 40 °C w porównaniu do kontroli, sugerują niższą aktywność proteaz, lignifikację, ekspansję ściany komórkowej i zmiany w architekturze polimerów ściany komórkowej, zwłaszcza pektyn. Wyniki te wzbogacają zrozumienie odpowiedzi na stres temperaturowy, która została wyczerpująco podsumowana przez Le Gall i in. (2015), gdzie autorzy zwrócili uwagę na zmiany w polisacharydach ściany komórkowej, celulozie, hemicelulozach i pektynach, a także biosyntezie ligniny w odpowiedzi na stres temperaturowy. W przeprowadzonej analizie proteomicznej nie udało się zidentyfikować żadnych AGP o zróżnicowanym poziomie obecności, co może być związane z faktem, że zmiany w obecności AGP, które zostały ujawnione przez analizy immunohistochemiczne, były tkankowo-specyficzne (Pinski i in., 2019b). Możliwym jest także, że ogólne zmiany w obecności AGP mogą nie być wystarczająco duże, aby znacząco różnić się między traktowaniami. Alternatywnie, ponieważ białka te są trudne do wykrycia ze względu na ich mały rozmiar i wysoki poziom glikozylacji, wymagają one specyficznego podejścia metodycznego, które rozpoczyna się od etapu deglikozylacji (Schultz i in., 2004). Zatem różnicujące traktowania AGP mogły pozostać niewykryte w analizie proteomicznej, podobnie jak ekstensyn, które są zwykle kowalencyjnie usieciowane z innymi składnikami ściany komórkowej (Albenne i in., 2013). Przeprowadzona analiza proteomiczna uzupełnia poprzednią analizę transkryptomiczną zmian w liściach *B. distachyon* w odpowiedzi na stres wywołany wysoką temperaturą. U roślin inkubowanych w temperaturze 42 °C przez 5 godz. autorzy zaobserwowali znaczne różnice w ekspresji genów związanych z białkami systemu fotosyntezy i siateczką śródplazmatyczną. Warto zauważyć, że wysoka temperatura indukowała również zwiększenie poziomu ekspresji genów zaangażowanych w splicing alternatywny matrycowego RNA (Chen i Li, 2016). Wyniki analizy proteomicznej zamieszczono w pracy **Pinski i in. (2021a)** umieszczonej w **rozdziale II.2** niniejszej pracy.

W celu sprecyzowania udziału białek ściany komórkowej w odpowiedzi na stres temperaturowy wybrano dwa geny kodujące FLA (*Bradi3g39740*) i PME (*Bradi3g24750*). Gen kodujący FLA wybrano bazując na wynikach analizy ekspresji genów w odpowiedzi na stres temperaturowy w liściach *B. distachyon,* gdzie zaobserwowano znaczny wzrost ekspresji genu

Bradi3g39740 (Pinski i in., 2019b). Z kolei, gen kodujący PME wybrano na podstawie danych literaturowych sugerujących znaczny udział białek modyfikujących pektyny w odpowiedzi na stres temperaturowy (Le Gall i in., 2015, Chen i in., 2018, Sista Kameshwar i Qin, 2018). Bazując na sekwencjach genów *FLA* i *PME* zdeponowanych w bazie Phytozome i sekwencjonowaniu ich kodujących sekwencji zaprojektowano jeden gRNA dla *FLA* i dwa dla *PME*. gRNA dla *FLA* wprowadzono do wektora pOsCas9. Ponieważ wektor ten pozwala na wprowadzenie tylko jednego gRNA, w przypadku *PME* wykorzystano zestaw umożliwiający przygotowanie wektora z kilkoma gRNA (trzech dla roślin jednoliściennych i ośmiu dla dwuliściennych) (Lowder i in., 2015). Ekspresja gRNA w wektorze w pOsCas9 regulowana była przez promotor U3 małego jądrowego RNA, z kolei w przypadku wektora dla *PME* oba gRNA posiadały promotor U6 małego jądrowego RNA. Sekwencja obu promotorów pochodziła z genomu ryżu (Lowder i in., 2015, Hus i in., 2020). Odpowiednie wektory przygotowano do transfekcji protoplastów, i wprowadzenia do komórek bakteryjnych *A. tumefacins* AGL1, które często są wykorzystywane do transformacji kalusa *B. distachyon* (Alves i in., 2009, Betekhtin i in., 2020). Funkcjonalność przygotowanych wektorów w edycji genomu oceniono wykorzystując test protoplastów. Z trzech testowanych gRNA edycję genomu w protoplastach uzyskano tylko dla gRNA *PME_BsrGI*, w odniesieniu do którego zaobserwowano delecję jednego nukleotydu (G lub T) między trzecim i czwartym nukleotydem powyżej regionu PAM (ang. *protospacer adjacent motif*) co pozostaje w zgodzie z mechanizmem działania białka Cas9 (Hus i in., 2020, Collias i Beisel, 2021). Nie wykryto żadnych zmian w genomie protoplastów w przypadku dwóch pozostałych gRNA (*FLA_BbsI* i *PME_AccI*), co nie oznacza jednak, że zaprojektowane gRNA są nieaktywne. Choć wykonanie testu wykorzystującego protoplasty jest stosunkowo szybkie, gdyż zajmuje tylko kilka dni, wydajność transformacji jest relatywnie niska, co skutkować może praktycznie niewykrywalną częstością mutacji (Vyacheslavova i in., 2012, Jung i in., 2015). Co więcej, w przypadku gatunków *Brachypodium* nie opracowano dotychczas skutecznej metody regeneracji protoplastów (Betekhtin i in., 2020, Pasternak i in., 2020). Technika taka umożliwiłaby modyfikację genomu protoplastów i ich regenerację omijając cechującą się niską wydajnością transformację kalusa z wykorzystaniem komórek *A. tumefaciens*. Regeneracja protoplastów w połączeniu z wykorzystaniem kompleksu rybonukleoproteiny Cas9 połączonej z gRNA umożliwiłoby uzyskiwanie zmodyfikowanych genetycznie roślin bez obcego materiału genetycznego. Kompleks rybonukleoproteiny Cas9 z gRNA cechuje się także wyższą specyficznością i niższą częstością

wprowadzania mutacji typu off-target (Zhang i in., 2021). W przypadku genu PME, dla którego zaprojektowano dwa gRNA oczekiwano delecji fragmentu znajdującego się pomiędzy dwoma gRNA (*PME_BsrGI* i *PME_AccI*). Oba gRNA rozdzielone są dwoma nukleotydami. Niemniej, w żadnej z czterech uzyskanych zmutowanych roślin nie zaobserwowano takiej delecji. Wynikać to może z bliskości obu gRNA co powodować może, że obie sekwencje docelowe cięte są raczej sekwencyjnie niż symultanicznie, co mogłoby indukować utratę fragmentu znajdującego się pomiędzy gRNA. Niemniej, podejście to umożliwia usuwanie długich fragmentów (do kilku tyś. par zasad) genomowego DNA (Do i in., 2019, Lopez i in., 2021). W dwóch roślinach obserwowano mutacje (insercje lub delecje jednego lub czterech nukleotydów) w obu gRNA dla obu alleli. W przypadku jednego mutanta nie zaobserwowano żadnych zmian w tylko jednym allelu dla gRNA *PME_AccI*. Co więcej, w czwartej roślinie obserwowano aktywność tylko gRNA *PME_BsrGI*. Wyniki te sugerują niższą aktywność gRNA *PME_AccI* w edycji genomu, co może być wyjaśnione różną wydajnością cięcia w zależności od zaprojektowanej sekwencji gRNA. W szczególności zawartość par GC, obecność puryn na końcu gRNA i dostępność regionu znajdującego się powyżej regionu PAM, mają największy wpływ na wydajność edycji genomu, jak wykazano na przykładzie edycji genomu topoli z wykorzystaniem systemu CRISPR/Cas9 (Bruegmann i in., 2019). W wyniku transformacji kalusa *B. distachyon* komórkami bakteryjnymi *A. tumefacins* AGL1 uzyskano cztery zmutowane rośliny w genie *FLA* ze zmianami obserwowanymi w obu allelach. Obserwowano głównie insercje jednego nukleotydu, choć w przypadku jednego allelu zidentyfikowano delecję jednego nukleotydu. Mutacje w postaci insercji lub delecji jednego do kilku nukleotydów są charakterystyczne dla mutacji wprowadzonych przez białko Cas9 u *B. distachyon* (Hus i in., 2020). Uzyskane wyniki dla inaktywacji genów *Bradi3g39740* i *Bradi3g24750* stanowią część pracy metodycznej **Hus i in. (2020)** zamieszczonej w **rozdziale II.3**. Praca ta zawierającej dokładny protokół inaktywacji genów z wykorzystaniem systemu CRISPR/Cas9 u *B. distachyon* i *B. hybridum*. Uzyskane indele (delecje lub insercje) w zmutowanych genach skutkują przesunięciem ramki odczytu a w efekcie powstaniem niefunkcjonalnego białka ze względu na przedwczesny kodon STOP lub całkowitą zmianą aminokwasów poniżej zmutowanej sekwencji. W przypadku mutantów w obu genach nie zaobserwowano znaczących różnic w fenotypie w normalnych dla *B. distachyon* warunkach wzrostu. Mutanty w obu genach wydały nasiona i rośliny z kolejnego pokolenia poddano wstępnej analizie odpowiedzi na warunku stresu temperaturowego. Nie zaobserwowano znaczących różnic

we wzroście roślin z inaktywowanymi genami *FLA* i *PME* w odpowiedzi na stres temperaturowy, natomiast wstępne badania odpowiedzi na stres solny wykazały znaczne spowolnienie ich wzrostu w obecności chlorku sodu i większą wrażliwość na stres solny manifestującą się niższą efektywnością kiełkowania niż u roślin genotypu referencyjnego (dane nieopublikowane). Brak efektu mutacji w przypadku stresu temperaturowego wynikać może z faktu, że oba geny, *FLA* i *PME*, należą do rodzin wielogenowych i ich inaktywacja może być kompensowana przez zmiany w profilu ekspresji innych genów w rodzinie (Seifert, 2018). Z kolei udział białek FLA i PME w odpowiedzi na stres solny został wykazany dla niektórych z białek należących do tych rodzin u *A. thaliana* (Seifert i in., 2014, Seifert, 2018, Yan i in., 2018).

W niniejszej pracy zastosowanie techniki immunobarwienia i analizy profilu ekspresji pozwoliły na charakteryzację tkankowo-specyficznych zmian w obecności i intensywności epitopów AGP i ekstensyn, jak też zmian w profilu ekspresji genów kodujących te białka w liściach *B. distachyon* w odpowiedzi na stres temperaturowy indukowany niską i wysoką temperaturą. Proteomika ściany komórkowej umożliwiła charakteryzację ogólnych zmian w obecności białek ściany komórkowej w wysokiej temperaturze. Uzyskane wyniki pogłębiają zrozumienie udziału białek ściany komórkowej w odpowiedzi na stres temperaturowy u *B. distachyon*, jak też mogą być wykorzystane w inżynierii genetycznej do zwiększania tolerancji roślin, w szczególności traw, na stres.

Rozdział I.5 Literatura

Acosta-Motos J, Ortuño M, Bernal-Vicente A, Diaz-Vivancos P, Sanchez-Blanco M, Hernandez J. 2017. Plant responses to salt stress: adaptive mechanisms. *Agronomy*, **7**: 18.

Albenne C, Canut H, Boudart G, Zhang Y, San Clemente H, Pont-Lezica R, Jamet E. 2009. Plant cell wall proteomics: mass spectrometry data, a trove for research on protein structure/function relationships. *Mol Plant,* **2**: 977-989.

Albenne C, Canut H, Hoffmann L, Jamet E. 2014. Plant cell wall proteins: a large body of data, but what about runaways? *Proteomes*, **2**: 224-242.

Albenne C, Canut H, Jamet E. 2013. Plant cell wall proteomics: the leadership of *Arabidopsis thaliana*. *Front Plant Sci,* **4**: 111.

Alves SC, Worland B, Thole V, Snape JW, Bevan MW, Vain P. 2009. A protocol for *Agrobacterium*-mediated transformation of *Brachypodium distachyon* community standard line Bd21. *Nat Protoc,* **4**: 638-649.

Bathke J, Konzer A, Remes B, McIntosh M, Klug G. 2019. Comparative analyses of the variation of the transcriptome and proteome of *Rhodobacter sphaeroides* throughout growth. *BMC Genomics*, **20**: 1-13.

Betekhtin A, Hus K, Rojek-Jelonek M, Kurczynska E, Nibau C, Doonan JH, Hasterok R. 2020. In vitro tissue culture in *Brachypodium*: applications and challenges. *Int J Mol Sci,* **21**: 1037.

Betekhtin A, Pinski A, Milewska-Hendel A, Kurczynska E, Hasterok R. 2019. Stability and instability processes in the calli of *Fagopyrum tataricum* that have different morphogenic potentials. *Plant Cell Tissue Organ Cult,* **137**: 343-357.

Betekhtin A, Rojek M, Milewska-Hendel A, Gawecki R, Karcz J, Kurczynska E, Hasterok R. 2016. Spatial distribution of selected chemical cell wall components in the embryogenic callus of *Brachypodium distachyon*. *PLoS One,* **11**: e0167426.

Betekhtin A, Rojek M, Nowak K, Pinski A, Milewska-Hendel A, Kurczynska E, Doonan JH, Hasterok R. 2018. Cell wall epitopes and endoploidy as reporters of embryogenic potential in *Brachypodium distachyon* callus culture. *Int J Mol Sci,* **19**: 3811.

Bita CE, Gerats T. 2013. Plant tolerance to high temperature in a changing environment: scientific fundamentals and production of heat stress-tolerant crops. *Front Plant Sci,* **4**: 273.

Bruegmann T, Deecke K, Fladung M. 2019. Evaluating the efficiency of gRNAs in CRISPR/Cas9 mediated genome editing in poplars. *Int J Mol Sci*, **20**: 3623.

Casero PJ, Casimiro I, Knox JP. 1998. Occurrence of cell surface arabinogalactan-protein and extensin epitopes in relation to pericycle and vascular tissue development in the root apex of four species. *Planta*, **204**: 252-259.

Castilleux R, Plancot B, Vicre M, Nguema-Ona E, Driouich A. 2021. Extensin, an underestimated key component of cell wall defence? *Ann Bot*, **127**: 709-713.

Chen J, Chen X, Zhang Q, Zhang Y, Ou X, An L, Feng H, Zhao Z. 2018. A cold-induced pectin methyl-esterase inhibitor gene contributes negatively to freezing tolerance but positively to salt tolerance in Arabidopsis. *J Plant Physiol*, **222**: 67-78.

Chen S, Li H. 2016. Heat stress regulates the expression of genes at transcriptional and post-transcriptional levels, revealed by RNA-seq in *Brachypodium distachyon*. *Front Plant Sci*, **7**: 2067.

Collias D, Beisel CL. 2021. CRISPR technologies and the search for the PAM-free nuclease. *Nat Commun*, **12**: 1-12.

Coomey JH, Sibout R, Hazen SP. 2020. Grass secondary cell walls, *Brachypodium distachyon* as a model for discovery. *New Phytol*, **227**: 1649-1667.

De Pinto A, Cenacchi N, Kwon HY, Koo J, Dunston S. 2020. Climate smart agriculture and global food-crop production. *PLoS One*, **15**: e0231764.

Debaeke P, Pellerin S, Scopel E. 2017. Climate-smart cropping systems for temperate and tropical agriculture: mitigation, adaptation and trade-offs. *Cah Agric*, **26**: 34002.

Do PT, Nguyen CX, Bui HT, Tran LTN, Stacey G, Gillman JD, Zhang ZJ, Stacey MG. 2019. Demonstration of highly efficient dual gRNA CRISPR/Cas9 editing of the homeologous GmFAD2-1A and GmFAD2-1B genes to yield a high oleic, low linoleic and alpha-linolenic acid phenotype in soybean. *BMC Plant Biol*, **19**: 1-14.

Douché T, San Clemente H, Burlat V, Roujol D, Valot B, Zivy M, Pont-Lezica R, Jamet E. 2013. *Brachypodium distachyon* as a model plant toward improved biofuel crops: search for secreted proteins involved in biogenesis and disassembly of cell wall polymers. *Proteomics*, **13**: 2438-2454.

Draper J, Mur LAJ, Jenkins G, Ghosh-Biswas GC, Bablak P, Hasterok R, Routledge APM. 2001. *Brachypodium distachyon*. A new model system for functional genomics in grasses. *Plant Physiol*, **127**: 1539-1555.

Ellis M, Egelund J, Schultz CJ, Bacic A. 2010. Arabinogalactan-proteins: key regulators at the cell surface? *Plant Physiol*, **153**: 403-419.

Faik A, Abouzouhair J, Sarhan F. 2006. Putative fasciclin-like arabinogalactan-proteins (FLA) in wheat (*Triticum aestivum*) and rice (*Oryza sativa*): identification and bioinformatic analyses. *Mol Genet Genomics*, **276**: 478-494.

Feiz L, Irshad M, Pont-Lezica RF, Canut H, Jamet E. 2006. Evaluation of cell wall preparations for proteomics: a new procedure for purifying cell walls from Arabidopsis hypocotyls. *Plant Methods*, **2**: 1-13.

Garaeva LD, Pozdeeva SA, Timofeeva OA, Khokhlova LP. 2006. Cell-wall lectins during winter wheat cold hardening. *Russ J Plant Physiol*, **53**: 746-750.

Gechev TS, Hille J, Woerdenbag HJ, Benina M, Mehterov N, Toneva V, Fernie AR, Mueller-Roeber B. 2014. Natural products from resurrection plants: potential for medical applications. *Biotechnol Adv*, **32**: 1091-1101.

Gong SY, Huang GQ, Sun X, Li P, Zhao LL, Zhang DJ, Li XB. 2012. GhAGP31, a cotton non-classical arabinogalactan protein, is involved in response to cold stress during early seedling development. *Plant Biol*, **14**: 447-457.

Gordon SP, Contreras-Moreira B, Woods DP, Des Marais DL, Burgess D, Shu S, Stritt C, Roulin AC, Schackwitz W, Tyler L, Martin J, Lipzen A, Dochy N, Phillips J, Barry K, Geuten K, Budak H, Juenger TE, Amasino R, Caicedo AL, Goodstein D, Davidson P, Mur LAJ, Figueroa M, Freeling M, Catalan P, Vogel JP. 2017. Extensive gene content variation in the *Brachypodium distachyon* pan-genome correlates with population structure. *Nat Commun*, **8**: 1-13.

Griffiths JS, Tsai AY, Xue H, Voiniciuc C, Sola K, Seifert GJ, Mansfield SD, Haughn GW. 2014. SALT-OVERLY SENSITIVE5 mediates Arabidopsis seed coat mucilage adherence and organization through pectins. *Plant Physiol*, **165**: 991-1004.

Ha MA, Vietor RJ, Jardine GD, Apperley DC, Jarvis MC. 2005. Conformation and mobility of the arabinan and galactan side-chains of pectin. *Phytochemistry*, **66**: 1817-1824.

Haider S, Pal R. 2013. Integrated analysis of transcriptomic and proteomic data. *Curr Genomics,* **14**: 91-110.

Hong SY, Park JH, Cho SH, Yang MS, Park CM. 2011. Phenological growth stages of *Brachypodium distachyon*: codification and description. *Weed Res,* **51**: 612-620.

Hus K, Betekhtin A, Pinski A, Rojek-Jelonek M, Grzebelus E, Nibau C, Gao M, Jaeger KE, Jenkins G, Doonan JH, Hasterok R. 2020. A CRISPR/Cas9-Based mutagenesis protocol for *Brachypodium distachyon* and its allopolyploid relative, *Brachypodium hybridum*. *Front Plant Sci,* **11**: 614.

International Brachypodium Initiative. 2010. Genome sequencing and analysis of the model grass *Brachypodium distachyon*. *Nature,* **463**: 763-768.

Janmohammadi M, Zolla L, Rinalducci S. 2015. Low temperature tolerance in plants: changes at the protein level. *Phytochemistry,* **117**: 76-89.

Jansson C, Vogel J, Hazen S, Brutnell T, Mockler T. 2018. Climate-smart crops with enhanced photosynthesis. *J Exp Bot,* **69**: 3801-3809.

Johnson KL, Cassin AM, Lonsdale A, Bacic A, Doblin MS, Schultz CJ. 2017. Pipeline to identify hydroxyproline-rich glycoproteins. *Plant Physiol,* **174**: 886-903.

Jung HI, Yan J, Zhai Z, Vatamaniuk OK. 2015. Gene functional analysis using protoplast transient assays. *Methods Mol Biol,* **1284**: 433-452.

Kreps JA, Wu Y, Chang HS, Zhu T, Wang X, Harper JF. 2002. Transcriptome changes for Arabidopsis in response to salt, osmotic, and cold stress. *Plant Physiol,* **130**: 2129-2141.

Larsen FH, Byg I, Damager I, Diaz J, Engelsen SB, Ulvskov P. 2011. Residue specific hydration of primary cell wall potato pectin identified by solid-state 13C single-pulse MAS and CP/MAS NMR spectroscopy. *Biomacromolecules,* **12**: 1844-1850.

Le Gall H, Philippe F, Domon JM, Gillet F, Pelloux J, Rayon C. 2015. Cell wall metabolism in response to abiotic stress. *Plants,* **4**: 112-166.

Liu X, Wolfe R, Welch LR, Domozych DS, Popper ZA, Showalter AM. 2016. Bioinformatic identification and analysis of extensins in the plant kingdom. *PLoS One,* **11**: e0150177.

Lopez FB, Fort A, Tadini L, Probst AV, McHale M, Friel J, Ryder P, Pontvianne F, Pesaresi P, Sulpice R, McKeown P, Brychkova G, Spillane C. 2021. Gene dosage compensation of rRNA transcript levels in *Arabidopsis thaliana* lines with reduced ribosomal gene copy number. *Plant Cell,* **33**: 1135–1150.

Lowder LG, Zhang D, Baltes NJ, Paul JW, Tang X, Zheng X, Voytas DF, Hsieh T-F, Zhang Y, Qi Y. 2015. A CRISPR/Cas9 toolbox for multiplexed plant genome editing and transcriptional regulation. *Plant Physiol,* **169**: 971-985.

Ma H, Zhao J. 2010. Genome-wide identification, classification, and expression analysis of the arabinogalactan protein gene family in rice (*Oryza sativa* L.). *J Exp Bot,* **61**: 2647-2668.

Mareri L, Romi M, Cai G. 2018. Arabinogalactan proteins: actors or spectators during abiotic and biotic stress in plants? *Plant Biosyst,* **153**: 173-185.

Moore JP, Farrant JM, Driouich A. 2014. A role for pectin-associated arabinans in maintaining the flexibility of the plant cell wall during water deficit stress. *Plant Signal Behav,* **3**: 102-104.

Nahar K, Hasanuzzaman M, Ahamed KU, Hakeem KR, Ozturk M, Fujita M. 2015. Plant responses and tolerance to high temperature stress: role of exogenous phytoprotectants. In: Hakeem KR, ed. *Crop Production and Global Environmental Issues*. Cham: Springer.

Niu Y, Xiang Y. 2018. An overview of biomembrane functions in plant responses to high-temperature stress. *Front Plant Sci,* **9**: 915.

Nothnagel EA. 1997. Proteoglycans and related components in plant cells. *Int Rev Cytol,* **174**: 195-291.

Novakovic L, Guo T, Bacic A, Sampathkumar A, Johnson KL. 2018. Hitting the wall-sensing and signaling pathways involved in plant cell wall remodeling in response to abiotic stress. *Plants,* **7**: 89.

Pasternak T, Lystvan K, Betekhtin A, Hasterok R. 2020. From single cell to plants: mesophyll protoplasts as a versatile system for investigating plant cell reprogramming. *Int J Mol Sci,* **21**: 4195.

Pereira AM, Pereira LG, Coimbra S. 2015. Arabinogalactan proteins: rising attention from plant biologists. *Plant Reprod,* **28**: 1-15.

Pfaffl MW. 2001. A new mathematical model for relative quantification in real-time RT–PCR. *Nucleic Acids Res,* **29**: e45-e45.

Pinski A, Betekhtin A, Hupert-Kocurek K, Mur LAJ, Hasterok R. 2019a. Defining the genetic basis of plant–endophytic bacteria interactions. *Int J Mol Sci,* **20**: 1947.

Pinski A, Betekhtin A, Sala K, Godel-Jedrychowska K, Kurczynska E, Hasterok R. 2019b. Hydroxyproline-rich glycoproteins as markers of temperature stress in the leaves of *Brachypodium distachyon*. *Int J Mol Sci,* **20**: 2571.

Pinski A, Betekhtin A, Skupien-Rabian B, Jankowska U, Jamet E, Hasterok R. 2021a. Changes in the cell wall proteome of leaves in response to high temperature stress in *Brachypodium distachyon*. *Int J Mol Sci,* **22**: 6750.

Pinski A, Roujol D, Pouzet C, Bordes L, Clemente HS, Hoffmann L, Jamet E. 2021b. Comparison of mass spectrometry data and bioinformatics predictions to assess the bona fide localization of proteins identified in cell wall proteomics studies. *Plant Sci,* **310**:110979.

Pushpalatha R, Gangadharan B. 2020. Is cassava (*Manihot esculenta* Crantz) a climate "smart" crop? A review in the context of bridging future food demand gap. *Trop Plant Biol,* **13**: 201-211.

Sala K, Malarz K, Barlow PW, Kurczyńska EU. 2017. Distribution of some pectic and arabinogalactan protein epitopes during *Solanum lycopersicum* (L.) adventitious root development. *BMC Plant Biol,* **17**: 1-16.

San Clemente H, Jamet E. 2015. WallProtDB, a database resource for plant cell wall proteomics. *Plant Methods,* **11**: 1-7.

Schultz CJ, Ferguson KL, Lahnstein J, Bacic A. 2004. Post-translational modifications of arabinogalactan-peptides of *Arabidopsis thaliana*. Endoplasmic reticulum and glycosylphosphatidylinositol-anchor signal cleavage sites and hydroxylation of proline. *J Biol Chem,* **279**: 45503-45511.

Seifert GJ. 2018. Fascinating fasciclins: a surprisingly widespread family of proteins that mediate interactions between the cell exterior and the cell surface. *Int J Mol Sci,* **19**: 1628.

Seifert GJ, Xue H, Acet T. 2014. The *Arabidopsis thaliana FASCICLIN LIKE ARABINOGALACTAN PROTEIN 4* gene acts synergistically with abscisic acid signalling to control root growth. *Ann Bot,* **114**: 1125-1133.

Seki M, Narusaka M, Ishida J, Nanjo T, Fujita M, Oono Y, Kamiya A, Nakajima M, Enju A, Sakurai T, Satou M, Akiyama K, Taji T, Yamaguchi-Shinozaki K, Carninci P, Kawai J, Hayashizaki Y, Shinozaki K. 2002. Monitoring the expression profiles of 7000

Arabidopsis genes under drought, cold and high-salinity stresses using a full-length cDNA microarray. *Plant J,* **31**: 279-292.

Sista Kameshwar AK, Qin W. 2018. Structural and functional properties of pectin and lignin–carbohydrate complexes de-esterases: a review. *Bioresour Bioprocess,* **5**: 1-16.

Skalska A, Stritt C, Wyler M, Williams HW, Vickers M, Han J, Tuna M, Savas Tuna G, Susek K, Swain M, Woycicki RK, Chaudhary S, Corke F, Doonan JH, Roulin AC, Hasterok R, Mur LAJ. 2020. Genetic and methylome variation in turkish *Brachypodium distachyon* accessions differentiate two geographically distinct subpopulations. *Int J Mol Sci,* **21**: 6700.

Taylor M. 2017. Climate-smart agriculture: what is it good for? *J Peasant Stud,* **45**: 89-107.

Tenhaken R. 2014. Cell wall remodeling under abiotic stress. *Front Plant Sci,* **5**: 771.

Tiwari S, Patel A, Singh M, Prasad SM. 2020. Regulation of temperature stress in plants. In: Tripathi DK, Singh VP, Chauhan DK, Sharma S, Prasad SM, Dubey NK, Ramawat N, eds. *Plant Life Under Changing Environment*. Academic Press: Elsevier.

Tyanova S, Temu T, Sinitcyn P, Carlson A, Hein MY, Geiger T, Mann M, Cox J. 2016. The Perseus computational platform for comprehensive analysis of (prote)omics data. *Nat Methods,* **13**: 731-740.

Varotto S, Tani E, Abraham E, Krugman T, Kapazoglou A, Melzer R, Radanovic A, Miladinovic D. 2020. Epigenetics: possible applications in climate-smart crop breeding. *J Exp Bot,* **71**: 5223-5236.

Vogel J. 2008. Unique aspects of the grass cell wall. *Curr Opin Plant Biol,* **11**: 301-307.

Vyacheslavova AO, Berdichevets IN, Tyurin AA, Shimshilashvili KR, Mustafaev ON, Goldenkova-Pavlova IV. 2012. Expression of heterologous genes in plant systems: new possibilities. *Russ J Genet,* **48**: 1067-1079.

Wang W, Vinocur B, Altman A. 2003. Plant responses to drought, salinity and extreme temperatures: towards genetic engineering for stress tolerance. *Planta,* **218**: 1-14.

Wang X, Liang H, Guo D, Guo L, Duan X, Jia Q, Hou X. 2019. Integrated analysis of transcriptomic and proteomic data from tree peony (*P. ostii*) seeds reveals key developmental stages and candidate genes related to oil biosynthesis and fatty acid metabolism. *Hortic Res,* **6**: 111.

Wisniewski JR, Zougman A, Nagaraj N, Mann M. 2009. Universal sample preparation method for proteome analysis. *Nat Methods,* **6**: 359-362.

Wolny E, Hasterok R. 2009. Comparative cytogenetic analysis of the genomes of the model grass *Brachypodium distachyon* and its close relatives. *Ann Bot,* **104**: 873-881.

Wu Y, Fan W, Li X, Chen H, Takac T, Samajova O, Fabrice MR, Xie L, Ma J, Samaj J, Xu C. 2017. Expression and distribution of extensins and AGPs in susceptible and resistant banana cultivars in response to wounding and *Fusarium oxysporum*. *Sci Rep,* **7**: 1-13.

Xu C, Takáč T, Burbach C, Menzel D, Šamaj J. 2011. Developmental localization and the role of hydroxyproline rich glycoproteins during somatic embryogenesis of banana (*Musa* spp. AAA). *BMC Plant Biol,* **11**: 1-12.

Yamauchi T, Noshita K, Tsutsumi N. 2021. Climate-smart crops: key root anatomical traits that confer flooding tolerance. *Breed Sci,* **71**: 51-61.

Yan J, He H, Fang L, Zhang A. 2018. Pectin methylesterase31 positively regulates salt stress tolerance in Arabidopsis. *Biochem Biophys Res Commun,* **496**: 497-501.

Yan Y, Takac T, Li X, Chen H, Wang Y, Xu E, Xie L, Su Z, Samaj J, Xu C. 2015. Variable content and distribution of arabinogalactan proteins in banana (*Musa* spp.) under low temperature stress. *Front Plant Sci,* **6**: 353.

Zhang S, Shen J, Li D, Cheng Y. 2021. Strategies in the delivery of Cas9 ribonucleoprotein for CRISPR/Cas9 genome editing. *Theranostics,* **11**: 614-648.

Zhang X, Ren Y, Zhao J. 2008. Roles of extensins in cotyledon primordium formation and shoot apical meristem activity in *Nicotiana tabacum*. *J Exp Bot,* **59**: 4045-4058.

Zhao C, Liu B, Piao S, Wang X, Lobell DB, Huang Y, Huang M, Yao Y, Bassu S, Ciais P, Durand JL, Elliott J, Ewert F, Janssens IA, Li T, Lin E, Liu Q, Martre P, Muller C, Peng S, Penuelas J, Ruane AC, Wallach D, Wang T, Wu D, Liu Z, Zhu Y, Zhu Z, Asseng S. 2017. Temperature increase reduces global yields of major crops in four independent estimates. *Proc Natl Acad Sci USA,* **114**: 9326-9331.

Rozdział II Publikacje wchodzące w skład rozprawy

II.1

Pinski A, Betekhtin A, Sala K, Godel-Jedrychowska K, Kurczynska E, Hasterok R.

Hydroxyproline-rich glycoproteins as markers of temperature stress in the leaves of *Brachypodium distachyon*

International Journal of Molecular Sciences, 2019, 20, 2571

IF_{2019} – 4,556; pkt MNiSW – 140

International Journal of
Molecular Sciences

MDPI

Article

Hydroxyproline-Rich Glycoproteins as Markers of Temperature Stress in the Leaves of *Brachypodium distachyon*

Artur Pinski [1], Alexander Betekhtin [1,*], Katarzyna Sala [2], Kamila Godel-Jedrychowska [2], Ewa Kurczynska [2,*] and Robert Hasterok [1]

[1] Department of Plant Anatomy and Cytology, Faculty of Biology and Environmental Protection, University of Silesia in Katowice, 40-032 Katowice, Poland; apinski@us.edu.pl (A.P.); robert.hasterok@us.edu.pl (R.H.)
[2] Department of Cell Biology, Faculty of Biology and Environmental Protection, University of Silesia in Katowice, 40-032 Katowice, Poland; katarzyna.sala@us.edu.pl (K.S.); kgodel@us.edu.pl (K.G.-J.)
* Correspondence: alexander.betekhtin@us.edu.pl (A.B.); ewa.kurczynska@us.edu.pl (E.K.); Tel.: +48-32-2009-484 (A.B.); +48-32-2009-447 (E.K.)

Received: 7 May 2019; Accepted: 23 May 2019; Published: 25 May 2019

Abstract: Plants frequently encounter diverse abiotic stresses, one of which is environmental thermal stress. To cope with these stresses, plants have developed a range of mechanisms, including altering the cell wall architecture, which is facilitated by the arabinogalactan proteins (AGP) and extensins (EXT). In order to characterise the localisation of the epitopes of the AGP and EXT, which are induced by the stress connected with a low (4 °C) or a high (40 °C) temperature, in the leaves of *Brachypodium distachyon*, we performed immunohistochemical analyses using the antibodies that bind to selected AGP (JIM8, JIM13, JIM16, LM2 and MAC207), pectin/AGP (LM6) as well as EXT (JIM11, JIM12 and JIM20). The analyses of the epitopes of the AGP indicated their presence in the phloem and in the inner bundle sheath (JIM8, JIM13, JIM16 and LM2). The JIM16 epitope was less abundant in the leaves from the low or high temperature compared to the control leaves. The LM2 epitope was more abundant in the leaves that had been subjected to the high temperatures. In the case of JIM13 and MAC207, no changes were observed at the different temperatures. The epitopes of the EXT were primarily observed in the mesophyll and xylem cells of the major vascular bundle (JIM11, JIM12 and JIM20) and no correlation was observed between the presence of the epitopes and the temperature stress. We also analysed changes in the level of transcript accumulation of some of the genes encoding EXT, EXT-like receptor kinases and AGP in the response to the temperature stress. In both cases, although we observed the upregulation of the genes encoding AGP in stressed plants, the changes were more pronounced at the high temperature. Similar changes were observed in the expression profiles of the EXT and EXT-like receptor kinase genes. Our findings may be relevant for genetic engineering of plants with increased resistance to the temperature stress.

Keywords: arabinogalactan proteins; *Brachypodium distachyon*; cell wall; extensins; immunohistochemistry; leaf; RT-qPCR; temperature stress

1. Introduction

Plant growth and productivity are compromised by various abiotic stresses, among which are high and low temperature stress. Even short periods of temperature stress may significantly decrease the yield, especially when it occurs during the crucial stages of plant development [1]. As was predicted,

heat waves and other extreme temperature events are to become more intense, frequent and long-lasting because of global climate change [2]. Thus, thermal stresses must be better understood in the context of the response and adaptation of plants, which may enable crops with improved thermotolerance to be obtained and bred [3].

Brachypodium distachyon L. Beauv. (Brachypodium), which is a member of the Pooideae subfamily, is a wild annual grass species that is widespread in the regions of the Mediterranean basin, Western Europe, the Middle East, south-west Asia, north-east Africa, North and South America and Australia. It is closely related to many temperate zone key cereals, including wheat, barley, rye, oats and various forage grasses [4]. Due to its numerous favourable biological features such as a relatively small nuclear genome that ranges from 270 Mb to 350 Mb (depending on the methodology that is used), small stature, self-fertility, a life cycle of less than four months and undemanding growth requirements, *B. distachyon* constitutes an excellent model species [5].

Low-temperature stress results in the downregulation of many photosynthesis-related proteins and, at the same time, the upregulation of the proteins that are involved in reactive oxygen species (ROS) scavenging, redox adjustment, cytoskeletal rearrangements, cryoprotection and cell wall remodelling [6]. Similar results are observed in plants that are stressed by a high temperature [7]. Though the cell wall structure is not primarily altered under heat stress, numerous studies have indicated various changes in its architecture. In low temperature stress, changes in the cell wall rigidity may be an important factor in thermotolerance. Changes in the cell wall are more pronounced in roots because they are more sensitive to temperature stresses than the aerial parts of a plant, though the adverse effect of such stress on leaves directly affects plant productivity. Alterations in the cell wall in response to temperature stress concern cellulose and hemicelluloses biosynthesis, pectin modifications by pectin methylesterases, lignin biosynthesis and changes in the abundance of hydroxyproline-rich glycoproteins (HRGP) [8].

HRGP are usually divided into three complex multigene families: (i) arabinogalactan proteins (AGP); (ii) extensins (EXT); and (iii) proline-rich proteins [9]. AGP are further divided into four sub-families according to their polypeptide core: classical AGP, lysine-rich AGP (Lys-rich AGP), arabinogalactan peptides (AG peptides) and fasciclin-like AGP (FLA) [10]. Typically, AGP are strongly O-glycosylated and most of them have glycosylphosphatidylinositol (GPI) anchors that attach the proteins to the plasma membrane, though some of them can be released into the wall matrix *via* GPI cleavage [11]. In connection with their abundance, ubiquitous presence and localisation, AGP play a crucial role in various biological processes such as cell division, cellular communication, programmed cell death, organ abscission, plant-microbe interactions, plant defence and growth as well as in the reproductive processes [12–14]. A decrease in the amount of AGP has also been linked with the loss of embryogenic potential in callus cultures of *B. distachyon* [15]. Despite many studies on the role of AGP in plant development, our understanding of their role in the reaction of the plant to temperature stress is still quite limited. Recent studies have shown that temperature stress strongly affects the distribution and content of AGP in the stigma and ovule of *Solanum lycopersicum* as well as in banana leaves and roots, which may indicate that AGP are differentially regulated in the response to temperature stress and that their expression and distribution is tissue specific [16–18].

Based on a bioinformatic analysis, EXT were divided into seven classes: classical, short, leucine-rich repeat extensins (LRX), proline-rich extensin-like receptor kinases (PERK), formin-homolog EXT (FH EXT), chimeric and long chimeric EXT. EXT are characterised by the presence of serine, which is followed by three to five proline residues. These prolines are hydroxylated and glycosylated [19]. EXT are known to play important roles in the response to wounding and pathogen infections [20]. This family was also indicated as playing an important role in root-microbe interactions [14,21]. A study on a *B. distachyon* callus showed that one of the chimeric EXT could be considered to be a good marker for embryogenic cells [15]. A chimeric leucine-rich repeat/extensin, LRX1, was shown to be required for root hair morphogenesis in *Arabidopsis thaliana* [22]. However, information on the synthesis and location of extensins in response to temperature stress is scarce.

Thus, the aim of this work was to investigate any changes in the distribution of the epitopes of AGP and EXT in *B. distachyon* leaves through an immunostaining analysis. This approach enabled the distribution of these epitopes and the changes in their leaves that had been stressed by a high or low temperature to be determined. We also determined the level of transcript accumulation of selected genes encoding EXT, EXT-like receptor kinases, and FLA in the leaves of *B. distachyon* that had been stressed by a high or low temperature using RT-qPCR.

2. Results

2.1. Distribution of the Epitopes of AGP and EXT in Leaves in Response to Temperature Stress

The distribution of the epitopes of AGP (JIM8, JIM13, JIM16, LM2 and MAC207), pectin/AGP (LM6) and EXT (JIM11, JIM12 and JIM20) in the leaves of *B. distachyon* under normal (21 °C) and thermal stress conditions (4 and 40 °C) was determined. Considering the phenotype, we observed no visible changes induced by the thermal stress. The general anatomy of a *B. distachyon* leaf is shown in Figure 1. In order to present the results clearly, only the antibodies for which changes in their localisation or the intensity of the fluorescence signal in different temperature conditions were observed, are presented in the main text. Figures A1–A5 show the localisation of the remaining epitopes, in which no changes were identified in their response to temperature treatment.

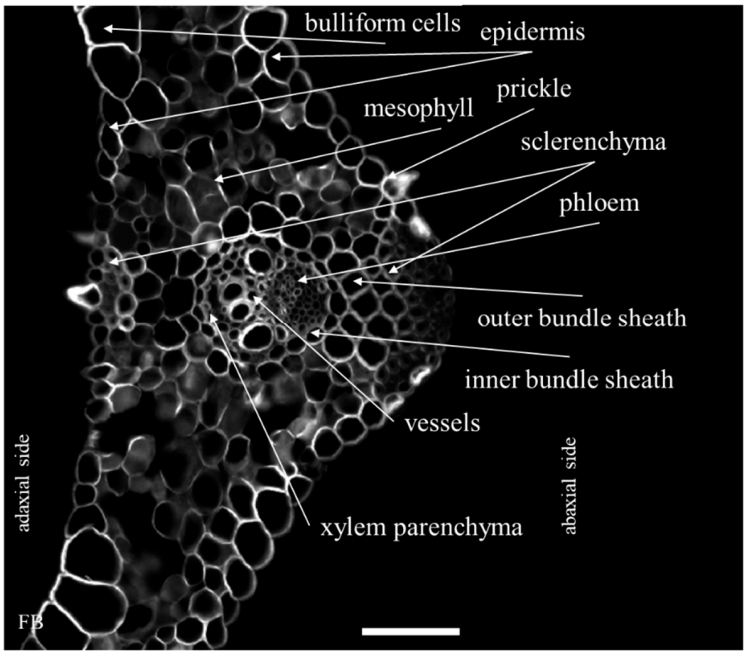

Figure 1. A cross-section of a *B. distachyon* leaf through the major vascular bundle (nomenclature according to Botha [23]) that had been stained with a fluorescent brightener (FB). Scale bar: 50 µm.

The occurrence of the epitopes of AGP was mostly associated with the vascular bundle. The JIM8 epitope was present in the walls and cellular compartments of the inner bundle sheath cells and phloem (Figure 2D–F). This epitope also occurred in the sclerenchyma fibres that were located next to the vascular bundle (Figure A1A–C) or were developing at the edge of the leaf blade (Figure A1D–F). The presence and spatial distribution of the JIM8 epitope were diverse at different temperatures. The JIM8 epitope was less represented in the leaves that were growing at a low temperature (Figure 2A–C). However, in the leaves that had been subjected to a temperature of 40 °C, an increase in the intensity of fluorescence signal was observed in the walls of phloem cells compared to the leaves that were growing at a low temperature (Figure 2G–I). JIM13 was found at the same locations as the JIM8 epitope (Figure A2A–F) and was additionally detected in the intercellular compartments (under intercellular compartments we

define the localisation of epitope within the cytoplasm endomembrane system or organelles that are associated with the biosynthesis and secretion pathway to the wall, however these are not visible on the light microscope level [24]) of the prickles (Figure A2G–I). There were no changes in the distribution of the JIM13 epitope or in the intensity of the fluorescence signal between the analysed temperatures. The JIM16 epitope in the control leaves was present in a low amount in the intercellular compartments of the inner and outer bundle sheath cells and phloem as well as in the xylem parenchyma (Figure 3D–F). This epitope was not detected in the xylem parenchyma in the leaves that were growing at 40 °C (Figure 3G–I) and in the leaves from 4 °C, the presence of this epitope was not detected (apart from single dots in the vascular bundle cells; Figure 3A–C). Another AGP epitope, LM2, occurred in the cellular compartments of bundle sheath, phloem and xylem parenchyma in the control leaves (Figure 4D–F). At a low temperature (4 °C), the occurrence of this epitope was very low (Figure 4A–C), while in the leaves that were growing at a high temperature, it was more abundant (Figure 4G–I) compared to the control plants (Figure 4D–F). Additionally, LM2, was detected in the intercellular compartments and/or walls of the epidermis and bulliform cells in the leaves from plants that had been subjected to a high temperature (Figure 5A–I). A signal in the mesophyll cells was detected only in the leaves that were growing at 40 °C (Figure 5G–I). The MAC207 epitope was present in large amounts in the intercellular compartments and/or walls of the phloem cells, mesophyll cells and bulliform cells (Figure A3A–F). At all of the temperatures, its fluorescence had a similar cellular distribution and intensity. The LM6 epitope was detected abundantly in the phloem, xylem parenchyma and, in lower amounts, in the cellular compartments and/or walls of the outer bundle sheath (Figure 6D–F). The fluorescence signal of this epitope in the leaves that were growing at 40 °C was more intense compared to the other temperature treatments (Figure 6G–I vs. Figure 6A–F). Outside the vascular bundle, LM6 was present in the cell walls and/or in the intercellular compartments of the mesophyll cells (Figure A4A–C).

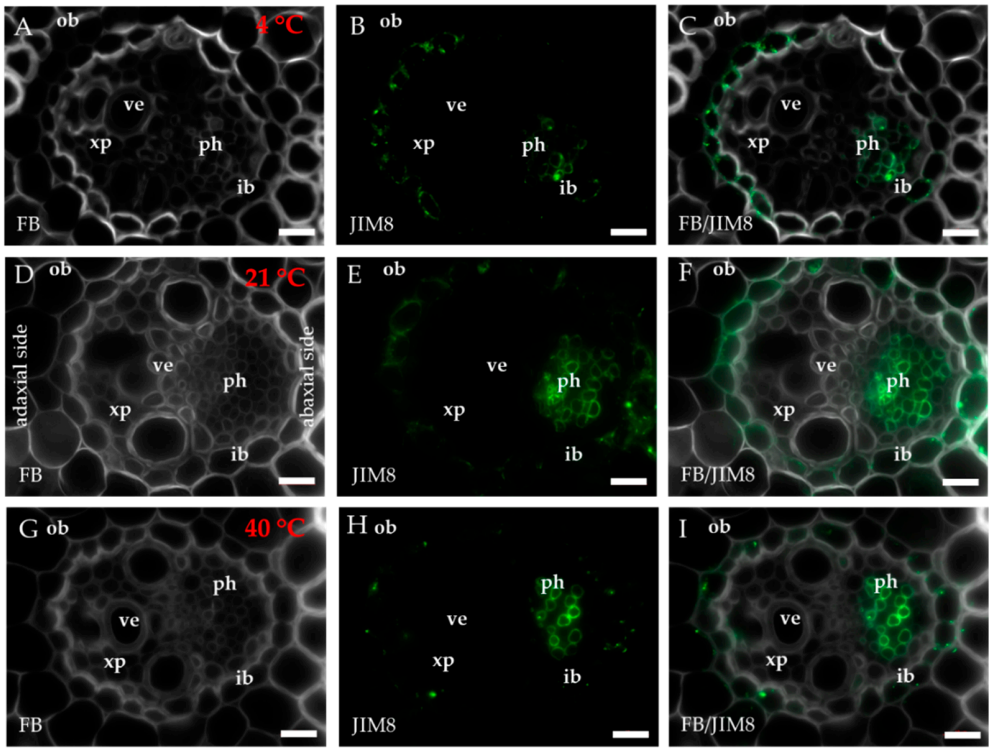

Figure 2. Immunolocalisation of the JIM8 epitope (**A**–**I**) in cross-sections of the *B. distachyon* leaves, (**A**–**I**): through the major vascular bundle. (**A**–**C**): 4 °C; (**D**–**F**): 21 °C; (**G**–**I**): 40 °C. Abbreviations: FB—fluorescent brightener, ib—inner bundle sheath, ob—outer bundle sheath, ph—phloem, ve—vessels, xp—xylem parenchyma. The green colour shows epitope occurrence. Scale bars: 10 µm.

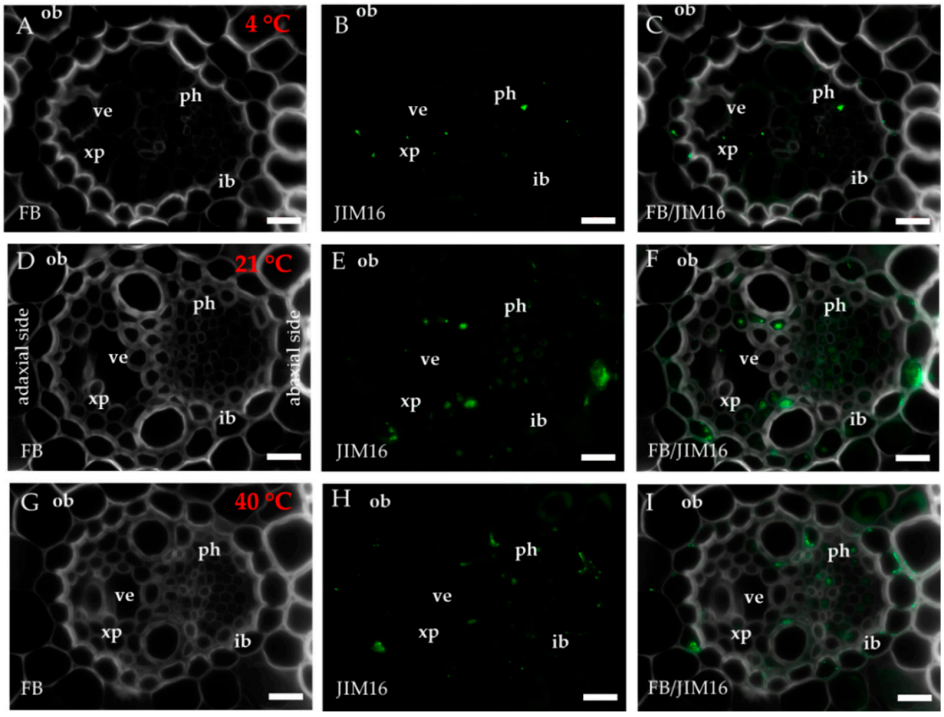

Figure 3. Immunolocalisation of the JIM16 epitope (**A**–**I**) in cross-sections of the *B. distachyon* leaves, (A-I): through the major vascular bundle. (**A**–**C**): 4 °C; (**D**–**F**): 21 °C; (**G**–**I**): 40 °C. Abbreviations: FB—fluorescent brightener, ib—inner bundle sheath, ob—outer bundle sheath, ph—phloem, ve—vessels, xp—xylem parenchyma. The green colour shows epitope occurrence. Scale bars: 10 µm.

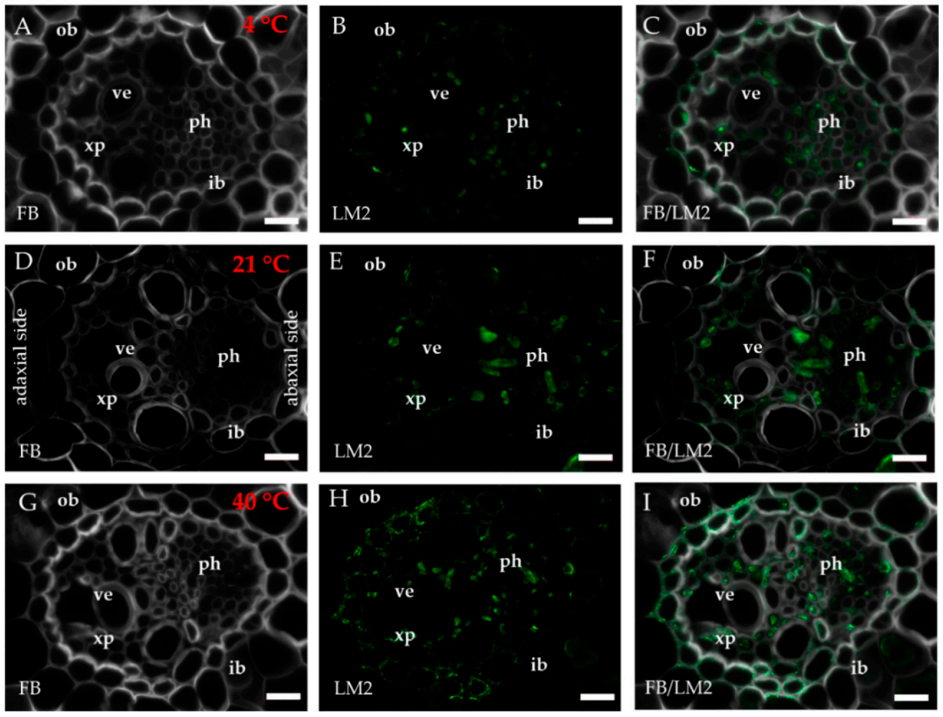

Figure 4. Immunolocalisation of the LM2 epitope (**A**–**I**) in cross-sections of the *B. distachyon* leaves, (**A**–**I**): through the major vascular bundle. (**A**–**C**): 4 °C; (**D**–**F**): 21 °C; (**G**–**I**): 40 °C. Abbreviations: FB—fluorescent brightener, ib—inner bundle sheath, ob—outer bundle sheath, ph—phloem, ve—vessels, xp—xylem parenchyma. The green colour shows epitope occurrence. Scale bars: 10 µm.

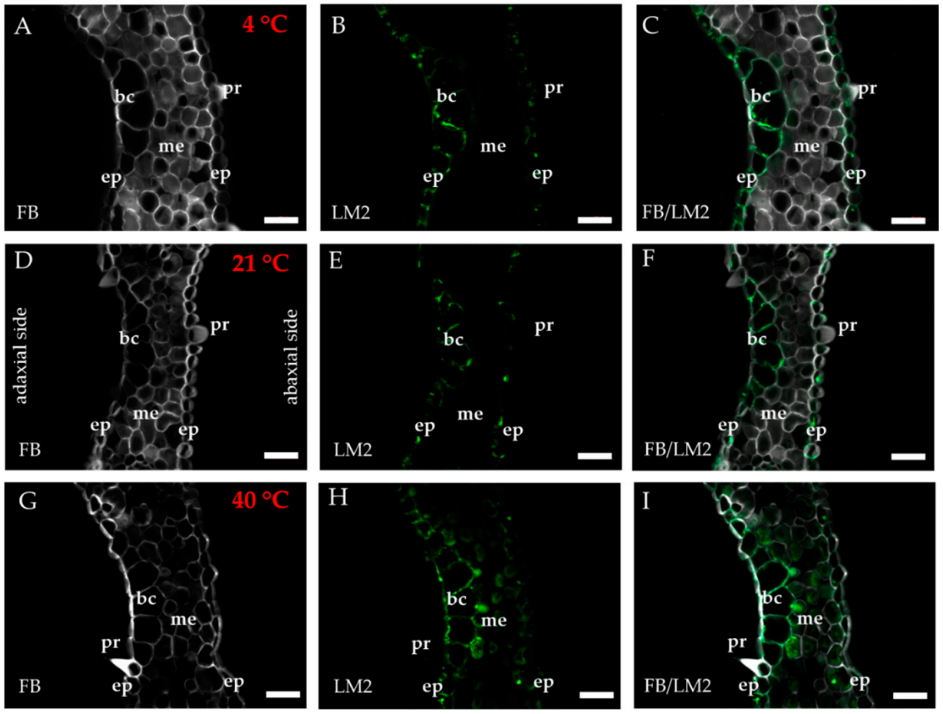

Figure 5. Immunolocalisation of the LM2 epitope (**A**–**I**) in cross-sections of the *B. distachyon* leaves, (**A**–**I**): through the mesophyll and bulliform cells. (**A**–**C**): 4 °C; (**D**–**F**): 21 °C; (**G**–**I**): 40 °C. Abbreviations: bc—bulliform cells, ep—epidermis, FB—fluorescent brightener, me—mesophyll, pr—prickle. The green colour shows epitope occurrence. Scale bars: 20 μm.

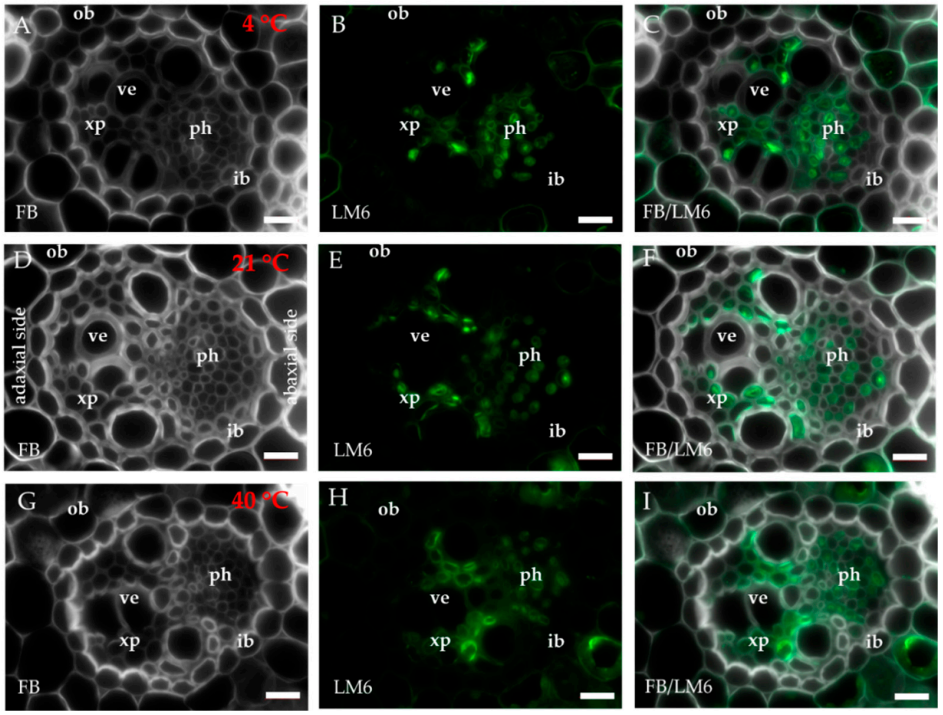

Figure 6. Immunolocalisation of the LM6 epitope (**A**–**I**) in cross-sections of the *B. distachyon* leaves, (**A**–**I**): through the major vascular bundle. (**A**–**C**): 4 °C; (**D**–**F**): 21 °C; (**G**–**I**): 40 °C. Abbreviations: FB—fluorescent brightener, ib—inner bundle sheath, ob—outer bundle sheath, ph—phloem, ve—vessels, xp—xylem parenchyma. The green colour shows epitope occurrence. Scale bars: 10 μm.

All three extensin epitopes that are recognised by the JIM11, JIM12 and JIM20 antibodies were mostly associated with the mesophyll cells. The JIM11 epitope was present only in the mesophyll cell walls (Figure A5A–C). In addition to occurring in the mesophyll cell walls (Figure A5D–F), JIM12 was also found in the walls of some of the outer bundle sheath cells and vessels (Figure A5G–I). The occurrence of the JIM20 epitope was similar to JIM12 (Figure A5J–O), but had an additional location in the walls and/or cellular compartments of the phloem (Figure A5M–O). All three extensin epitopes occurred abundantly and there were no differences in their distribution or in the intensity of the fluorescence signal among the temperatures that were analysed.

2.2. Analysis of the Level of Transcript Accumulation of the Genes Encoding the FLA, EXT and EXT-Like Receptor Kinases

In this study, we determined the level of transcript accumulation of five different genes encoding *FLA* (*Bradi4g34420*, *Bradi2g00220*, *Bradi5g18950*, *Bradi3g39740* and *Bradi2g60270*). The transcript accumulation levels of *Bradi4g34420* and *Bradi2g00220* increased in both temperatures, 4 and 40 °C, compared to the control conditions (Figure 7A). The increase in expression of the *Bradi4g34420* gene at 40 °C (4.7-fold) was higher than at 4 °C (1.9-fold) (Figure 7A). In the case of the *Bradi5g18950* gene, the expression at 4 °C was approximately the same as in the control, while its expression at 40 °C was 6-fold higher (Figure 7A). A similar pattern of expression was found for the *Bradi3g39740* gene, though there was only a slight (1.7-fold) increase in its expression at 4 °C (Figure 7B). Interestingly, there was a dramatic increase (28-fold) in the expression of this gene at 40 °C. Notably, the expression of the *Bradi2g60270* gene was only detectable in the leaves at 40 °C. Generally, temperature stress resulted in a higher level of transcript accumulation of *FLA*, though the increase was more pronounced at 40 °C.

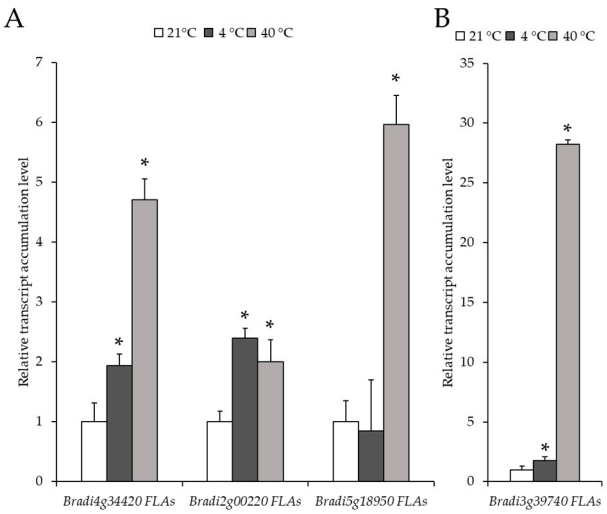

Figure 7. Relative level of transcript accumulation of the fasciclin-like AGP (*FLA)* genes: (**A**) *Bradi4g34420*, *Bradi2g00220* and *Bradi5g18950* and (**B**) *Bradi3g39740*. The relative expression levels were normalised to an internal control (*Bradi1g32860*, gene encoding ubiquitin) and calibrated to the control. Asterisks indicate significant differences from the control using the Student's t-test ($p < 0.05$; mean ± SD, $n = 3$).

The level of transcript accumulation of nine different genes encoding EXT and EXT-like receptor kinases were also determined. Each gene was assigned to a group based on its structure: *FH EXT* (*Bradi1g22980*, *Bradi3g59780* and *Bradi4g03720*), *chimeric EXT* (*Bradi4g11250* and *Bradi3g12902*) and *PERK EXT* (*Bradi2g00900*, *Bradi2g49240*, *Bradi1g07010* and *Bradi3g31967*). The level of transcript accumulation of the *Bradi1g22980* gene in the treated plants was not statistically different from the control (Figure 8A). The level of transcript accumulation of two other *FH EXT*, *Bradi3g59780* and *Bradi4g03720* was only statistically higher at 40 °C (Figure 8A). Conversely, the level of transcript accumulation of the *chimeric*

EXT, *Bradi4g11250*, increased significantly at 4 °C, though there was no clear difference in its expression for the *Bradi3g12902* gene (Figure 8B). When considering *PERK*, a higher transcript accumulation of the *Bradi2g00900* gene at 4 °C and a higher level of transcript accumulation of the *Bradi2g49240* gene at 4 °C and 40 °C was determined (Figure 8C). Intriguingly, the expression of the other *PERK* gene, *Bradi3g31967*, was only observed in the temperature-stressed samples (Figure 8D). The distribution of all of the epitopes together with changes in the level of transcript accumulation of the analysed genes are summarised in Figure 9.

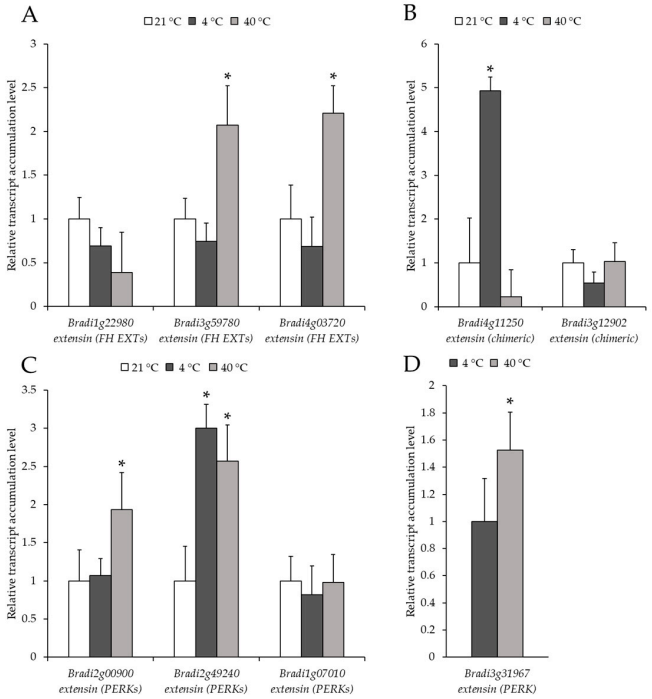

Figure 8. Relative level of transcript accumulation of the extensins (EXT) genes: (**A**) formin-homolog (FH) EXT: *Bradi1g22980*, *Bradi3g59780*, *Bradi4g03720*, (**B**) chimeric EXT: *Bradi4g11250*, *Bradi3g12902*, (**C**) proline-rich extensin-like receptor kinase (PERK): *Bradi2g00900*, *Bradi2g49240*, *Bradi1g07010* and (**D**) *Bradi3g31967*. The relative expression levels were normalised to an internal control (*Bradi1g32860*, gene encoding ubiquitin) and calibrated to the control. Asterisks indicate significant differences from the control using the Student's t-test ($p < 0.05$; mean ± SD, $n = 3$).

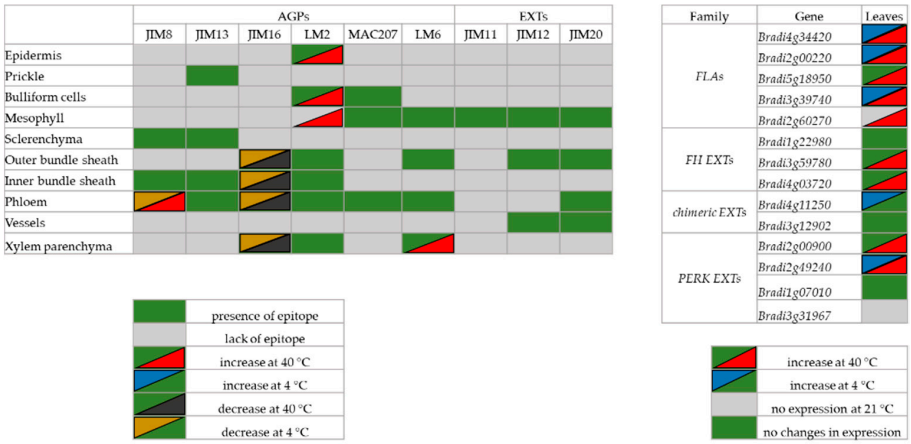

Figure 9. Consolidated results of the distribution of the epitopes EXT and AGP in the leaves of *B. distachyon* and changes in the level of transcript accumulation of the analysed genes.

3. Discussion

Although immunohistochemical analyses are widely used to study changes in the chemical components of the cell wall during different developmental processes, in vivo and in vitro information concerning the presence and distribution of the cell wall proteins in leaves that have been subjected to biotic and/or abiotic stresses are scarce and remain largely unexplored [16,18,25]. Previous studies have primarily focused on the differential expression of AGP in response to temperatures stresses in roots and seedlings; however, the involvement of AGP in the response to temperature stress has rarely been studied in leaves [16]. For example, the transient appearance of two AGP proteins in *Triticum aestivum* in response to a low temperature were observed, thus indicating their involvement in the activation of the plant cell defence [16,26]. In transgenic *A. thaliana* plants, non-classical AGP improved the freezing tolerance of seedlings [27]. Temperature stress is one of the factors that limit plant growth and productivity [2,28]. Therefore, data showing changes in the distribution of individual cell wall components, particularly AGP, in connection with temperature stress, are particularly important as the results can be used in genetic engineering for stress tolerance [29].

In the present study, while the distribution of the epitopes of the analysed AGP and EXT was primarily observed in the major vascular bundles (nomenclature according to Botha [23]) and sclerenchyma cells, in the case of the LM2 and MAC207 epitopes, they were present in the mesophyll and epidermal cells, especially in the bulliform cells. Generally, the results for *B. distachyon* presented here are similar to those that have been described for banana leaves in terms of the distribution of epitopes in leaf tissues [18]. In banana, the JIM8 epitope increased in abundance at lower temperatures, thus indicating its role in the tolerance to strong chilling stress [18]. In the pistils of *Solanum lycopersicum* cv Micro-Tom, a high temperature strongly affected the distribution of the JIM8 epitope, which decreased in the stigma and ovule [17]. These varied results with respect to this and other epitopes mean that further intensive studies are necessary. Moreover, such results may indicate that the changes in the chemical composition of the cell walls in response to temperature stress are species-specific. In banana leaves, the presence of the JIM16 epitope was higher in a tolerant cultivar at low temperature stress, thus suggesting that these epitopes may be involved in determining the tolerance of banana to temperature stress [18]. Among the analysed epitopes, the LM2 epitope was detected in most of the leaf tissues and an increase of the LM2 epitope as a response to high temperature stress was observed. A similar distribution was detected in banana leaves, in which this epitope was found in the phloem, bundle sheath, mesophyll and epidermal cells. Low temperature treatment increased the abundance of this epitope in banana [18]. In the leaves of *Tilia x euchlora*, the LM2 epitope was present in the epidermis, hypodermis and parenchyma cells, although as a response to salt stress [25]. Such results may indicate that this wall epitope may be a marker of the plant response to diverse stresses. The abundant presence of the LM6 antibody in *B. distachyon* leaves was found. As LM6 antibody exhibits a high affinity to the (1-5)-α-L-arabinosyl residues, it detects the (1-5)-α-L-arabinan (a pectin rhamnogalacturonan I side chain), however, it can also bind to some AGP (http://www.plantprobes.net/index.php). Thus, the increase in the fluorescence signal in the xylem parenchyma of the temperature-stressed plants may not necessarily indicate changes in the presence of AGP. The function of the arabinan side chains is not well understood and their roles are postulated to be an involvement in the rehydration of the cell wall and flexibility [30–33]. The more abundant presence of the wall components that are recognised by LM6 antibody, especially in the cytoplasmic compartments, that were observed in our study indicate that leaves react to temperature stress by synthesising and depositing (1-5)-α-L-arabinans into the cell walls.

As has been shown in previous studies, analyses of the distribution and changes in the signal intensity of epitopes can be compared with the expression profiles of the genes encoding the proteins that are targeted by these antibodies [15,34]. In this work, we focused on the FLA that have been implicated in modulation of signalling upstream of cell wall polymer biosynthesis, remodelling, as well as in the stress response as one of the AGP sub-families [35–37]. We found an increase in the level of transcript accumulation of the *FLA* in response to temperature stress, which concurs with the

immunohistochemistry observations that have been made for the LM2 antibody. It is worth noting that the increase in the level of transcript accumulation of these genes was more pronounced at the high temperature. However, in wheat, four genes encoding *FLA* had a decreased level of transcript accumulation in response to low temperature stress [38]. Similarly, two other *FLA* genes (*OsFLA1* and *OsFLA4*) were downregulated by cold stress in rice [39]. This may reflect intrinsic differences between the analysed species or might be the result of fragmentariness of the conducted experiments, which only focus on a few of the numerous *FLA* genes that are present in a genome. The *Bradi5g18950* gene, which was analysed in our work, exhibited a higher level of transcript accumulation at the high temperature and it was previously shown to be upregulated in a 30-day-old callus that was characterised by an increased embryogenic potential. Conversely, the *Bradi3g39740* gene was linked with a gradual loss of embryogenic potential in *B. distachyon* [15]. Temperature stresses that are induced by low or high temperatures inhibit water uptake, which immediately leads to a slowing down of leaf growth. This observation was correlated with a loss of turgor in leaf cells and an adjustment of the osmoticum, which enables cells to regain turgor [40]. AGP are well known for their water-holding properties [41]. For example, in the resurrection plants, side chains of pectin are highly enriched in arabinose-rich polymers, including AGP. Their presence can prevent water loss during desiccation [8]. In *Coffea arabica* plants that had been subjected to heat stress, there were extensive changes in the cell wall of the leaves. The plants accumulated a higher content of arabinose and galactose, which may suggest that the response of coffee leaves to heat stress is related to type II arabinogalactans and pectins. Moreover, during heat stress, the palisade parenchyma cells were more separated and thinner relative to the control, which resulted in a decreased thickness of the leaves [42]. It has been hypothesised that the organs that are susceptible to water loss such as leaves increase the thickness of the cell walls, thereby limiting desiccation through the production of specific molecules such as AGP [16]. Our results seem to support this hypothesis.

Similar to the temperature stress, salt stress results in a decrease of available water due to a reduction in osmotic potential of the soil solution, which leads to a water deficit [8]. AGP have also been shown to play an important part in the salt stress response and an upregulation of *AGP* in salt-adapted tobacco BY-2 cell cultures was observed. It has been proposed that AGP act as a possible sodium carrier via vesicle trafficking from the apoplast to the vacuoles in salt-adapted tobacco BY-2 cells [43]. A significant upregulation of the *FLA* genes in the salt stress response was observed in the roots of *Populus trichocarpa* [44]. Moreover, AGP were found to act as pectin plasticisers [8,45]. As was shown for an *FLA sos5* (*salt-overly sensitive*) mutant of *A. thaliana*, it exhibits a root-swelling phenotype under salt stress [46]. Further studies showed that the SOS5 protein mediates adherence via its interaction with the cell wall pectin [47]. *At-FLA4* is one of the *FLA* genes in *A. thaliana* that encodes the predicted lipid-anchored glycoprotein and it was shown to positively regulate cell wall biosynthesis and root growth by modulating abscisic acid signalling. Moreover, an *At-fla4* mutant was found to be sensitive to the salt stress [37]. It has been suggested that *At-fla4* might interact with the pectin network via the covalent or non-covalent interactions of its glycans. *At-fla4* may mechanically link pectin with the *AtFei1* and *AtFei2* receptor kinases and the plasma membrane, thus contributing to some biophysical properties such as swelling and interpolymer connectivity [48]. As was indicated by another inactivated mutant of *A. thaliana*, the *FLA1* gene is involved in the early events of lateral root and shoot development in tissue cultures [49]. Considering the salt stress response, it is possible that the upregulation of *FLA* and the increased signal intensity of some of the epitopes of AGP during temperature stress may link with other cell wall polymers such as pectins and thus may modulate the signalling pathways. As has been shown by a number of studies on various species, the pectin content increases during cold stress. Conversely, it decreases during heat stress [8].

An immunohistochemical analysis of the distribution of the *EXT* using the JIM11, JIM12 and JIM20 antibodies showed the presence of all of these epitopes in the mesophyll and the JIM12 and JIM20 epitopes in the vessels. Although no immunohistochemical studies targeting the EXT using the JIM11, JIM12 and JIM20 antibodies were done in the leaves, the distribution of these epitopes has been

widely studied in the callus embryos and roots [20,50–53]. For example, changes in the signal intensity of the JIM11 and JIM12 antibodies were connected with a gradual loss of embryogenic potential in *B. distachyon* callus cultures [15]. Zhang, et al. [54] showed that the EXT that are recognised by the JIM20 antibody were present in the pollen tubes and transmitting tissue of *Nicotiana tabacum* and that the application of hydroxyproline synthesis inhibitor, 3,4-dehydro-L-proline, decreased pollen tube growth. However, studies dedicated to the role of EXT in abiotic stress and especially temperature stress are still scarce. In our study, while we did not observe any changes in the selected epitopes of the EXT in the mesophyll, outer bundle sheath, phloem or vessels at the level of the immunohistochemical analyses, we found an increase of *EXT* and *EXT-like receptor kinase* level of transcript accumulation in the response to temperature stresses, especially during the high temperature stress. This may be partially explained by the fact that we used only three antibodies that bind to the EXT, but it is possible that the application of other anti-EXT antibodies could reveal some changes. Additionally, the effectiveness of immunohistochemical analyses is limited, since it does not provide sufficient resolution and does not focus on individual genes, as is the case of RT-qPCR-based analyses. Changes in the *EXT* gene expression greatly depended on the class of extensins that were being analysed as was shown for *A. thaliana* plants that had been subjected to low temperature stress [55]. Another transcriptomic analysis of the *A. thaliana* response to cold stress showed the downregulation of one of the *PERK* genes [56]. In our experiment, we found that the *PERK extensin*, *Bradi3g31967*, was only expressed in the stressed leaves. The genes that belong to this class have been found in the apical dominance, floral organ defects and root cell elongation [57]. An increased accumulation level of the *PERK4* gene transcript in *A. thaliana* was observed in response to abscisic acid, which is a key regulator of abiotic stress tolerance in plants [58,59]. *PERK1* mRNA from *Brassica napus* was shown to be dramatically and rapidly accumulated in response to wounding and moderately accumulated in response to infection by the fungal pathogen *Sclerotinia sclerotiorum* [60]. Interestingly, the LRX proteins were found to regulate salt tolerance in *A. thaliana*. A triple mutant in the *LRX* genes exhibited a severe salt hypersensitivity and these genes were determined to be an important sensor of the cell wall integrity signals [61]. Moreover, recent studies have hinted at the role of EXT in the plant defence against phytopathogens as well as in interactions with beneficial microorganisms [14,21,62]. EXT have also been implicated in aluminium resistance and its accumulation in the cell walls of pea roots was observed [63]. The changes in the plant cell wall in response to temperature stress are diverse and not only include AGP and EXT, but also alterations in cellulose, hemicellulose, pectin and lignin biosynthesis [8]. Further investigations into the changes in cell wall proteomes could unravel the involvement of other proteins in the stress response because the proteome of the *B. distachyon* cell walls is complex and consists of at least 594 proteins [64–68].

4. Materials and Methods

4.1. Plant Material

The plants of the *B. distachyon* reference genotype Bd21 that were used is this experiment were cultivated in pots that had been filled with soil mixed with vermiculite at a ratio of 3:1 in a greenhouse. The seeds of *B. distachyon* genotype Bd21 (accession number: PI 254867) were sourced from the collection held by the United States Department of Agriculture—National Plant Germplasm System. The plants were grown in the greenhouse under a 16 h/8 h light/dark photoperiod at 21 ± 1 °C and were illuminated by lamps emitting white light at an intensity of 10 000 lx. For the low temperature stress, the plants were incubated at 4 °C for 24 h and for the high temperature stress, the plants were incubated at 40 °C for 24 h in growing chambers [69]. Plants at the fourth stage of principal growth according to the Hong, et al. [70] were used in this experiment. This stage is referred to as booting and is characterised by the emergence of the head at the top of the growing shoot. The flag leaf was harvested and used to isolate the RNA and to perform the RT-qPCR analysis. For the immunohistochemistry

analysis, the middle part of the leaf was collected because this permitted clear observations of the major vascular bundle, epidermis, bulliform cells, mesophyll and sclerenchyma.

4.2. Sample Preparation

To determine the chemistry of the cell wall, a set of monoclonal antibodies against the specific cell wall epitopes of the AGP (antibodies JIM8, JIM13, JIM16, LM2, MAC207), pectin/AGP (LM6) and EXT (JIM11, JIM12 and JIM20) (Plant Probes, Leeds, UK) were used. The references and information on the antibodies are shown in Table 1. The leaves were excised, fixed and embedded in Steedman's wax [20,71]. Transverse sections of the leaf blade (7 µm thick) were cut using a HYRAX M40 rotary microtome (Zeiss, Oberkochen, Germany) and collected on microscopic slides coated with poly-L-lysine (Menzel Gläser, Braunscheig, Germany).

4.3. Immunohistochemistry

The sections were de-waxed and rehydrated in an ethanol series (three times in 100, 90 and 50% ethanol in phosphate buffered saline PBS, *v*/*v*, each for 10 min) and PBS (10 min) [71]. The detailed procedure for immunochemical analysis and histological section observation was as previously described [20]. The slides were stained with 0.01% (*w*/*v*) fluorescent brightener 28 (FB) (Sigma-Aldrich, St. Louis, MO, USA) in PBS, which was used to visualise cell walls due to its affinity to cellulose. Two biological replicates were performed with at least eight sections for each replicate.

4.4. RT-qPCR

In order to characterise the level of transcript accumulation of the selected genes, RT-qPCR was performed using a LightCycler® 480 SYBR Green I Master in a LightCycler® 480 Real-Time PCR System (Roche, Basel, Switzerland). The total RNA was isolated from the leaves of *B. distachyon*. The primers used in this research are shown in Table A1. The genes encoding extensins with their division into classes were as previously described [19]. The *FLA* genes were selected based on the annotation found in the Phytozome database (https://phytozome.jgi.doe.gov/pz/portal.html). The detailed procedure for RT-qPCR was as in Betekhtin, et al. [72]. Briefly, the isolated RNA were treated with the DNase (QIAGEN, Hilden, Germany), and subsequently used for first-strand cDNA generation. Samples were run in the LightCycler® 480 Real-Time PCR System (Roche, Basel, Switzerland). The PCR conditions were as follow: 5 min at 95 °C, 45 cycles of 10 s at 95 °C, 20 s at 60 °C and 10 s at 72 °C with signal acquisition. Ubiquitin was used as the reference gene and analysis was performed using the $2^{-\Delta\Delta CT}$ method. The significant differences between the samples and control were calculated using the Student's *t*-test.

Table 1. The antibodies that were used for the immunocytochemistry, the epitopes they recognise and the relevant references.

Antibody	Epitope	References
	AGP	
JIM8	Arabinogalactan	[73]
JIM13	(β)GlcA1->3(α)GalA1->2Rha	[74–76]
JIM16	AGP glycan	[74–76]
LM2	β-linked GlcA	[75,77]
MAC207	(β)GlcA1->3(α)GalA1->2Rha	[74,75,78,79]
	Pectin/AGP	
LM6	(1-5)-α-L-arabinosyl residues, can also bind to some AGP	[80,81]
	EXT	
JIM11	Extensin	[74,82]
JIM12	Extensin	[82]
JIM20	Extensin	[82]

5. Conclusions

In our work, we demonstrated changes in the abundance and diversified expression of the epitopes of the AGP genes encoding FLA, EXT and EXT-like receptor kinases in the leaves of *B. distachyon* in response to temperature stress.

The main findings are as follows:

1. An increase in the JIM8 signal in the walls of phloem cells at 40 °C and a decrease at 4 °C.
2. An increase in the abundance of the LM2 epitope in the leaves of plants that had been subjected to the high temperature.
3. A decrease in the JIM16 signal intensity at 4 and 40 °C.
4. The upregulation of some *FLA*, *EXT* and *EXT-like* receptor *kinases* genes in response to temperature stress (4 and 40 °C).
5. The expression of the *PERK EXT* gene *Bradi3g31967* only in the leaves under low and high temperature stress.

To summarise, our results extend the knowledge about the presence of these epitopes in connection with temperature stress in *B. distachyon*. A precise dissection of the functions of AGP and EXT in response to abiotic stresses and to temperature stress, among others, requires the use of specific mutants whose availability is still limited. However, recent developments in the site-directed mutagenesis techniques such as CRISPR/Cas9 should allow the selective targeting of these genes, which may be helpful to better understand their roles.

Author Contributions: Conceptualisation, A.P., A.B.; methodology, A.P., A.B., K.S., K.G.-J.; validation, A.P., K.S., A.B.; formal analysis, A.P., K.S., A.B.; investigation, A.P., K.S., A.B.; resources, R.H., E.K.; data curation, A.P., A.B., K.S.; writing—original draft preparation, A.P., A.B., K.S., E.K.; writing—review and editing, A.P., A.B., K.S., E.K., R.H.; visualisation, A.P.; supervision, A.B., R.H.; funding acquisition, R.H., E.K.

Funding: This research was funded by the National Science Centre Poland (grant DEC-2014/14/M/NZ2/00519).

Conflicts of Interest: The authors declare no conflict of interest.

Abbreviations

AG Peptides	Arabinogalactan peptides
AGP	Arabinogalactan proteins
EXT	Extensins
FH EXT	Formin-homolog EXT
FLA	Fasciclin-like AGP
GPI	Glycosylphosphatidylinositol
HRGP	Hydroxyproline-rich glycoproteins
LRX	Leucine-rich repeat extensins
Lys-rich AGP	Lysine-rich arabinogalactan proteins
PBS	Phosphate-buffered saline
PERK	Proline-rich extensin-like receptor kinases
ROS	Reactive oxygen species
RT-qPCR	Reverse transcription-quantitative polymerase chain reaction

Appendix A

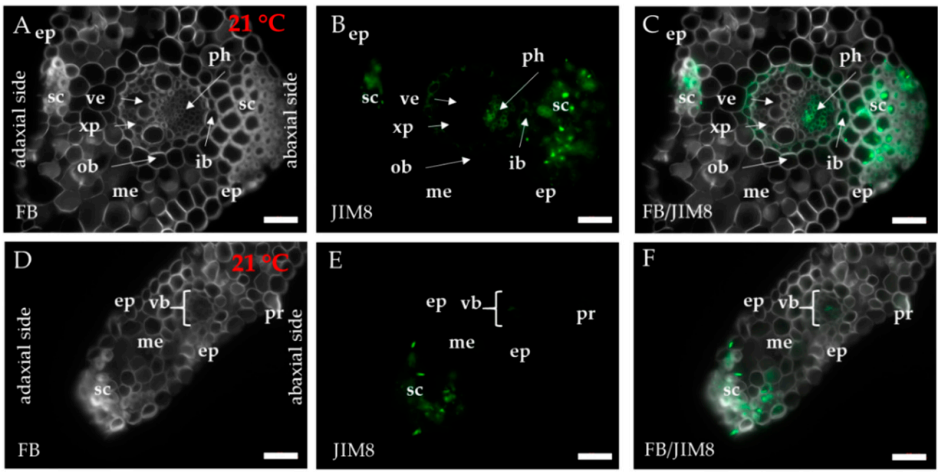

Figure A1. Immunolocalisation of the JIM8 epitope (**A**–**F**) in cross-sections of *B. distachyon* leaves (21 °C), (**A**–**C**): through the major vascular bundle; (**D**–**F**): through the edge of the leaf blade. The white arrows point to the respective parts of the leaf. Abbreviations: ep—epidermis, FB—fluorescent brightener, ib—inner bundle sheath, me—mesophyll, ob—outer bundle sheath, ph—phloem, pr—prickle, sc—sclerenchyma, vb—vascular bundle, ve—vessels, xp—xylem parenchyma. The green colour shows epitope occurrence. Scale bars: 20 μm.

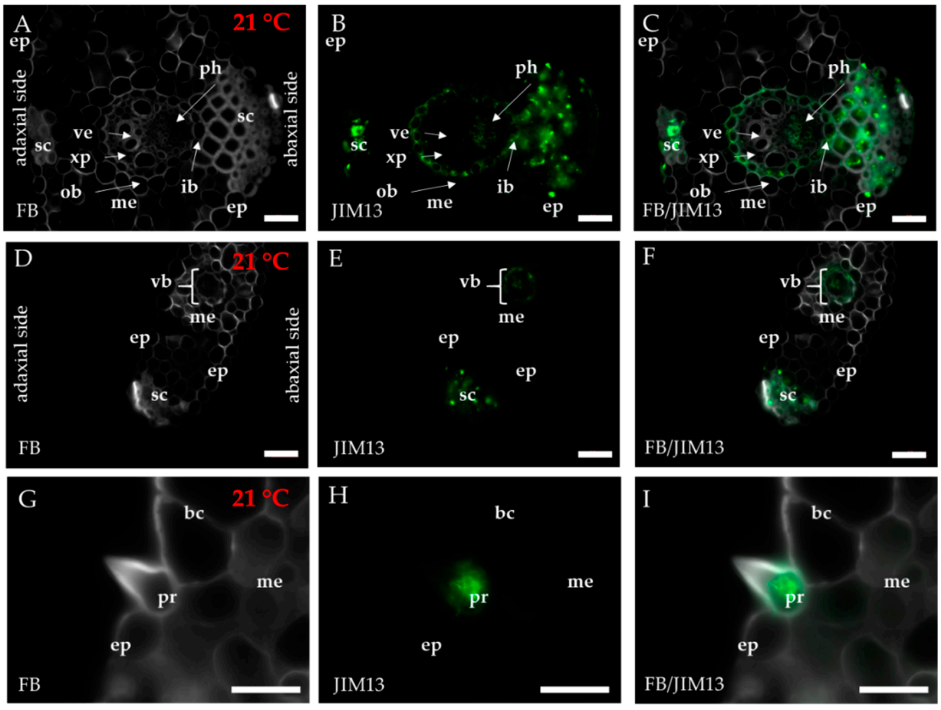

Figure A2. Immunolocalisation of the JIM13 epitope (**A**–**I**) in cross-sections of *B. distachyon* leaves (21 °C), (**A**–**C**): through the major vascular bundle; (**D**–**F**): through the edge of the leaf blade; (**G**–**I**): prickle. The white arrows point to the respective parts of the leaf. Abbreviations: bc—bulliform cells, ep—epidermis, FB—fluorescent brightener, ib—inner bundle sheath, me—mesophyll, ob—outer bundle sheath, ph—phloem, pr—prickle, sc—sclerenchyma, vb—vascular bundle, ve—vessels, xp—xylem parenchyma. The green colour shows epitope occurrence. Scale bars: 20 μm.

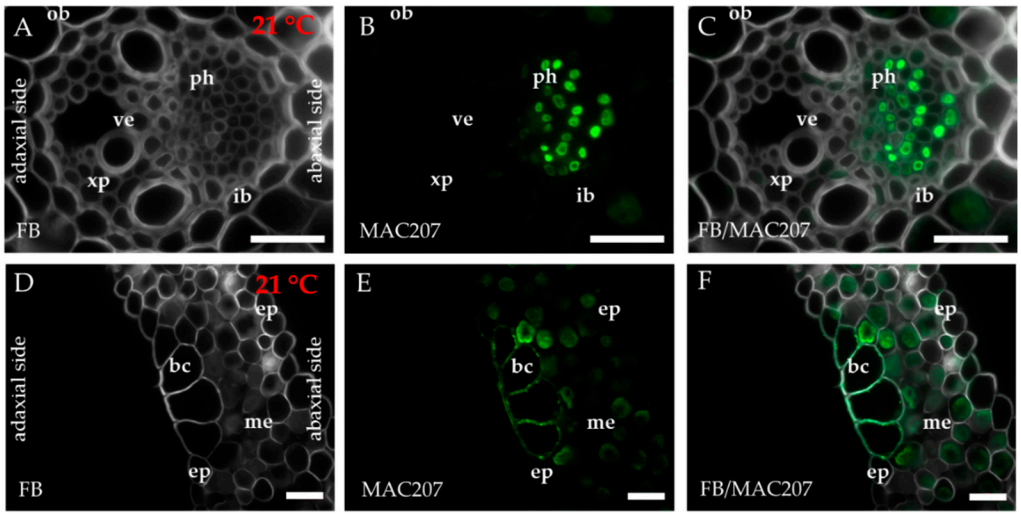

Figure A3. Immunolocalisation of the MAC207 epitope in cross-sections of *B. distachyon* leaves (21 °C), (**A**–**C**): through the major vascular bundle; (**D**–**F**): through the mesophyll and bulliform cells. Abbreviations: ep—epidermis, b—bulliform cells, FB—fluorescent brightener, ib—inner bundle sheath, me—mesophyll, ob—outer bundle sheath, ph—phloem, ve—vessels, xp—xylem parenchyma. The green colour shows epitope occurrence. Scale bars: 20 μm.

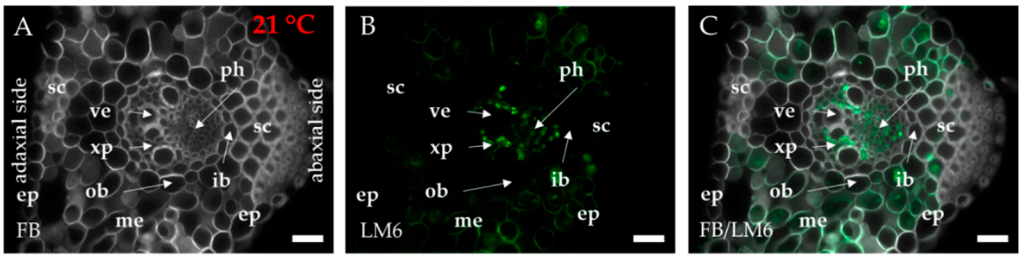

Figure A4. Immunolocalisation of the LM6 epitope (**A**–**C**) in cross-sections of *B. distachyon* leaves (21 °C), through the major vascular bundle. The white arrows point to the respective parts of the leaf. Abbreviations: ep—epidermis, FB—fluorescent brightener, ib—inner bundle sheath, me—mesophyll, o—outer bundle sheath, ph—phloem, sc—sclerenchyma ve—vessels, xp—xylem parenchyma. The green colour shows epitope occurrence. Scale bars: 20 μm.

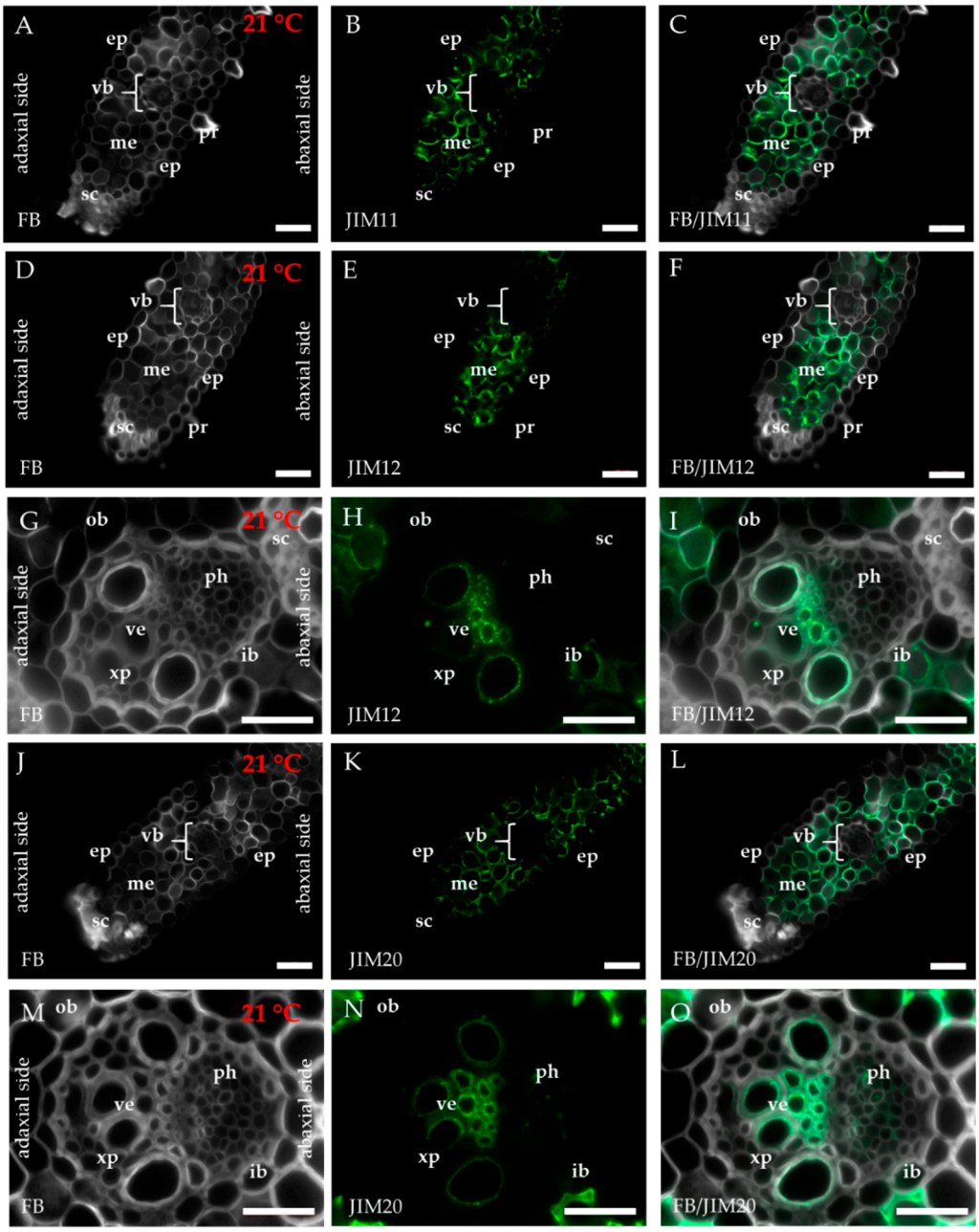

Figure A5. Immunolocalisation of the JIM11 (**A**–**I**), JIM12 (**D**–**I**) and JIM20 (**J**–**O**) epitopes in cross-sections of *B. distachyon* leaves (21 °C), (**A**–**F**,**J**–**L**): through the edge of the leaf blade; (**G**–**I**,**M**–**O**): through the major vascular bundle. Abbreviations: bc—bulliform cells, ep—epidermis, FB—fluorescent brightener, ib—inner bundle sheath, me—mesophyll, ob—outer bundle sheath, p— phloem, pr—prickle, sc—sclerenchyma, vb—vascular bundle, ve—vessels, xp—xylem parenchyma. The green colour shows epitope occurrence. Scale bars: 20 μm.

Table A1. The oligonucleotide primers that were used for the RT-qPCR reaction with relevant descriptions of the genes.

Genes	Description of the Genes	Primer Sequence (5′-3′)
Bradi1g32860	*ubiquitin*	pF-GAGGGTGGACTCCTTTTGGA pR-TCCACACTCCACTTGGTGCT
	***EXT* and *EXT*-like receptor kinase**	
Bradi4g11250	*extensin (chimeric EXT)*	pF-GCGACTGCGACAATGATGTG pR-ACCCCTTGCTAAGCCCTCTA
Bradi3g12902	*extensin (chimeric EXT)*	pF-CATCTGGACCTGCCAATGGT pR-TCCCAGTTTTGGAGTCTCGC
Bradi3g59780	*formin-homolog extensin (FH EXT)*	pF-GATGAATGCCGGAACAGCAC pR-GTGGAGAAGAGTGGTGCCTC
Bradi4g03720	*formin-homolog extensin (FH EXT)*	pF-GAAGCAGATTGAGGCCGAGA pR-CGCGCCTCCATCTTTTGATT
Bradi1g22980	*formin-homolog extensin (FH EXT)*	pF-CAGCAGAGCCTGTTGCTTGAC pR-TTCTAGGTTTCCGTGCATGAGT
Bradi2g49240	*proline-rich extensin-like receptor kinase (PERK)*	pF-TTCTCAGCCGTTGGGAGATG pR-GGAAGGTCCCCAAAGTCTCG
Bradi1g07010	*proline-rich extensin-like receptor kinase (PERK)*	pF-CCTCCACGGTAAAGGGCTG pR-GATCCGTGGATGGCAGTCTT
Bradi3g31967	*proline-rich extensin-like receptor kinase (PERK)*	pF-CCGTCGCCATTAAGAATCTGC pR-GATTCTTGTGCCGAACTCGC
Bradi2g00900	*proline-rich extensin-like receptor kinase (PERK)*	pF-TAACTTTGAGGCACAGGTTGCT pR-AGCCATGTATCCAAAAGTCCCC
	FLA	
Bradi2g00220	*fasciclin-like arabinogalactan protein*	pF-AGCTCAACAGCTCCCAGAC pR-CGAAAGCGAGTTGAGCGTG
Bradi5g18950	*fasciclin-like arabinogalactan protein*	pF-AATAAAGGGAAGTCACCGTCGC pR-CCGTTCTTCTTGTCATGGACCT
Bradi4g34420	*fasciclin-like arabinogalactan protein*	pF-CACATCCTCCAGATGCACGTC pR-CCGGACTCCTGGAACATGG
Bradi3g39740	*fasciclin-like arabinogalactan protein*	pF-GTACTATTCCCTGGCGGAGTTC pR-CCATGTTGTCGGTGAGGTTGAG
Bradi2g60270	*fasciclin-like arabinogalactan protein*	pF-AGCAGAGCAATCCTCTAGTAGC pR-TGGGTTCTTCTCGCCATTGTTA

References

1. Barlow, K.M.; Christy, B.P.; O'Leary, G.J.; Riffkin, P.A.; Nuttall, J.G. Simulating the impact of extreme heat and frost events on wheat crop production: A review. *Field Crops Res.* **2015**, *171*, 109–119. [CrossRef]
2. Hatfield, J.L.; Prueger, J.H. Temperature extremes: Effect on plant growth and development. *Weather Clim. Extrem.* **2015**, *10*, 4–10. [CrossRef]
3. Ohama, N.; Sato, H.; Shinozaki, K.; Yamaguchi-Shinozaki, K. Transcriptional regulatory network of plant heat stress response. *Trends Plant Sci.* **2017**, *22*, 53–65. [CrossRef]
4. Garvin, D.F.; Gu, Y.Q.; Hasterok, R.; Hazen, S.P.; Jenkins, G.; Mockler, T.C.; Mur, L.A.J.; Vogel, J.P. Development of genetic and genomic research resources for *Brachypodium distachyon*, a new model system for grass crop research. *Crop Sci.* **2008**, *48*, S-69. [CrossRef]
5. International Brachypodium Initiative. Genome sequencing and analysis of the model grass *Brachypodium distachyon*. *Nature* **2010**, *463*, 763–768. [CrossRef] [PubMed]

6. Janmohammadi, M.; Zolla, L.; Rinalducci, S. Low temperature tolerance in plants: Changes at the protein level. *Phytochemistry* **2015**, *117*, 76–89. [CrossRef]
7. Bita, C.E.; Gerats, T. Plant tolerance to high temperature in a changing environment: Scientific fundamentals and production of heat stress-tolerant crops. *Front. Plant Sci.* **2013**, *4*, 273. [CrossRef]
8. Le Gall, H.; Philippe, F.; Domon, J.M.; Gillet, F.; Pelloux, J.; Rayon, C. Cell wall metabolism in response to abiotic stress. *Plants* **2015**, *4*, 112–166. [CrossRef] [PubMed]
9. Johnson, K.L.; Cassin, A.M.; Lonsdale, A.; Bacic, A.; Doblin, M.S.; Schultz, C.J. Pipeline to identify hydroxyproline-rich glycoproteins. *Plant Physiol.* **2017**, *174*, 886–903. [CrossRef] [PubMed]
10. Pereira, A.M.; Pereira, L.G.; Coimbra, S. Arabinogalactan proteins: Rising attention from plant biologists. *Plant Reprod.* **2015**, *28*, 1–15. [CrossRef] [PubMed]
11. Showalter, A.M.; Basu, D. Extensin and arabinogalactan-protein biosynthesis: Glycosyltransferases, research challenges, and biosensors. *Front. Plant Sci.* **2016**, *7*, 814. [CrossRef] [PubMed]
12. Su, S.; Higashiyama, T. Arabinogalactan proteins and their sugar chains: Functions in plant reproduction, research methods, and biosynthesis. *Plant Reprod.* **2018**, *31*, 67–75. [CrossRef]
13. Baetz, U.; Martinoia, E. Root exudates: The hidden part of plant defense. *Trends Plant Sci.* **2014**, *19*, 90–98. [CrossRef] [PubMed]
14. Pinski, A.; Betekhtin, A.; Hupert-Kocurek, K.; Mur, L.A.J.; Hasterok, R. Defining the genetic basis of plant–endophytic bacteria interactions. *Int. J. Mol. Sci.* **2019**, *20*, 1947. [CrossRef] [PubMed]
15. Betekhtin, A.; Rojek, M.; Nowak, K.; Pinski, A.; Milewska-Hendel, A.; Kurczynska, E.; Doonan, J.H.; Hasterok, R. Cell wall epitopes and endoploidy as reporters of embryogenic potential in *Brachypodium distachyon* callus culture. *Int. J. Mol. Sci.* **2018**, *19*, 3811. [CrossRef] [PubMed]
16. Mareri, L.; Romi, M.; Cai, G. Arabinogalactan proteins: Actors or spectators during abiotic and biotic stress in plants? *Plant Biosyst.* **2018**, *153*, 173–185. [CrossRef]
17. Mareri, L.; Faleri, C.; Romi, M.; Mariani, C.; Cresti, M.; Cai, G. Heat stress affects the distribution of JIM8-labelled arabinogalactan proteins in pistils of *Solanum lycopersicum* cv Micro-Tom. *Acta Physiol. Plant* **2016**, *38*, 184. [CrossRef]
18. Yan, Y.; Takac, T.; Li, X.; Chen, H.; Wang, Y.; Xu, E.; Xie, L.; Su, Z.; Samaj, J.; Xu, C. Variable content and distribution of arabinogalactan proteins in banana (*Musa* spp.) under low temperature stress. *Front. Plant Sci.* **2015**, *6*, 353. [CrossRef]
19. Liu, X.; Wolfe, R.; Welch, L.R.; Domozych, D.S.; Popper, Z.A.; Showalter, A.M. Bioinformatic identification and analysis of extensins in the plant kingdom. *PLoS ONE* **2016**, *11*, e0150177. [CrossRef]
20. Betekhtin, A.; Rojek, M.; Milewska-Hendel, A.; Gawecki, R.; Karcz, J.; Kurczynska, E.; Hasterok, R. Spatial distribution of selected chemical cell wall components in the embryogenic callus of *Brachypodium distachyon*. *PLoS ONE* **2016**, *11*, e0167426. [CrossRef]
21. Castilleux, R.; Plancot, B.; Ropitaux, M.; Carreras, A.; Leprince, J.; Boulogne, I.; Follet-Gueye, M.L.; Popper, Z.A.; Driouich, A.; Vicre, M. Cell wall extensins in root-microbe interactions and root secretions. *J. Exp. Bot.* **2018**, *69*, 4235–4247. [CrossRef] [PubMed]
22. Baumberger, N.; Ringli, C.; Keller, B. Systematic identification of novel protein domain families associated with nuclear functions. *Genome Res.* **2002**, *12*, 47–56.
23. Botha, C.E. A tale of two neglected systems-structure and function of the thin- and thick-walled sieve tubes in monocotyledonous leaves. *Front. Plant Sci.* **2013**, *4*, 297. [CrossRef]
24. Gawecki, R.; Sala, K.; Kurczyńska, E.U.; Świątek, P.; Płachno, B.J. Immunodetection of some pectic, arabinogalactan proteins and hemicellulose epitopes in the micropylar transmitting tissue of apomictic dandelions (*Taraxacum*, Asteraceae, Lactuceae). *Protoplasma* **2016**, *254*, 657–668. [CrossRef] [PubMed]
25. Milewska-Hendel, A.; Baczewska, A.H.; Sala, K.; Dmuchowski, W.; Brągoszewska, P.; Gozdowski, D.; Jozwiak, A.; Chojnacki, T.; Swiezewska, E.; Kurczynska, E. Quantitative and qualitative characteristics of cell wall components and prenyl lipids in the leaves of *Tilia* x *euchlora* trees growing under salt stress. *PLoS ONE* **2017**, *12*, e0172682. [CrossRef]
26. Garaeva, L.D.; Pozdeeva, S.A.; Timofeeva, O.A.; Khokhlova, L.P. Cell-wall lectins during winter wheat cold hardening. *Russ. J. Plant. Physiol.* **2006**, *53*, 746–750. [CrossRef]
27. Gong, S.Y.; Huang, G.Q.; Sun, X.; Li, P.; Zhao, L.L.; Zhang, D.J.; Li, X.B. GhAGP31, a cotton non-classical arabinogalactan protein, is involved in response to cold stress during early seedling development. *Plant. Biol.* **2012**, *14*, 447–457. [CrossRef] [PubMed]

28. Kang, Y.; Khan, S.; Ma, X. Climate change impacts on crop yield, crop water productivity and food security—A review. *Prog. Nat. Sci.* **2009**, *19*, 1665–1674. [CrossRef]
29. Wang, W.; Vinocur, B.; Altman, A. Plant responses to drought, salinity and extreme temperatures: Towards genetic engineering for stress tolerance. *Planta* **2003**, *218*, 1–14. [CrossRef]
30. Larsen, F.H.; Byg, I.; Damager, I.; Diaz, J.; Engelsen, S.B.; Ulvskov, P. Residue specific hydration of primary cell wall potato pectin identified by solid-state 13C single-pulse MAS and CP/MAS NMR spectroscopy. *Biomacromolecules* **2011**, *12*, 1844–1850. [CrossRef] [PubMed]
31. Ha, M.A.; Vietor, R.J.; Jardine, G.D.; Apperley, D.C.; Jarvis, M.C. Conformation and mobility of the arabinan and galactan side-chains of pectin. *Phytochemistry* **2005**, *66*, 1817–1824. [CrossRef]
32. Tenhaken, R. Cell wall remodeling under abiotic stress. *Front. Plant. Sci.* **2014**, *5*, 771. [CrossRef]
33. Moore, J.P.; Farrant, J.M.; Driouich, A. A role for pectin-associated arabinans in maintaining the flexibility of the plant cell wall during water deficit stress. *Plant. Signal. Behav.* **2014**, *3*, 102–104. [CrossRef]
34. Betekhtin, A.; Pinski, A.; Milewska-Hendel, A.; Kurczynska, E.; Hasterok, R. Stability and instability processes in the calli of *Fagopyrum tataricum* that have different morphogenic potentials. *Plant. Cell Tissue Organ. Cult.* **2019**, 1–15. [CrossRef]
35. Xue, H.; Seifert, G.J. Fasciclin like arabinogalactan protein 4 and respiratory burst oxidase homolog d and F independently modulate abscisic acid signaling. *Plant. Signal. Behav.* **2015**, *10*, e989064. [CrossRef]
36. Johnson, K.L.; Jones, B.J.; Bacic, A.; Schultz, C.J. The fasciclin-like arabinogalactan proteins of Arabidopsis. A multigene family of putative cell adhesion molecules. *Plant. Physiol.* **2003**, *133*, 1911–1925. [CrossRef]
37. Seifert, G.J.; Xue, H.; Acet, T. The *Arabidopsis thaliana FASCICLIN LIKE ARABINOGALACTAN PROTEIN 4* gene acts synergistically with abscisic acid signalling to control root growth. *Ann. Bot.* **2014**, *114*, 1125–1133. [CrossRef]
38. Faik, A.; Abouzouhair, J.; Sarhan, F. Putative fasciclin-like arabinogalactan-proteins (FLA) in wheat (*Triticum aestivum*) and rice (*Oryza sativa*): Identification and bioinformatic analyses. *Mol. Genet. Genom.* **2006**, *276*, 478–494. [CrossRef]
39. Ma, H.; Zhao, J. Genome-wide identification, classification, and expression analysis of the arabinogalactan protein gene family in rice (*Oryza sativa* L.). *J. Exp. Bot.* **2010**, *61*, 2647–2668. [CrossRef]
40. Nahar, K.; Hasanuzzaman, M.; Ahamed, K.U.; Hakeem, K.R.; Ozturk, M.; Fujita, M. Plant responses and tolerance to high temperature stress: Role of exogenous phytoprotectants. In *Crop Production and Global Environmental Issues*; Hakeem, K.R., Ed.; Springer International Publishing: Cham, The Netherlands, 2015; pp. 385–435.
41. Ellis, M.; Egelund, J.; Schultz, C.J.; Bacic, A. Arabinogalactan-proteins: Key regulators at the cell surface? *Plant. Physiol.* **2010**, *153*, 403–419. [CrossRef]
42. Lima, R.B.; dos Santos, T.B.; Vieira, L.G.; Ferrarese Mde, L.; Ferrarese-Filho, O.; Donatti, L.; Boeger, M.R.; Petkowicz, C.L. Heat stress causes alterations in the cell-wall polymers and anatomy of coffee leaves (*Coffea arabica* L.). *Carbohydr. Polym.* **2013**, *93*, 135–143. [CrossRef]
43. Olmos, E.; Garcia De La Garma, J.; Gomez-Jimenez, M.C.; Fernandez-Garcia, N. Arabinogalactan proteins are involved in salt-adaptation and vesicle trafficking in tobacco by-2 cell cultures. *Front. Plant Sci.* **2017**, *8*, 1092. [CrossRef]
44. Zang, L.; Zheng, T.; Chu, Y.; Ding, C.; Zhang, W.; Huang, Q.; Su, X. Genome-wide analysis of the fasciclin-like arabinogalactan protein gene family reveals differential expression patterns, localization, and salt stress response in *Populus*. *Front. Plant Sci.* **2015**, *6*, 1140. [CrossRef] [PubMed]
45. Lamport, D.T.; Kieliszewski, M.J.; Showalter, A.M. Salt stress upregulates periplasmic arabinogalactan proteins: Using salt stress to analyse AGP function. *New Phytol.* **2006**, *169*, 479–492. [CrossRef] [PubMed]
46. Shi, H.; Kim, Y.; Guo, Y.; Stevenson, B.; Zhu, J.K. The Arabidopsis SOS5 locus encodes a putative cell surface adhesion protein and is required for normal cell expansion. *Plant. Cell* **2002**, *15*, 19–32. [CrossRef] [PubMed]
47. Griffiths, J.S.; Tsai, A.Y.; Xue, H.; Voiniciuc, C.; Sola, K.; Seifert, G.J.; Mansfield, S.D.; Haughn, G.W. SALT-OVERLY SENSITIVE5 mediates Arabidopsis seed coat mucilage adherence and organization through pectins. *Plant Physiol.* **2014**, *165*, 991–1004. [CrossRef] [PubMed]
48. Seifert, G.J. Fascinating fasciclins: A surprisingly widespread family of proteins that mediate interactions between the cell exterior and the cell surface. *Int. J. Mol. Sci.* **2018**, *19*, 1628. [CrossRef] [PubMed]

49. Johnson, K.L.; Kibble, N.A.; Bacic, A.; Schultz, C.J. A fasciclin-like arabinogalactan-protein (FLA) mutant of *Arabidopsis thaliana*, *fla1*, shows defects in shoot regeneration. *PLoS ONE* **2011**, *6*, e25154. [CrossRef]
50. Wu, Y.; Fan, W.; Li, X.; Chen, H.; Takac, T.; Samajova, O.; Fabrice, M.R.; Xie, L.; Ma, J.; Samaj, J.; et al. Expression and distribution of extensins and AGPs in susceptible and resistant banana cultivars in response to wounding and *Fusarium oxysporum*. *Sci. Rep.* **2017**, *7*, 42400. [CrossRef]
51. Casero, P.J.; Casimiro, I.; Knox, J.P. Occurrence of cell surface arabinogalactan-protein and extensin epitopes in relation to pericycle and vascular tissue development in the root apex of four species. *Planta* **1998**, *204*, 252–259. [CrossRef]
52. Zhang, X.; Ren, Y.; Zhao, J. Roles of extensins in cotyledon primordium formation and shoot apical meristem activity in *Nicotiana tabacum*. *J. Exp. Bot.* **2008**, *59*, 4045–4058. [CrossRef] [PubMed]
53. Xu, C.; Takáč, T.; Burbach, C.; Menzel, D.; Šamaj, J. Developmental localization and the role of hydroxyproline rich glycoproteins during somatic embryogenesis of banana (*Musa* spp. AAA). *BMC Plant. Biol.* **2011**, *11*, 38. [CrossRef]
54. Zhang, X.; Ma, H.; Qi, H.; Zhao, J. Roles of hydroxyproline-rich glycoproteins in the pollen tube and style cell growth of tobacco (*Nicotiana tabacum* L.). *J. Plant. Physiol.* **2014**, *171*, 1036–1045. [CrossRef] [PubMed]
55. Seki, M.; Narusaka, M.; Ishida, J.; Nanjo, T.; Fujita, M.; Oono, Y.; Kamiya, A.; Nakajima, M.; Enju, A.; Sakurai, T.; et al. Monitoring the expression profiles of 7000 Arabidopsis genes under drought, cold and high-salinity stresses using a full-length cDNA microarray. *Plant. J.* **2002**, *31*, 279–292. [CrossRef] [PubMed]
56. Kreps, J.A.; Wu, Y.; Chang, H.S.; Zhu, T.; Wang, X.; Harper, J.F. Transcriptome changes for Arabidopsis in response to salt, osmotic, and cold stress. *Plant. Physiol.* **2002**, *130*, 2129–2141. [CrossRef]
57. Hwang, Y.; Lee, H.; Lee, Y.S.; Cho, H.T. Cell wall-associated ROOT HAIR SPECIFIC 10, a proline-rich receptor-like kinase, is a negative modulator of Arabidopsis root hair growth. *J. Exp. Bot.* **2016**, *67*, 2007–2022. [CrossRef]
58. Dar, N.A.; Amin, I.; Wani, W.; Shafiq, A.; Shikari, A.B.; Wani, S.H.; Masoodi, K.Z. Abscisic acid: A key regulator of abiotic stress tolerance in plants. *Plant. Gene* **2017**, *11*, 106–111. [CrossRef]
59. Bai, L.; Zhang, G.; Zhou, Y.; Zhang, Z.; Wang, W.; Du, Y.; Wu, Z.; Song, C.P. Plasma membrane-associated proline-rich extensin-like receptor kinase 4, a novel regulator of Ca signalling, is required for abscisic acid responses in *Arabidopsis thaliana*. *Plant. J.* **2009**, *60*, 314–327. [CrossRef] [PubMed]
60. Silva, N.F.; Goring, D.R. The proline-rich, extensin-like receptor kinase-1 (PERK1) gene is rapidly induced by wounding. *Plant. Mol. Biol.* **2002**, *50*, 667–685. [CrossRef]
61. Zhao, C.; Zayed, O.; Yu, Z.; Jiang, W.; Zhu, P.; Hsu, C.C.; Zhang, L.; Tao, W.A.; Lozano-Duran, R.; Zhu, J.K. Leucine-rich repeat extensin proteins regulate plant salt tolerance in Arabidopsis. *Proc. Natl. Acad. Sci. USA* **2018**, *115*, 13123–13128. [CrossRef]
62. Irizarry, I.; White, J.F. *Bacillus amyloliquefaciens* alters gene expression, ROS production and lignin synthesis in cotton seedling roots. *J. Appl. Microbiol.* **2018**, *124*, 1589–1603. [CrossRef]
63. Sujkowska-Rybkowska, M.; Borucki, W. Accumulation and localization of extensin protein in apoplast of pea root nodule under aluminum stress. *Micron* **2014**, *67*, 10–19. [CrossRef]
64. Francin-Allami, M.; Merah, K.; Albenne, C.; Rogniaux, H.; Pavlovic, M.; Lollier, V.; Sibout, R.; Guillon, F.; Jamet, E.; Larre, C. Cell wall proteomic of *Brachypodium distachyon* grains: A focus on cell wall remodeling proteins. *Proteomics* **2015**, *15*, 2296–2306. [CrossRef]
65. Calderan-Rodrigues, M.J.; Guimarães Fonseca, J.; de Moraes, F.E.; Vaz Setem, L.; Carmanhanis Begossi, A.; Labate, C.A. Plant cell wall proteomics: A focus on monocot species, *Brachypodium distachyon*, *Saccharum* spp. and *Oryza sativa*. *Int. J. Mol. Sci.* **2019**, *20*, 1975. [CrossRef] [PubMed]
66. Douche, T.; San Clemente, H.; Burlat, V.; Roujol, D.; Valot, B.; Zivy, M.; Pont-Lezica, R.; Jamet, E. *Brachypodium distachyon* as a model plant toward improved biofuel crops: Search for secreted proteins involved in biogenesis and disassembly of cell wall polymers. *Proteomics* **2013**, *13*, 2438–2454. [CrossRef] [PubMed]
67. Francin-Allami, M.; Lollier, V.; Pavlovic, M.; San Clemente, H.; Rogniaux, H.; Jamet, E.; Guillon, F.; Larre, C. Understanding the remodelling of cell walls during *Brachypodium distachyon* grain development through a sub-cellular quantitative proteomic approach. *Proteomes* **2016**, *4*, 21. [CrossRef]
68. Zhang, M.; Chen, G.X.; Lv, D.W.; Li, X.H.; Yan, Y.M. N-linked glycoproteome profiling of seedling leaf in *Brachypodium distachyon* L. *J. Proteome Res.* **2015**, *14*, 1727–1738. [CrossRef] [PubMed]

69. Priest, H.D.; Fox, S.E.; Rowley, E.R.; Murray, J.R.; Michael, T.P.; Mockler, T.C. Analysis of global gene expression in *Brachypodium distachyon* reveals extensive network plasticity in response to abiotic stress. *PLoS ONE* **2014**, *9*, e87499. [CrossRef]
70. Hong, S.Y.; Park, J.H.; Cho, S.H.; Yang, M.S.; Park, C.M. Phenological growth stages of *Brachypodium distachyon*: Codification and description. *Weed Res.* **2011**, *51*, 612–620. [CrossRef]
71. Sala, K.; Malarz, K.; Barlow, P.W.; Kurczyńska, E.U. Distribution of some pectic and arabinogalactan protein epitopes during *Solanum lycopersicum* (L.) adventitious root development. *BMC Plant. Biol.* **2017**, *17*, 25. [CrossRef] [PubMed]
72. Betekhtin, A.; Milewska-Hendel, A.; Chajec, L.; Rojek, M.; Nowak, K.; Kwasniewska, J.; Wolny, E.; Kurczynska, E.; Hasterok, R. 5-azacitidine induces cell death in a tissue culture of *Brachypodium distachyon*. *Int. J. Mol. Sci.* **2018**, *19*, 1806. [CrossRef] [PubMed]
73. Pennell, R.I.; Janniche, L.; Kjellbom, P.; Scofield, G.N.; Peart, J.M.; Roberts, K. Developmental regulation of a plasma membrane arabinogalactan protein epitope in oilseed rape flowers. *Plant. Cell* **1991**, *3*, 1317–1326. [CrossRef] [PubMed]
74. Yates, E.A.; Knox, J.P. Investigations into the occurrence of plant cell surface epitopes in exudate gums. *Carbohydr. Polym.* **1994**, *24*, 281–286. [CrossRef]
75. Yates, E.A.; Valdor, J.F.; Haslam, S.M.; Morris, H.R.; Dell, A.; Mackie, W.; Knox, J.P. Characterization of carbohydrate structural features recognized by anti-arabinogalactan-protein monoclonal antibodies. *Glycobiology* **1996**, *6*, 131–139. [CrossRef]
76. Knox, J.P.; Linstead, P.J.; Peart, J.; Cooper, C.; Roberts, K. Developmentally regulated epitopes of cell surface arabinogalactan proteins and their relation to root tissue pattern formation. *Plant. J.* **1991**, *1*, 317–326. [CrossRef] [PubMed]
77. Smallwood, M.; Yates, E.A.; Willats, W.G.T.; Martin, H.; Knox, J.P. Immunochemical comparison of membrane-associated and secreted arabinogalactan-proteins in rice and carrot. *Planta* **1996**, *198*, 452–459. [CrossRef]
78. Bradley, D.J.; Wood, E.A.; Larkins, A.P.; Galfre, G.; Butcher, G.W.; Brewin, N.J. Isolation of monoclonal antibodies reacting with peribacteroid membranes and other components of pea root nodules containing *Rhizobium leguminosarum*. *Planta* **1988**, *173*, 149–160. [CrossRef] [PubMed]
79. Pennell, R.I.; Knox, J.P.; Scofield, G.N.; Selvendran, R.R.; Roberts, K. A family of abundant plasma membrane-associated glycoproteins related to the arabinogalactan proteins is unique to flowering plants. *J. Cell. Biol.* **1989**, *108*, 1967–1977. [CrossRef]
80. Willats, W.G.T.; Marcus, S.E.; Knox, J.P. Generation of a monoclonal antibody specific to (1→5)-α-L-arabinan. *Carbohydr. Res.* **1998**, *308*, 149–152. [CrossRef]
81. El-Tantawy, A.A.; Solis, M.T.; Da Costa, M.L.; Coimbra, S.; Risueno, M.C.; Testillano, P.S. Arabinogalactan protein profiles and distribution patterns during microspore embryogenesis and pollen development in *Brassica napus*. *Plant. Reprod.* **2013**, *26*, 231–243. [CrossRef] [PubMed]
82. Smallwood, M.; Beven, A.; Donovan, N.; Neill, S.J.; Peart, J.; Roberts, K.; Knox, J.P. Localization of cell wall proteins in relation to the developmental anatomy of the carrot root apex. *Plant. J.* **1994**, *5*, 237–246. [CrossRef]

II.2

Pinski A, Betekhtin A, Skupien-Rabian B, Jankowska U, Jamet E, Hasterok R.

Changes in the cell wall proteome of leaves in response to temperature stress in *Brachypodium distachyon*

International Journal of Molecular Sciences, 2021, 22, 6750

IF_{2020} – 5,923; pkt MNiSW – 140

Ze względu na obszerność, dane suplementarne dla tej pracy znajdują się pod linkiem: https://www.mdpi.com/article/10.3390/ijms22136750/s1, jak też zostały dołączone w postaci elektronicznej.

International Journal of
Molecular Sciences

MDPI

Article

Changes in the Cell Wall Proteome of Leaves in Response to High Temperature Stress in *Brachypodium distachyon*

Artur Pinski [1,*], Alexander Betekhtin [1,*], Bozena Skupien-Rabian [2], Urszula Jankowska [2], Elisabeth Jamet [3] and Robert Hasterok [1]

[1] Plant Cytogenetics and Molecular Biology Group, Institute of Biology, Biotechnology and Environmental Protection, Faculty of Natural Sciences, University of Silesia in Katowice, 40-032 Katowice, Poland; robert.hasterok@us.edu.pl
[2] Proteomics and Mass Spectrometry Core Facility, Malopolska Centre of Biotechnology, Jagiellonian University, 31-007 Krakow, Poland; bozena.skupien-rabian@uj.edu.pl (B.S.-R.); urszula.jankowska@uj.edu.pl (U.J.)
[3] Laboratoire de Recherche en Sciences Végétales, Université de Toulouse, CNRS, UPS, 31326 Auzeville Tolosane, France; jamet@lrsv.ups-tlse.fr
* Correspondence: apinski@us.edu.pl (A.P.); alexander.betekhtin@us.edu.pl (A.B.)

Abstract: High temperature stress leads to complex changes to plant functionality, which affects, i.a., the cell wall structure and the cell wall protein composition. In this study, the qualitative and quantitative changes in the cell wall proteome of *Brachypodium distachyon* leaves in response to high (40 °C) temperature stress were characterised. Using a proteomic analysis, 1533 non-redundant proteins were identified from which 338 cell wall proteins were distinguished. At a high temperature, we identified 46 differentially abundant proteins, and of these, 4 were over-accumulated and 42 were under-accumulated. The most significant changes were observed in the proteins acting on the cell wall polysaccharides, specifically, 2 over- and 12 under-accumulated proteins. Based on the qualitative analysis, one cell wall protein was identified that was uniquely present at 40 °C but was absent in the control and 24 proteins that were present in the control but were absent at 40 °C. Overall, the changes in the cell wall proteome at 40 °C suggest a lower protease activity, lignification and an expansion of the cell wall. These results offer a new insight into the changes in the cell wall proteome in response to high temperature.

Keywords: *Brachypodium distachyon*; cell wall proteomics; glycoside hydrolase; leaves; high temperature stress

Citation: Pinski, A.; Betekhtin, A.; Skupien-Rabian, B.; Jankowska, U.; Jamet, E.; Hasterok, R. Changes in the Cell Wall Proteome of Leaves in Response to High Temperature Stress in *Brachypodium distachyon*. *Int. J. Mol. Sci.* **2021**, *22*, 6750. https://doi.org/10.3390/ijms22136750

Academic Editor: Setsuko Komatsu

Received: 4 June 2021
Accepted: 21 June 2021
Published: 23 June 2021

1. Introduction

In recent years, plant productivity has been increasingly threatened by climate change, primarily extreme climate events, altered rainfall patterns and increasing global mean land and ocean surface temperatures [1]. Multimethod analyses predict that each Celsius degree increase in the global mean temperature will negatively impact the yields of four major crops: maize, wheat, rice and soybean, which will result in food scarcity. However, it should be noted that the results are highly heterogeneous regarding geographical areas and crops with some estimations of a positive impact [2]. Simultaneously, there is also a need to increase food production because of the growing population (an additional two billion-plus people by 2050), a decrease of arable land and switch in the use of land for biofuel production and other industries [3]. In order to cope with the negative impact of climate changes and need to increase food production, there is an urgency to develop new climate-smart crops that fit into the climate-smart agriculture approach [3–5]. The development of such crops can be done using genetic engineering and breeding as well by exploiting epigenetic variations [6,7]. However, this requires detailed knowledge about the molecular mechanisms that underlie the various stress responses [8–12]. In order to facilitate the development of climate-smart crops, *Brachypodium distachyon* was proposed

as a model plant for temperate grasses [13,14] because it offers a suite of advantages: undemanding growth requirements, small stature, short life cycle, relatively small genome and established protocols for efficient genomic editing [3,15–18]. Large collections of natural accessions with well-described genetic diversity and variation in DNA methylation are also available [19,20]. *B. distachyon* constitutes a useful target for genetically manipulating the cell wall composition as the cell wall of grasses differs from that of dicots in the aspects of major structural polysaccharides and the abundance of pectins, phenolic compounds and proteins [14,21]. The most notable and exciting area for discovery is that of lignin formation in grasses [16].

Temperature stress induced by high temperatures, leads to complex changes in the photosynthesis efficiency, reactive oxygen species scavenging, redox adjustment, cytoskeletal rearrangements and cell wall remodelling [22,23]. Although they constitute less than 10% of the dry mass for dicots and 1% for monocots, the cell wall proteins (CWPs) participate in cell wall remodelling, signalling and its overall scaffolding structure [9,14,24,25]. To facilitate their analysis, CWPs are usually divided into nine functional classes: proteins acting on carbohydrates, oxido-reductases, proteases, proteins related to lipid metabolism, proteins that are possibly involved in signalling, proteins that have predicted interaction domains, miscellaneous proteins, structural proteins and proteins with an unknown function. CWPs can be identified through a proteomic analysis using liquid chromatography tandem-mass spectrometry (LC-MS/MS). The process begins with the purification of the cell walls, followed by the extraction of CWPs using salt solutions. It is difficult to obtain a full representation of CWPs because the cell wall is an open compartment that has no surrounding structure, which results in the loss of some CWPs during the isolation procedure and because some CWPs are covalently linked to other cell wall components. Additionally, the isolated CWPs are contaminated with intracellular proteins that require further bioinformatic analysis [24,25]. Using such approaches, has enabled 699 *B. distachyon* CWPs to be identified in the leaves, stems and seeds (data available at *WallProtDB*, http://www.polebio.lrsv.ups-tlse.fr/WallProtDB/, accessed on 29 March 2021, [26]).

In a previous work, we investigated the response of the hydroxyproline-rich glycoproteins (HRGPs) to temperature stress in leaves. We showed a differential response of the HRGPs to temperature stress with more pronounced changes in the levels of the mRNAs encoding the AGPs at a high temperature [27]. Although the roots and reproductive organs are more sensitive to temperature, the response of the leaves directly affects plant productivity [9,28].

However, it is known that high temperature stress affects other CWPs beside HRGPs [9] but there are only a few studies on monocots [29,30]. In order to analyse these changes in the cell wall proteome of *B. distachyon* more broadly, a cell wall proteomics approach was used. This study aimed to characterise the changes in the cell wall proteome of *B. distachyon* leaves in response to high (40 °C) temperature stress.

2. Results

2.1. Isolating the Cell Wall Proteins

The CWPs were isolated from about 3 g of the fresh leaves of *B. distachyon,* which enabled about 0.75 mg proteins (0.25 mg proteins per g fresh leaves) to be extracted. The proteins, which were separated using 1D-electrophoresis, showed a reproducible band pattern across all four of the biological replicates. None of the samples showed visible protein degradation patterns with presence of distinct bands from the largest proteins to the smallest ones. The 1D-electrophoretic patterns were slightly different between the control (21 °C) and plants subjected to 40 °C treatment (Figure A1).

2.2. Overall Proteome Data Analysis

In the two different treatments (control and 40 °C), 1533 non-redundant proteins were identified through an LC-MS/MS analysis. Of these, only 338 CWPs were identified (22.05% of the total identified unique proteins) based on the prediction of a signal peptide

by at least one bioinformatics tool (SignalP, TargetP or Phobius) and the absence of any known intracellular retention domain [26]. A protein was validated in a given sample when at least two unique peptides were present and in a given treatment when it was present in at least three of the four biological replicates. To make sure that high temperature treatment was not deleterious to plants, the amount of a few proteins related to the cell death process was checked, namely Bradi5g25970, Bradi1g37780, Bradi4g28680, Bradi1g60800, Bradi1g64680, Bradi2g02000, Bradi2g52470, and Bradi4g44667 [31,32]. No change in their level of accumulation was observed.

In this study, 39 new CWPs were identified compared to those that were already recorded in *WallProtDB*, which increases the number of experimentally validated CWPs in *B. distachyon* to 738. The number of CWPs that were identified for each treatment differed, and the highest number in the control—311 (21.9%) and the lowest number at 40 °C -253 (16.8%) (Table S1). The number of identified CWPs was different between the control and 40 °C; fewer CWPs were present predominantly in the proteins acting on cell wall polysaccharides and oxido-reductases functional classes at 40 °C (Table 1). The principal component analysis showed that the samples from 40 °C were grouped together and were separate from the control, which suggests significant differences between them (Figure 1A). The first factor explained 56.4% of the changes between the control and samples at 40 °C. Moreover, a hierarchical clustering for CWPs showed the control samples with samples at 40 °C forming a separate branch (Figure 1B). The protein molecular masses were predominantly concentrated in the 20-60 kDa range, but proteins up to 120 kDa were also identified, which showed a good coverage of the different molecular masses (Figure 1C). In most of the proteins, there was high protein sequence coverage with the identified peptides (Figure 1D). A sequence coverage of more than 20% was observed for 80% of the proteins.

Table 1. Number of unique proteins and CWPs that were identified for the control and 40 °C and classified into the functional classes (classified as in *WallProtDB*). The percentage of the proteins identified in the functional classes compared to the total number of CWPs for each treatment is indicated in brackets.

Functional Class	Control	40 °C
Proteins acting on cell wall polysaccharides	87 (28%)	65 (25.7%)
Proteases	57 (18.3%)	48 (19%)
Oxido-reductases	52 (16.7%)	39 (15.4%)
Proteins related to lipid metabolism	38 (12.2%)	32 (12.6%)
Proteins with interaction domains (with proteins or polysaccharides)	9 (2.9%)	9 (3.6%)
Proteins possibly involved in signalling	7 (2.3%)	5 (2%)
Structural proteins	3 (1%)	3 (1.2%)
Miscellaneous	35 (11.3%)	33 (13%)
Unknown function	23 (7.4%)	19 (7.5%)
Total number of CWPs	311	253
Total number of unique proteins	1423	1505

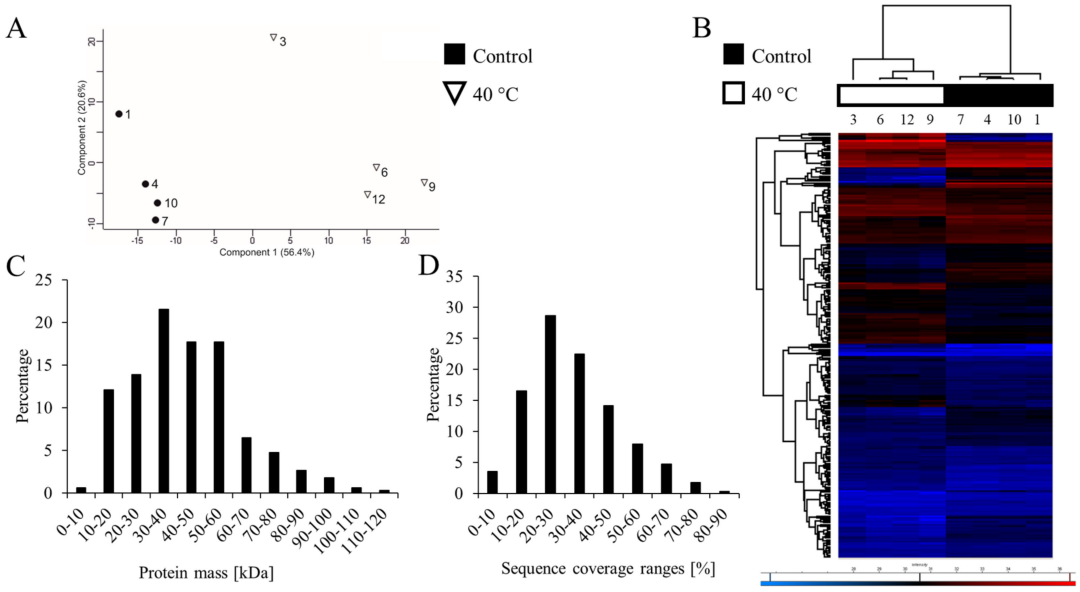

Figure 1. General features of the proteomic analysis. (**A**) Principal component analysis scatterplot in which each point represents a biological replicate. (**B**) The hierarchical clustering of the differentially abundant proteins (DAPs) that were identified in the experiment. (**C**) The molecular mass distribution of the proteins. The X-axis represents the theoretical molecular mass (kDa); the Y-axis represents the percentage of CWPs within each mass range. (**D**) Sequence coverage distribution for the identified proteins. The X-axis represents the sequence coverage ranges; the Y-axis represents the percentage of CWPs within each sequence coverage range.

2.3. Qualitative Analysis

For the qualitative analysis, only CWPs were included. The percentage of the contributions of the functional classes was different for each treatment and the differences were most prominent in the classes of proteins acting on the cell wall polysaccharides, proteases, oxido-reductases and miscellaneous proteins (Table 1). A lower contribution was observed at 40 °C (15.4% vs. 16.7% in the control) for the proteins acting on cell wall polysaccharides and oxido-reductases. Simultaneously, there was a higher representation of the miscellaneous proteins at 40 °C (13.0%) than in the control (11.3%). Using a more rigorous approach, a protein was found to be exclusively present in a given treatment when it was identified in all four biological replicates and was absent in the other temperature treatment. This approach revealed 25 differentially present CWPs (Table S1). One protein was found to be exclusively present at 40 °C (Bradi4g14920) while being absent in the control and 24 proteins were found to be present in the control but not at 40 °C.

2.4. Quantitative Analysis

Only CWPs were considered for the quantitative analysis. To identify the differentially abundant proteins (DAPs), a protein had to be present in at least three of the four biological replicates for a given treatment. Considering the differences between the control and 40 °C, 46 DAPs were identified. Of these, 4were over-accumulated and 42 were under-accumulated. A classification of CWPs into the functional classes showed changes in the abundance of CWPs in seven; both an over-accumulation and under-accumulation were observed in three of them (Table 2). Notably, the most significant changes were in the class of proteins acting on cell wall polysaccharides with 2 over- and 12 under-accumulated proteins. Looking at the level of protein families, most of the DAPs were classified as glycoside hydrolases (GHs) (11 DAPs), Asp proteases (6), class III peroxidases (CIII Prxs) (4) and GDSL-lipases/acylhydrolases (4) (Table S1). The abundance differences ranged from a 23.2-fold increase at 40 °C for Bradi4g09430 (xylanase inhibitor/class II chitinase of the GH18 family according to the CAZy database, http://www.cazy.org/, accessed on

29 March 2021) to a 15.8-fold decrease for Bradi1g52050 (polygalacturonase of the GH28 family according to the CAZy database) compared to the control (Table 3).

Table 2. DAPs for the 40 °C treatment compared to the control and classified into their functional classes (according to the classification introduced in *WallProtDB*).

Functional Class	Over-Accumulated DAPs	Under-Accumulated DAPs
Proteins acting on cell wall polysaccharides	2	12
Proteases	1	11
Miscellaneous	1	4
Unknown function	-	2
Oxido-reductases	-	6
Proteins related to lipid metabolism	-	6
Proteins with interaction domains (with proteins or polysaccharides)	-	1
Total number	4	42

Table 3. DAPs for the 40 °C treatment compared to the control.

Protein	Fold Change	q-Value	Functional Class	(Putative) Function
Over-Accumulated DAPs at 40 °C				
Bradi1g20950	1.8	0.00518	Miscellaneous	dirigent protein
Bradi4g02700	2.9	0	Proteases	peptidase M20
Bradi4g09430	23.2	0.00190	Proteins acting on cell wall polysaccharides	GH18 (xylanase inhibitor/class II chitinase)
Bradi4g09417	5.9	0	Proteins acting on cell wall polysaccharides	GH18 (xylanase inhibitor/class II chitinase)
Under-Accumulated DAPs at 40 °C				
Bradi3g18680	−7.9	0.00229	Miscellaneous	dienelactone hydrolase
Bradi4g41300	−3.3	0.00285	Miscellaneous	dirigent protein
Bradi3g37670	−1.7	0.00407	Miscellaneous	germin (cupin domain)
Bradi1g57590	−5.6	0.00405	Miscellaneous	SCP-like extracellular protein (PR-1)
Bradi3g59210	−5.6	0.00133	Oxido-reductases	laccase
Bradi4g05980	−2.7	0.00139	Oxido-reductases	CIII Prx (BdiPrx117)
Bradi1g58997	−2.8	0	Oxido-reductases	CIII Prx (BdiPrx35)
Bradi2g12170	−2.5	0.00115	Oxido-reductases	CIII Prx (BdiPrx62)
Bradi3g09080	−1.7	0.00409	Oxido-reductases	CIII Prx (BdiPrx96)
Bradi1g77560	−2.4	0.00326	Oxido-reductases	plastocyanin (blue copper-binding protein)
Bradi1g36160	−1.7	0.00876	Proteases	Asp protease (Peptidase family A1)
Bradi3g61060	−2.6	0.00393	Proteases	Asp protease (Peptidase family A1)
Bradi4g12160	−2.7	0.00282	Proteases	Asp protease (Peptidase family A1)
Bradi1g19070	−3.1	0	Proteases	Asp protease (Peptidase family A1)
Bradi2g25850	−3.8	0.00567	Proteases	Asp protease (Peptidase family A1)
Bradi3g56660	−8	0	Proteases	Asp protease (Peptidase family A1)
Bradi1g09729	−1.9	0.00348	Proteases	Cys protease (papain family) (Peptidase family C1A)
Bradi1g09737	−2.2	0.00266	Proteases	Cys protease (papain family) (Peptidase family C1A)
Bradi3g01320	−1.5	0.00198	Proteases	Ser carboxypeptidase (Peptidase family S10)
Bradi1g60600	−1.7	0.00998	Proteases	Ser carboxypeptidase (Peptidase family S10)
Bradi3g57140	−3.1	0.00123	Proteases	Ser protease (subtilisin) (Peptidase family S8)
Bradi2g45320	−4.2	0.00155	Proteins acting on cell wall polysaccharides	expressed protein (Trichome Birefringence-like domain)
Bradi1g10940	−3.9	0.00301	Proteins acting on cell wall polysaccharides	GH1 (β-glucosidase)
Bradi1g10930	−4.3	0.00165	Proteins acting on cell wall polysaccharides	GH1 (β-glucosidase)
Bradi3g18590	−5.5	0	Proteins acting on cell wall polysaccharides	GH16 (endoxyloglucan transferase)
Bradi1g25517	−3.8	0.00279	Proteins acting on cell wall polysaccharides	GH17 (β-1,3-glucosidase)
Bradi2g60441	−5.8	0.00131	Proteins acting on cell wall polysaccharides	GH17 (β-1,3-glucosidase)
Bradi2g47210	−1.9	0	Proteins acting on cell wall polysaccharides	GH19
Bradi1g52050	−15.8	0	Proteins acting on cell wall polysaccharides	GH28 (polygalacturonase)
Bradi1g08570	−2	0.00902	Proteins acting on cell wall polysaccharides	GH3
Bradi1g08550	−7.1	0	Proteins acting on cell wall polysaccharides	GH3
Bradi1g67760	−1.6	0.00346	Proteins acting on cell wall polysaccharides	GH35 (β-galactosidase)
Bradi2g31690	−2.5	0.00116	Proteins acting on cell wall polysaccharides	GH5 (cellulase)
Bradi1g14983	−1.5	0.00398	Proteins related to lipid metabolism	glycerophosphoryl diester phosphodiesterase
Bradi1g49010	−2.4	0.00149	Proteins related to lipid metabolism	GDSL-lipase/acylhydrolase
Bradi1g23120	−3.5	0.00962	Proteins related to lipid metabolism	GDSL-lipase/acylhydrolase
Bradi1g38780	−3.8	0.00161	Proteins related to lipid metabolism	GDSL-lipase/acylhydrolase
Bradi1g50897	−7.4	0.00117	Proteins related to lipid metabolism	GDSL-lipase/acylhydrolase
Bradi1g21870	−6.3	0	Proteins related to lipid metabolism	lipid transfer protein/trypsin-alpha amylase inhibitor
Bradi4g37090	−3.5	0.00113	Proteins with interaction domains (with proteins or polysaccharides)	expressed protein (LysM domain)
Bradi2g43230	−2.2	0.00728	Unknown function	expressed protein (DUF642)
Bradi3g29710	−1.6	0.00943	Unknown function	Plant Basic Secreted Protein (BSP)

2.5. Expression of Six Genes Encoding the DAPs

RT-qPCR was used to analyse the expression levels of six genes encoding the DAPs and showed a contrasting differential level of accumulation between the 40 °C treatment and the control (Table 3): *Bradi1g52050* encodes a polygalacturonase (GH28), *Bradi1g38780* a GDSL-lipase/acylhydrolase, *Bradi1g25517* an endo-β-1,3-glucosidase (GH17), *Bradi1g58997* a CIII Prx (BdiPrx35), *Bradi4g09417* a class II chitinase (GH18) and *Bradi4g09430* another GH18. The relative expression levels of five genes at 40 °C showed similar trends as those for the proteomics results (Figure 2). In contrast, the relative expression levels of one remaining gene had a trend opposite to the result of the proteomic analysis, although the differences were small. It is worth noting that the proteomic analysis showed changes in the abundancy of proteins that were accumulated or degraded during the entire treatment period (24 h), while the expression analysis showed the levels of gene expression at a specific timepoint (after 24 h). Moreover, the relationship between the expression level of a given gene and the biosynthesis of the encoded protein is complex and is subject to various levels of regulation, which makes proteomic analysis more informative regarding the actual changes in the cell wall proteomes [33,34].

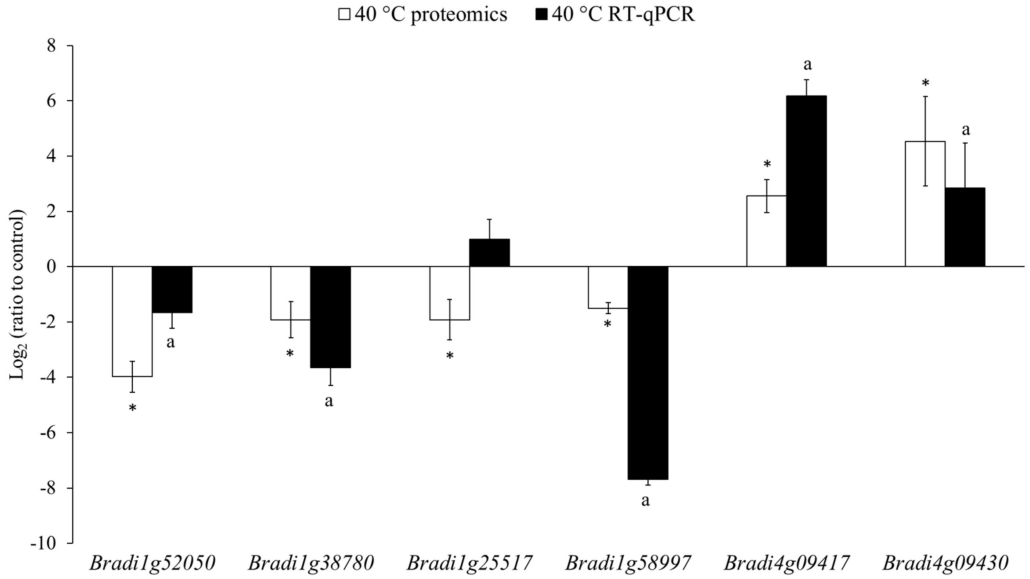

Figure 2. Comparison between the relative expression levels of the six genes that were measured using RT-qPCR and the relative level of the accumulation of the encoded proteins. *Bradi1g52050* encodes a polygalacturonase (GH28), *Bradi1g38780* a GDSL-lipase/acylhydrolase, *Bradi1g25517* an endo-β-1,3-glucosidase (GH17), *Bradi1g58997* a CIII Prx (BdiPrx35), *Bradi4g09417* a class II chitinase (GH18) and *Bradi4g09430* another GH18. The polyubiquitin gene (*Bradi1g32860*) was used as the reference gene for the RT-qPCR measurements and the control treatment (at 21 °C) as the reference group for all the calculations. The error bars of RT-qPCR results represent the standard deviations that were calculated from three biological replicates and two technical replicates for each biological replicate. The letter "a" indicates significant differences from the control using the Student's t-test ($p < 0.05$; mean ± SD, $n = 3$). The error bars indicated for the quantitative proteomic results represent the standard deviations that were calculated from four biological replicates. Asterisks indicate significant differences from the control using the Student's *t*-test with the permutation-based FDR set to 1% (q-value < 0.01).

3. Discussion

3.1. Proteins Acting on Cell Wall Polysaccharides

Glycoside hydrolases (GHs) are enzymes that are able to rearrange the plant cell wall polysaccharides, thereby participating in plant development and the response to stress [35]. The treatment at 40 °C resulted in significant changes in the proteins that belong

to the GH family with an over-accumulation of two GH18, an under-accumulation of 11 GHs (GH1, GH3, GH5, GH16, GH17, GH19 and GH28) and the absence of three GHs (GH1, GH3 and GH10). GH18 is among the most interesting GH families as its members can be xylanase inhibitors or class II chitinases. This family has more representatives in grasses than in dicots, thus they constitute promising candidates for further investigating their role in the cell wall [36]. The Bradi4g09430 protein, which was over-accumulated at 40 °C, was characterised as a xylanase inhibitor [37]. Such proteins reversibly inhibit the xylanases that belong to GH10 (the Bradi5g04640 GH10 was absent at 40 °C) and GH11 [38]. The inhibition of xylanases can limit the early stages of fungal infections [37]. GH18 can also work in synergy with GH19 (chitinases) to promote antifungal activity [39]. The members of GH3 family exhibit broad substrate specificities acting on arabinoxylans and (1-3)(1-4)-β-D glucans, which are the most common hemicelluloses in grasses [40]. GH16 have xyloglucan endotransglucosylase/hydrolases activity and are likely to be involved in xyloglucan remodelling, although their effect on the cell wall mechanics seems to be relatively weak [41]. GH1 exhibit a β-glycosidases activity and are involved in lignification, the defence against herbivory and the hydrolysis of the cell wall-derived oligosaccharides during germination [42]. Finally, GH28 exhibits polygalacturonase activity, which catalyses pectin depolymerisation, which can result in cell wall loosening [39].

Previous studies have indicated the role of expansins in the heat stress response through the loosening of the cell walls [9]. In our experiment, we identified three expansins that were present in the control but were absent at 40 °C. Such an absence aligns with previous experiments, which showed differential changes in the expression of the expansin genes that are specific to a species and/or the expansin isoforms [9]. For example, in *Brassica napus* seedlings, the expression of *EXPA5* was reduced ten-fold at 38 °C, and in the case of *Populus simonii*, 13 genes encoding expansins were also down-regulated at 42 °C [43,44]. On the other hand, in *Agrostis scabra,* the up-regulation of one of expansin gene was positively correlated with a better heat tolerance [45]. Indeed, a few studies have suggested that although the cell wall loosening by expansins promotes plant growth and development, it makes plants more vulnerable to biotic and abiotic stresses [46,47].

The trichome birefringence-like (TBL) proteins through the O-acetylation of cell wall polysaccharides (either hemicelluloses or pectins) affect their physicochemical properties of polymers [48]. Notably, as has been shown in *Arabidopsis thaliana,* the TBL proteins are essential for the plant response to various biotic and abiotic stresses [49]. In *A. thaliana,* exposure to aluminium resulted in a decrease in the *TBL27* transcript accumulation and the mutant in this gene had a higher aluminium accumulation in the hemicellulose fraction than the wild type [48]. In *Oryza sativa*, a double mutant that was impaired in the TBL genes (*tbl1 tbl2*) exhibited a stunted growth phenotype with varying degrees of dwarfism [50]. In response to heat stress, we observed a decreased abundance of the Bradi2g45230 TBL protein and the lack of another one (Bradi2g07000), which were both present in the control. This could lead to a lower level of the O-acetylation of the cell wall polymers.

Pectins can undergo various modifications in the cell wall, among which is the demethylesterification by pectin methylesterases (PMEs) [51]. One PME was absent at 40 °C compared to the control together with one pectate lyase that catalyses the eliminative cleavage of de-esterified pectin. The changes in the degree of pectin methylesterification and its consequence of the formation of the so-called egg-boxes with the calcium ions have previously been described, although the mechanism and effect on heat tolerance remain to be elucidated [52,53].

3.2. Proteases

The proteases break the peptide bonds and control key plant processes such as protein transport, activity and half-live [36]. Our results revealed the under-accumulation of several proteases (aspartyl, cysteine and serine) and the absence of a few proteases (aspartyl, cysteine, serine and peptidase C13) at 40 °C, although they were present in the control. Only one peptidase that belongs to the M20 family was over-accumulated at 40 °C.

Overall, at 40 °C, the presence of the proteases seemed to decrease compared to the control, which suggests a lower proteolytic activity. The *Bradi5g26620* and *Bradi5g16960* encoding proteases, which were absent at 40 °C, have been proposed as novel candidate genes that might participate in grain programmed cell death [54].

3.3. Miscellaneous Proteins and Proteins of a Yet Unknown Function

The miscellaneous class includes CWPs with diverse functions, among others, the dirigent proteins, which are involved in lignan and lignin biosynthesis that are involved in plant development and the response to a pathogen infection or abiotic stress [36,55]. In our analysis, one over-accumulated and one under-accumulated dirigent protein were identified. Numerous genes encoding the dirigent proteins were found to be up-regulated in response to salt stress in the roots of *B. distachyon*, among which *Bradi1g20950* encoding a CWP that was found among the over-accumulated CWPs in this experiment [56]. In *Medicago sativa*, a gene encoding a dirigent protein was up-regulated due to heat stress [57]. Though a few studies have shown changes in the expression of the genes encoding the dirigent proteins, the molecular mechanisms underpinning their involvement in stress responses remain to be elucidated [55]. The next group of miscellaneous proteins - the germin proteins - has also been indicated to respond to abiotic stresses with genes that exhibit various expression changes as has been shown for rice that had been subjected to desiccation, salt or cold stress [58]. The one germin protein was under-accumulated at 40 °C compared to the control. Another protein, an SCP-like extracellular protein, was also found to be under-accumulated. Dienelactone hydrolase catalyses the conversion of dienelactone to maleylacetate and participates in the degradation of the haloaromatic compounds. The under-accumulation of a dienelactone hydrolase (Bradi3g18680) that was observed in this study may cause a decrease in the degradation of these secondary metabolites as has been suggested to explain a similar decrease in the abundance of a dienelactone hydrolase in the roots of soybean in response to a NaCl treatment [59]. Although the DUF642 protein family has been shown to be involved in the development and growth of plants and the response to various stresses, its precise function remains unknown [60]. In the fruit mesocarp of *Prunus persica*, the under-accumulation of a DUF642 protein was observed after a post-harvest heat treatment [61]. There was a similar under-accumulation of Bradi2g43230, which belongs to the DUF642 protein family. At the same time, a DUF538 protein was identified in the control, while it was absent at 40 °C. The DUF538 proteins are predicted to have esterase-type hydrolytic activity towards the bacterial lipopolysaccharides and chlorophyll molecules. Recently, the DUF538 proteins were also predicted to have pectin methylesterase activity [62].

3.4. Oxido-Reductases

The CIII Prxs belong to a large multigenic family and have dual hydroxylic and peroxidative cycles that allow them to build rigid cell walls or loosen them [63]. The specific function of a given CIII Prx remains elusive due to their substrate diversity and spatiotemporal regulation of the expression of their genes. However, for some CIII Prxs of *A. thaliana*, a role in cell wall dynamics could be attributed [63]. In the *B. distachyon* genome, 143 CIII Prxs genes have been annotated, though none of them was linked with a specific function [63,64]. In our experiment, we found four under-accumulated CIII Prxs at 40 °C and one only present in the control. We also observed the under-accumulation of a laccase and a blue copper-binding protein and the absence of one multicopper oxidase and a blue copper-binding protein at 40 °C. Taken together, this suggests a perturbation in the oxidative state of the cell wall and decreased lignification processes under heat stress.

3.5. Proteins Related to Lipid Metabolism

The GDSL-lipases/acylhydrolases play essential roles in plant growth and development, organ morphogenesis, the stress response and lipid metabolism as well as hydrolysing and synthesising various lipids [65]. Though genes encoding GDSL-lipases/acylhydrolases are

usually up-regulated in response to biotic stresses, a few experiments have also suggested their role in abiotic stresses. For example, an overexpression of *A. thaliana LTL1* leads to an increased salt tolerance [66]. Notably, the expression of GDSL-lipases/acylhydrolases varies significantly in response to salt stress as was shown for *B. distachyon* roots [56]. In the experiment presented here, four GDSL-lipases/acylhydrolases were under-accumulated at 40 °C, suggesting a decrease in hydrolysis and lipid synthesis in response to heat stress. Additionally, two GDSL-lipases/acylhydrolases present in the control were absent at 40 °C (Bradi3g39622 and Bradi1g01920). The under-accumulation of a glycerophosphoryl diester phosphodiesterase (GDPL) could suggest some changes in the primary cell wall organisation since it was shown that a mutant of *A. thaliana* with inactivated *SHV3* encoding a GDPL exhibited a ruptured root hair phenotype. This phenotype was suppressed by adding borate, which is involved in rhamnogalactunonan II cross-linking [67].

3.6. Proteins with Interaction Domains (with Proteins or Polysaccharides)

At 40 °C, the under-accumulated Bradi4g37090 protein had two LysM domains with a possible glycosylphosphatidylinositol anchor. Though proteins with the LysM domain can have different structures, they mediate the recognition of the different N-acetylglucosamine-containing ligands that facilitate microbial infection and symbiosis [68]. In our data, we also found a protein with a Barwin domain (Bradi4g14920) that was only present at 40 °C. The Barwin domain itself can bind carbohydrates and has an antifungal, ribonuclease or DNase activity [69]. Interestingly, proteins with this domain were previously observed to be over-accumulated in response to heat stress (after 6 h and 12 h) in rice [70]. The gene encoding this protein with a Barwin domain was also found to be upregulated in *B. distachyon* roots inoculated with *Pseudomonas fluorescens* SBW25 [71]. Taken together, this suggests the importance of Bradi4g14920 in the response to heat stress as well as in root defence mechanisms in response to bacterial colonisation. Such involvement in different stresses can be explained by the crosstalk between cellular signalling events [72]. Though, recent studies have shown that the plant responses to combinations of multiple stress conditions are unique and require species-specific studies [73].

3.7. Cell Wall Response to Temperature Stress

The changes in the cell wall proteome of the leaves at 40 °C compared to the control suggest a lower protease activity, lignification, an expansion of the cell wall and changes in the architecture of the cell wall polymers, especially the pectins. This enriches our understanding of the heat stress response that was robustly summarised by Le Gall et al. [9], where the authors highlighted the changes in the cell wall polysaccharides, cellulose, hemicelluloses and pectins, as well as lignin biosynthesis in response to heat stress. Moreover, *AGPs* are usually up-regulated under heat stress, which we showed in our previous work using RT-qPCR, and specific AGP epitopes accumulate as was shown by immunochemistry using specific antibodies. Interestingly, we could not identify any AGPs among the DAPs, which could be related to the fact that the changes in the AGP composition that were revealed by immunohistochemistry were tissue specific. However, one FLA (Bradi1g76630) was absent at 40 °C but was present in the control. The overall increase in their abundance might not be high enough to be significantly different between the treatments [27]. Alternatively, because these proteins are difficult to detect due to their small size and high level of glycosylation, they require specific approaches that begin with a deglycosylation step [74]. Thus, AGPs may have escaped our analysis like EXTs that are usually covalently cross-linked to other cell wall components [75]. Our study complements previous transcriptomic analysis of *B. distachyon* leaf response to the heat stress. In *B. distachyon* plants that have been treated at 42°C during 5 h, Chen et al. [29] observed differences in the expression of genes related to the photosynthesis-antenna proteins and the endoplasmic reticulum. Notably, high temperature also induced alternative splicing by up-regulation of gene expression involved in RNA splicing.

4. Materials and Methods

4.1. Plant Material and Treatment

Plants of the *B. distachyon* reference genotype Bd21 (accession number: PI 254867) were used and were treated as was previously described [27]. Briefly, the plants were grown in a greenhouse under a 16 h/8 h light/dark photoperiod at 21 ± 1 °C for four weeks and were illuminated by lamps emitting white light at an intensity of 150 µmol photons m^{-2} s^{-1}. The plants were then transferred to growth chambers for 24 h at 40 °C for the high temperature treatment. For the control treatment, the plants were kept at 21 °C. The relative humidity was maintained at around 50% for all temperatures. For each of four biological replications of the control and 40 °C treatment, plants from subsequent cultivations were used.

4.2. Cell Wall Proteins Isolation

To isolate CWPs, whole leaves of *B. distachyon* (from the control and 40 °C treatment) were collected. For each experiment, around 3 g fresh leaves were used. The cell wall was extracted as was previously described [76,77]. The samples were washed in distilled water and placed in a blender with 100 mL of a 5 mM acetate buffer (Merck, Darmstadt, Germany) (pH 4.6) that had been supplemented with 0.4 M sucrose (Chempur, Piekary Slaskie, Poland), a protease inhibitor cocktail (55 µL/g material) (P9599, Merck) and 0.5 g polyvinylpyrrolidone (Merck). The mixture was ground in the blender at full speed three times for 2 min. The cell walls were separated from the cytoplasmic fluids by centrifugations (Eppendorf AG, Hamburg, Germany) for 15 min at 3000 g at 4 °C. The supernatant was gently decanted, and the pellets were washed with a cold 5 mM acetate buffer (pH 4.6) that had been supplemented with 0.6 M sucrose and centrifuged again for 15 min at 3000 g at 4 °C. The supernatant was gently decanted, and the cell walls were washed with cold 5 mM acetate buffer (pH 4.6) that had been supplemented with 1 M sucrose. Lastly, the samples were centrifuged for 15 min at 3000 g at 4 °C. After the supernatant was removed, the pelleted material was placed on a nylon net (25 µm pore size) and washed with 1 L of a 5 mM acetate buffer (pH 4.6) to remove the sucrose. Then, the material was thinly spread in a plastic bag and frozen at −80 °C. The frozen material was ground in liquid nitrogen in a mortar with a pestle and lyophilised (Christ, Osterode am Harz, Germany) for two days. The dried powder was used to extract CWPs using salt solutions. Five mL of 0.2 M $CaCl_2$ in a 5 mM acetate buffer (pH 4.6) that had been supplemented with a 3.75 µL protease inhibitor cocktail was added to each sample. The samples were then vortexed for 30 min at 4 °C and centrifuged for 15 min at 5000 g at 4 °C. The supernatant was collected in a fresh tube and the extraction was repeated once with 0.2 M $CaCl_2$ (Merck) in a 5 mM acetate buffer (pH 4.6) and twice with 2 M LiCl (Merck) in a 5 mM acetate buffer (pH 4.6). The collected supernatants were desalted using Econo-Pac 10 DG columns (Bio-Rad, Hercules, CA, USA) that had been equilibrated with 0.1 M formic acid ammonium salt (Merck). The desalted samples were lyophilised and resuspended in distilled water. The protein concentration was measured using the Pierce BCA Protein Assay Kit according to the manufacturer's instructions (Thermo Fisher Scientific, Waltham, MA, USA). For each sample, 200 µg of the isolated proteins were transferred into separate tubes, lyophilised and saved for further proteomic analysis.

4.3. Sodium Dodecyl Sulphate Polyacrylamide Gel Electrophoresis (SDS-PAGE)

The quality and integrity of the isolated proteins were checked by separating them using SDS-PAGE. For the SDS-PAGE, a 12% separating gel was prepared, and for each well, 60 µg of the protein sample was mixed with a 4× Laemmli Sample Buffer (Merck) and heated in a water bath for 10 min before being applied to the gel [78]. As a protein ruler, a 5 µL Precision Plus Protein Kaleidoscope Prestained Protein Standards (Bio-Rad), 10 to 250 kDa, was used. After electrophoresis, the gel was washed three times with distilled water for 15 min. Then, it was stained with Coomassie® blue using an EZBlue™ Gel Staining Reagent (Merck) for 1 h and then washed three times with distilled water for 15 min and then overnight. The gels were scanned using a Brother MFC-J3530DW Business Smart Inkjet Printer All-in-One (Brother Industries, Nagoya, Japan).

4.4. Protein Tryptic Digestion and LC-MS/MS Analysis

The isolated proteins were suspended in a urea solution (8 M urea in 50 mM ammonium bicarbonate; BioShop Canada Inc., Burlington, Canada and Merck, respectively) to a concentration of 2 µg/µL and then 100 µg of proteins were prepared according to the FASP protocol [79]. The protein samples (100 µg) were diluted four times with the urea solution, reduced with 50 mM dithiothreitol (BioShop Canada Inc.) and incubated for 15 min at room temperature. Then, the samples were centrifuged (21 000 g, 15 min, 20 °C), transferred into filtration columns (30 kDa membrane cut-off, VIVACON 500, Sartorius Stedim Biotech GmbH, Göttingen, Germany) and centrifuged (14 000 g, 15 min, 20 °C). The 30 kDa membrane cut-off was used to increase the peptide yield and decrease sample preparation time while retaining small proteins [80]. The proteins remaining on the filter were washed with 200 µL of the urea solution and alkylated with 54 mM iodoacetamide (Merck) (20 min of incubation at room temperature in the dark). In the following steps, the proteins were washed three times with 100 µL of the urea solution and then three times with 100 µL of 50 mM ammonium bicarbonate (ABC) (Merck). After washing, trypsin (Promega, Madison, WI, USA) was added to the samples with an enzyme to protein ratio of 1:60. The lyophilised enzyme was suspended in 50 mM ABC to a final volume of 75 µL per sample. Digestion was performed overnight at 37 °C. The next day, the columns were transferred into new collection tubes, 40 µL of 50 mM ABC were added to the columns and the samples were centrifuged (14 000 g, 10 min, 20 °C). Then, the peptides were eluted with 40 µL of 50 mM ABC and 50 µL of 0.5 M NaCl. The obtained filtrate was collected and vacuum dried. The resulting peptide mixture was suspended in 100 µL of a loading buffer (2% acetonitrile with 0.05% trifluoroacetic acid; JT Baker, Phillipsburg, NJ, USA and Merk, respectively) and 1 µL of the solution was used for the LC-MS/MS analysis, which was performed on a Q Exactive mass spectrometer (Thermo Fisher Scientific) equipped with a PicoView nanospray source (DPV-550, New Objective, Aarle-Rixtel, The Netherlands) and coupled with a nanoHPLC (UltiMate 3000 RSLCnano System, Thermo Fisher Scientific). The peptides were loaded onto a pre-column (AcclaimPep-Map100 C18, Thermo Fisher Scientific; ID 75 µm, length 20 mm, particle size 3 µm, pore size 100 Å) and then eluted from an analytical column (AcclaimPepMapRLSC C18, Thermo Fisher Scientific; ID 75 µm, length 500 mm, particle size 2 µm, pore size 100 Å) in the presence of 0.05% formic acid (JT Baker) using a linear gradient of acetonitrile (2%–40%) for 240 min. The mass spectrometric measurement was performed in the data-dependent mode using the Top12 method. The MS and MS/MS spectra were acquired at resolutions of 70 000 and 17 500, respectively. The performance of the LC-MS/MS platform was monitored using the QCloud quality control system [81].

4.5. Bioinformatic Analysis

The LC-MS/MS data were processed using the MaxQuant software package (version 1.5.8.3) including the Andromeda search engine [82,83]. The protein sequences of *B. distachyon* Bd21 were downloaded from the Phytozome database (https://phytozome.jgi.doe.gov/pz/portal.html, accessed on 10 February 2021) (version 3.2, number of sequences 56,847). The search was done using the default parameters with minor modifications. The standard list of variable modifications, methionine oxidation and the acetylation of the protein N-termini was completed with proline oxidation. The false discovery rate (FDR) for the peptide and protein identification was set to 1%. Label free quantification (LFQ) was also enabled. The resulting table with the protein group identifications and quantitative information (LFQ intensities) was uploaded to the Perseus platform for further processing and statistical analysis [84]. The protein groups from the decoy database, contaminants and proteins only identified by site were filtered out. The data were log-transformed, and the matrix was filtered for the protein groups that had valid LFQ values in at least three replicates within each group. Then, any missing values were imputed from a normal distribution. Principal component analysis and hierarchical clustering were performed in Perseus using the default settings. The Student's t-test with the permutation-based FDR set to 1% was used to reveal changes between the treatments. The resulting list of differential protein groups was additionally filtered for the protein groups that had been identified

based on at least two specific peptides. A fold change threshold of 1.5 was used. Moreover, the protein groups that had been detected in all of the replicates from one experimental group and none of the other group replicates were considered to be qualitative differences.

4.6. RT-qPCR Analysis

To correlate the proteomic analysis results, six genes were selected to characterise the level of their transcript accumulation using RT-qPCR. Three genes (*Bradi1g52050*, *Bradi4g09417* and *Bradi4g09430*) were selected based on the highest differences in the accumulation of the proteins between the control and the 40 °C treatment, and the three other genes (*Bradi1g38780*, *Bradi1g25517* and *Bradi1g58997*) were selected to represent proteins from different families. The RNA for the control and treated leaves were isolated as described previously [27]. The primers that were used are listed in Table A1. The detailed procedure for RT-qPCR was also previously described [27]. Since we have already shown that the level of expression of the polyubiquitin gene (*Bradi1g32860*) was stable under different temperature treatments it was used as a reference [27]. The analysis was performed using the $2^{-\Delta\Delta CT}$ method. The control treatment (at 21 °C) was used as the reference group. Three biological replicates were performed with two technical replicates for each. The analysis of the statistical differences between the treatments and the control was done with Student's t-test (TIBCO Software Inc., Palo Alto, CA, USA). As mentioned in Section 4.4, the proteomics data were log-transformed, and the Student's t-test with the permutation-based FDR set to 1% was used for statistical analysis of differences between the treatments and the control (Perseus, Max-Planck Institute of Biochemistry, Martinsried, Germany).

5. Conclusions

In this work, we focused on the changes in the cell wall proteome in response to high (40 °C) temperature treatment. We showed that a high temperature resulted in qualitative and quantitative changes compared to the control (21 °C). The qualitative analysis indicated a lower contribution of the proteins acting on cell wall polysaccharides and oxidoreductases and a higher representation of the miscellaneous proteins at 40 °C. Further, a quantitative analysis revealed 46 DAPs: 4 were over-accumulated and 42 were under-accumulated. Overall, this suggests a lower protease activity, lignification, an expansion of the cell wall and changes in the architecture of the cell wall polymers, especially the pectins at 40 °C. Our results provide a new insight into the changes in the cell wall proteome in response to high temperature, and also present potential new targets for further studies of the cell wall response to high temperature stress, such as *Bradi4g09430* (GH18, xylanase inhibitor/class II chitinase) and *Bradi1g52050* (GH28, polygalacturonase).

Supplementary Materials: The following are available online at https://www.mdpi.com/article/10.3390/ijms22136750/s1.

Author Contributions: Conceptualisation, A.P. and A.B.; methodology, A.P., B.S.-R., U.J. and E.J.; validation, A.P., B.S.-R., U.J. and E.J.; formal analysis, A.P., B.S.-R., U.J. and E.J.; investigation, A.P. and E.J.; resources, R.H.; data curation, A.P. and E.J.; writing—original draft preparation, A.P.; writing—review and editing, all authors; visualisation, A.P., B.S.-R. and U.J.; supervision, A.P. and A.B.; funding acquisition, R.H. All authors have read and agreed to the published version of the manuscript.

Funding: The work was co-financed by the funds granted under the Research Excellence Initiative of the University of Silesia in Katowice. E.J. wishes to thank the CNRS and the Toulouse 3 University for funding her research.

Data Availability Statement: The mass spectrometry data were deposited at the ProteomeXchange Consortium [85] via the MassIVE repository with the dataset identifier PXD025679. The cell wall proteomics data have been deposited at *WallProtDB* http://www.polebio.lrsv.ups-tlse.fr/WallProtDB/, accessed on 29 March 2021).

Acknowledgments: A.P. is thankful to ERASMUS for funding his stay at LRSV. The authors thank Hélène San Clemente for including the proteomics data in *WallProtDB*.

Conflicts of Interest: The authors declare no conflict of interest. The funders had no role in the design of the study; in the collection, analyses or interpretation of data; in the writing of the manuscript or in the decision to publish the results.

Appendix A

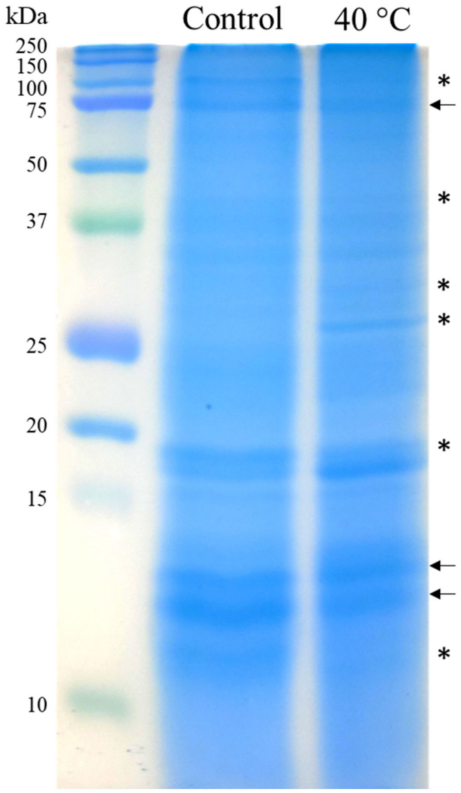

Figure A1. The 1D-electrophoretic patterns of the proteins that were isolated from the purified cell walls of the *B. distachyon* leaves that had been treated at 40 °C and the control. Sixty µg of the proteins were analysed for each sample. After electrophoresis, the proteins were stained with Coomassie blue. Some of the bands of similar intensity across all treatments are marked with arrows. The bands differentiating plants treated at 40 °C from those at the control are marked with asterisks.

Table A1. The oligonucleotide primers that were used for the RT-qPCR analysis with the relevant descriptions of the genes.

Genes	Description of the Genes	Primer Sequences (5′→3′)
Bradi1g32860	Ubiquitin	GAGGGTGGACTCCTTTTGGA TCCACACTCCACTTGGTGCT
Bradi1g52050	GH28	CGACATGGTGGTCGAAATAC GTGACGTTGGAGATGAAGATG
Bradi1g38780	GDSL/lipase acylhydrolase	CCCTCTGTAAATCGGAGAAAG CGGAGAACAATGGAGCATTA
Bradi1g25517	GH17	GCGAGTTCAAAGACGACAT GTACGTGTAGTACGGGTAGAT
Bradi1g58997	class III peroxidase (BdiPrx35)	GGTCCTTCGACAACCAGTA TAGTCCTCGAGTCGGTGTA
Bradi4g09417	GH18	CTCCCTCATAGCTCTCCTATC GAGCCTTCGTCCTTGTTC
Bradi4g09430	GH18	AGGTTCTACATCGGGCTTAC GCCGTAGTTCTCCTTCTTCT

References

1. Debaeke, P.; Pellerin, S.; Scopel, E. Climate-smart cropping systems for temperate and tropical agriculture: Mitigation, adaptation and trade-offs. *Cah. Agric.* **2017**, *26*, 34002. [CrossRef]
2. Zhao, C.; Liu, B.; Piao, S.; Wang, X.; Lobell, D.B.; Huang, Y.; Huang, M.; Yao, Y.; Bassu, S.; Ciais, P.; et al. Temperature increase reduces global yields of major crops in four independent estimates. *Proc. Natl. Acad. Sci. USA* **2017**, *114*, 9326–9331. [CrossRef]
3. Jansson, C.; Vogel, J.; Hazen, S.; Brutnell, T.; Mockler, T. Climate-smart crops with enhanced photosynthesis. *J. Exp. Bot.* **2018**, *69*, 3801–3809. [CrossRef]
4. De Pinto, A.; Cenacchi, N.; Kwon, H.Y.; Koo, J.; Dunston, S. Climate smart agriculture and global food-crop production. *PLoS ONE* **2020**, *15*, e0231764. [CrossRef]
5. Taylor, M. Climate-smart agriculture: What is it good for? *J. Peasant Stud.* **2017**, *45*, 89–107. [CrossRef]
6. Pushpalatha, R.; Gangadharan, B. Is cassava (*Manihot esculenta* Crantz) a climate "smart" crop? A review in the context of bridging future food demand gap. *Trop. Plant. Biol.* **2020**, *13*, 201–211. [CrossRef]
7. Varotto, S.; Tani, E.; Abraham, E.; Krugman, T.; Kapazoglou, A.; Melzer, R.; Radanovic, A.; Miladinovic, D. Epigenetics: Possible applications in climate-smart crop breeding. *J. Exp. Bot.* **2020**, *71*, 5223–5236. [CrossRef] [PubMed]
8. Yamauchi, T.; Noshita, K.; Tsutsumi, N. Climate-smart crops: Key root anatomical traits that confer flooding tolerance. *Breed. Sci.* **2021**, 20119. [CrossRef]
9. Le Gall, H.; Philippe, F.; Domon, J.M.; Gillet, F.; Pelloux, J.; Rayon, C. Cell wall metabolism in response to abiotic stress. *Plants* **2015**, *4*, 112–166. [CrossRef] [PubMed]
10. Acosta-Motos, J.; Ortuño, M.; Bernal-Vicente, A.; Diaz-Vivancos, P.; Sanchez-Blanco, M.; Hernandez, J. Plant responses to salt stress: Adaptive mechanisms. *Agronomy* **2017**, *7*, 18. [CrossRef]
11. Niu, Y.; Xiang, Y. An overview of biomembrane functions in plant responses to high-temperature stress. *Front. Plant. Sci.* **2018**, *9*, 915. [CrossRef]
12. Fahad, S.; Bajwa, A.A.; Nazir, U.; Anjum, S.A.; Farooq, A.; Zohaib, A.; Sadia, S.; Nasim, W.; Adkins, S.; Saud, S.; et al. Crop production under drought and heat stress: Plant responses and management options. *Front. Plant. Sci.* **2017**, *8*, 1147. [CrossRef] [PubMed]
13. Mur, L.A.J.; Corke, F.M.K.; Doonan, J.H. Brachypodium: A model temperate grass. *eLS* **2015**. [CrossRef]
14. Vogel, J. Unique aspects of the grass cell wall. *Curr. Opin. Plant. Biol.* **2008**, *11*, 301–307. [CrossRef] [PubMed]
15. Hus, K.; Betekhtin, A.; Pinski, A.; Rojek-Jelonek, M.; Grzebelus, E.; Nibau, C.; Gao, M.; Jaeger, K.E.; Jenkins, G.; Doonan, J.H.; et al. A CRISPR/Cas9-Based mutagenesis protocol for *Brachypodium distachyon* and its allopolyploid relative, *Brachypodium hybridum*. *Front. Plant. Sci.* **2020**, *11*, 614. [CrossRef] [PubMed]
16. Coomey, J.H.; Sibout, R.; Hazen, S.P. Grass secondary cell walls, *Brachypodium distachyon* as a model for discovery. *N. Phytol.* **2020**, *227*, 1649–1667. [CrossRef]
17. Alves, S.C.; Worland, B.; Thole, V.; Snape, J.W.; Bevan, M.W.; Vain, P. A protocol for *Agrobacterium*-mediated transformation of *Brachypodium distachyon* community standard line Bd21. *Nat. Protoc.* **2009**, *4*, 638–649. [CrossRef]
18. International_Brachypodium_Initiative. Genome sequencing and analysis of the model grass *Brachypodium distachyon*. *Nature* **2010**, *463*, 763–768. [CrossRef]
19. Gordon, S.P.; Contreras-Moreira, B.; Woods, D.P.; Des Marais, D.L.; Burgess, D.; Shu, S.; Stritt, C.; Roulin, A.C.; Schackwitz, W.; Tyler, L.; et al. Extensive gene content variation in the *Brachypodium distachyon* pan-genome correlates with population structure. *Nat. Commun.* **2017**, *8*, 2184. [CrossRef]
20. Skalska, A.; Stritt, C.; Wyler, M.; Williams, H.W.; Vickers, M.; Han, J.; Tuna, M.; Savas Tuna, G.; Susek, K.; Swain, M.; et al. Genetic and methylome variation in Turkish *Brachypodium distachyon* accessions differentiate two geographically distinct subpopulations. *Int. J. Mol. Sci.* **2020**, *21*, 6700. [CrossRef]
21. Rancour, D.M.; Marita, J.M.; Hatfield, R.D. Cell wall composition throughout development for the model grass *Brachypodium distachyon*. *Front. Plant. Sci.* **2012**, *3*, 266. [CrossRef]
22. Bita, C.E.; Gerats, T. Plant tolerance to high temperature in a changing environment: Scientific fundamentals and production of heat stress-tolerant crops. *Front. Plant. Sci.* **2013**, *4*, 273. [CrossRef]
23. Janmohammadi, M.; Zolla, L.; Rinalducci, S. Low temperature tolerance in plants: Changes at the protein level. *Phytochemistry* **2015**, *117*, 76–89. [CrossRef]
24. Albenne, C.; Canut, H.; Boudart, G.; Zhang, Y.; San Clemente, H.; Pont-Lezica, R.; Jamet, E. Plant cell wall proteomics: Mass spectrometry data, a trove for research on protein structure/function relationships. *Mol. Plant.* **2009**, *2*, 977–989. [CrossRef]
25. Albenne, C.; Canut, H.; Hoffmann, L.; Jamet, E. Plant cell wall proteins: A large body of data, but what about runaways? *Proteomes* **2014**, *2*, 224–242. [CrossRef] [PubMed]
26. San Clemente, H.; Jamet, E. WallProtDB, a database resource for plant cell wall proteomics. *Plant. Methods* **2015**, *11*, 2. [CrossRef] [PubMed]
27. Pinski, A.; Betekhtin, A.; Sala, K.; Godel-Jedrychowska, K.; Kurczynska, E.; Hasterok, R. Hydroxyproline-rich glycoproteins as markers of temperature stress in the leaves of *Brachypodium distachyon*. *Int. J. Mol. Sci.* **2019**, *20*, 2571. [CrossRef]
28. Liu, J.; Pang, C.; Wei, H.; Song, M.; Meng, Y.; Ma, J.; Fan, S.; Yu, S. iTRAQ-facilitated proteomic profiling of anthers from a photosensitive male sterile mutant and wild-type cotton (*Gossypium hirsutum* L.). *J. Proteomics* **2015**, *126*, 68–81. [CrossRef]

29. Chen, S.; Li, H. Heat stress regulates the expression of genes at transcriptional and post-transcriptional levels, revealed by RNA-seq in *Brachypodium distachyon*. *Front. Plant. Sci.* **2016**, *7*, 2067. [CrossRef] [PubMed]
30. Xu, J.; Belanger, F.; Huang, B. Differential gene expression in shoots and roots under heat stress for a geothermal and non-thermal *Agrostis* grass species contrasting in heat tolerance. *Environ. Exp. Bot.* **2008**, *63*, 240–247. [CrossRef]
31. Xu, G.; Wang, S.; Han, S.; Xie, K.; Wang, Y.; Li, J.; Liu, Y. Plant Bax Inhibitor-1 interacts with ATG6 to regulate autophagy and programmed cell death. *Autophagy* **2017**, *13*, 1161–1175. [CrossRef]
32. Minina, E.A.; Filonova, L.H.; Fukada, K.; Savenkov, E.I.; Gogvadze, V.; Clapham, D.; Sanchez-Vera, V.; Suarez, M.F.; Zhivotovsky, B.; Daniel, G. Autophagy and metacaspase determine the mode of cell death in plants. *J. Cell Biol. Biol.* **2013**, *203*, 917–927. [CrossRef] [PubMed]
33. Wang, X.; Liang, H.; Guo, D.; Guo, L.; Duan, X.; Jia, Q.; Hou, X. Integrated analysis of transcriptomic and proteomic data from tree peony (*P. ostii*) seeds reveals key developmental stages and candidate genes related to oil biosynthesis and fatty acid metabolism. *Hortic. Res.* **2019**, *6*, 111. [CrossRef] [PubMed]
34. Haider, S.; Pal, R. Integrated analysis of transcriptomic and proteomic data. *Curr. Genom.* **2013**, *14*, 91–110. [CrossRef]
35. Calderan-Rodrigues, M.J.; Fonseca, J.G.; San Clemente, H.; Labate, C.A.; Jamet, E. Glycoside hydrolases in plant cell wall proteomes: Predicting functions that could be relevant for improving biomass transformation processes. In *Advances in Biofuels and Bioenergy*; Nageswara-Rao, M., Soneji, J.R., Eds.; IntechOpen: London, UK, 2018. [CrossRef]
36. Calderan-Rodrigues, M.J.; Guimarães Fonseca, J.; de Moraes, F.E.; Vaz Setem, L.; Carmanhanis Begossi, A.; Labate, C.A. Plant cell wall proteomics: A focus on monocot species, *Brachypodium distachyon*, *Saccharum* spp. and *Oryza sativa*. *Int. J. Mol. Sci.* **2019**, *20*, 1975. [CrossRef] [PubMed]
37. Sonah, H.; Chavan, S.; Katara, J.; Chaudhary, J.; Kadam, S.; Patil, G.; Deshmukh, R. Genome-wide identification and characterization of Xylanase Inhibitor Protein (XIP) genes in cereals. *Indian J. Genet.* **2016**, *76*, 159–166. [CrossRef]
38. Durand, A.; Hughes, R.; Roussel, A.; Flatman, R.; Henrissat, B.; Juge, N. Emergence of a subfamily of xylanase inhibitors within glycoside hydrolase family 18. *FEBS J.* **2005**, *272*, 1745–1755. [CrossRef] [PubMed]
39. Minic, Z. Physiological roles of plant glycoside hydrolases. *Planta* **2008**, *227*, 723–740. [CrossRef]
40. Francin-Allami, M.; Merah, K.; Albenne, C.; Rogniaux, H.; Pavlovic, M.; Lollier, V.; Sibout, R.; Guillon, F.; Jamet, E.; Larré, C. Cell wall proteomic of *Brachypodium distachyon* grains: A focus on cell wall remodeling proteins. *Proteomics* **2015**, *15*, 2296–2306. [CrossRef]
41. Cosgrove, D.J. Catalysts of plant cell wall loosening. *F1000Res.* **2016**, *5*, 119. [CrossRef]
42. Xu, Z.; Escamilla-Trevino, L.L.; Zeng, L.; Lalgondar, M.; Bevan, D.R.; Winkel, B.S.J.; Mohamed, A.; Cheng, C.-L.; Shih, M.-C.; Poulton, J.E.; et al. Functional genomic analysis of *Arabidopsis thaliana* glycoside hydrolase family 1. *Plant. Mol. Biol.* **2004**, *55*, 343–367. [CrossRef]
43. Song, Y.; Ci, D.; Tian, M.; Zhang, D. Comparison of the physiological effects and transcriptome responses of *Populus simonii* under different abiotic stresses. *Plant. Mol. Biol.* **2014**, *86*, 139–156. [CrossRef] [PubMed]
44. Yu, E.; Fan, C.; Yang, Q.; Li, X.; Wan, B.; Dong, Y.; Wang, X.; Zhou, Y. Identification of heat responsive genes in *Brassica napus* siliques at the seed-filling stage through transcriptional profiling. *PLoS ONE* **2014**, *9*, e101914. [CrossRef] [PubMed]
45. Xu, J.; Tian, J.; Belanger, F.C.; Huang, B. Identification and characterization of an expansin gene *AsEXP1* associated with heat tolerance in C3 *Agrostis* grass species. *J. Exp. Bot.* **2007**, *58*, 3789–3796. [CrossRef] [PubMed]
46. Tan, J.; Wang, M.; Shi, Z.; Miao, X. *OsEXPA10* mediates the balance between growth and resistance to biotic stress in rice. *Plant. Cell Rep.* **2018**, *37*, 993–1002. [CrossRef]
47. Ding, X.; Cao, Y.; Huang, L.; Zhao, J.; Xu, C.; Li, X.; Wang, S. Activation of the indole-3-acetic acid-amido synthetase GH3-8 suppresses expansin expression and promotes salicylate- and jasmonate-independent basal immunity in rice. *Plant. Cell* **2008**, *20*, 228–240. [CrossRef]
48. Zhu, X.F.; Sun, Y.; Zhang, B.C.; Mansoori, N.; Wan, J.X.; Liu, Y.; Wang, Z.W.; Shi, Y.Z.; Zhou, Y.H.; Zheng, S.J. Trichome Birefringence-Like27 affects aluminum sensitivity by modulating the O-acetylation of xyloglucan and aluminum-binding capacity in Arabidopsis. *Plant. Physiol.* **2014**, *166*, 181–189. [CrossRef]
49. Nafisi, M.; Stranne, M.; Fimognari, L.; Atwell, S.; Martens, H.J.; Pedas, P.R.; Hansen, S.F.; Nawrath, C.; Scheller, H.V.; Kliebenstein, D.J.; et al. Acetylation of cell wall is required for structural integrity of the leaf surface and exerts a global impact on plant stress responses. *Front. Plant. Sci.* **2015**, *6*, 550. [CrossRef]
50. Gao, Y.; He, C.; Zhang, D.; Liu, X.; Xu, Z.; Tian, Y.; Liu, X.H.; Zang, S.; Pauly, M.; Zhou, Y.; et al. Two trichome birefringence-like proteins mediate xylan acetylation, which is essential for leaf blight resistance in rice. *Plant. Physiol.* **2017**, *173*, 470–481. [CrossRef]
51. Chen, J.; Liu, W.; Liu, C.M.; Li, T.; Liang, R.H.; Luo, S.J. Pectin modifications: A review. *Crit. Rev. Food Sci. Nutr.* **2015**, *55*, 1684–1698. [CrossRef]
52. Tenhaken, R. Cell wall remodeling under abiotic stress. *Front. Plant. Sci.* **2014**, *5*, 771. [CrossRef] [PubMed]
53. Wu, H.C.; Bulgakov, V.P.; Jinn, T.L. Pectin methylesterases: Cell wall remodeling proteins are required for plant response to heat stress. *Front. Plant. Sci.* **2018**, *9*, 1612. [CrossRef] [PubMed]
54. Saada, S.; Solomon, C.U.; Drea, S. Programmed cell death in the developing *Brachypodium distachyon* grain. *bioRxiv* **2019**. [CrossRef]

55. Paniagua, C.; Bilkova, A.; Jackson, P.; Dabravolski, S.; Riber, W.; Didi, V.; Houser, J.; Gigli-Bisceglia, N.; Wimmerova, M.; Budinska, E.; et al. Dirigent proteins in plants: Modulating cell wall metabolism during abiotic and biotic stress exposure. *J. Exp. Bot.* **2017**, *68*, 3287–3301. [CrossRef] [PubMed]
56. Guo, X.; Wang, Q.; Liu, Y.; Zhang, X.; Zhang, L.; Fan, S. Screening of salt stress responsive genes in *Brachypodium distachyon* (L.) Beauv. by transcriptome analysis. *Plants* **2020**, *9*, 1622. [CrossRef] [PubMed]
57. Behr, M.; Legay, S.; Hausman, J.F.; Guerriero, G. Analysis of cell wall-related genes in organs of *Medicago sativa* l. under different abiotic stresses. *Int. J. Mol. Sci.* **2015**, *16*, 16104–16124. [CrossRef]
58. Li, L.; Xu, X.; Chen, C.; Shen, Z. Genome-wide characterization and expression analysis of the germin-like protein family in rice and Arabidopsis. *Int. J. Mol. Sci.* **2016**, *17*, 1622. [CrossRef]
59. Sobhanian, H.; Razavizadeh, R.; Nanjo, Y.; Ehsanpour, A.A.; Jazii, F.R.; Motamed, N.; Komatsu, S. Proteome analysis of soybean leaves, hypocotyls and roots under salt stress. *Proteome Sci.* **2010**, *8*, 19. [CrossRef]
60. Cruz-Valderrama, J.E.; Gomez-Maqueo, X.; Salazar-Iribe, A.; Zuniga-Sanchez, E.; Hernandez-Barrera, A.; Quezada-Rodriguez, E.; Gamboa-deBuen, A. Overview of the role of cell wall DUF642 proteins in plant development. *Int. J. Mol. Sci.* **2019**, *20*, 3333. [CrossRef]
61. Bustamante, C.A.; Budde, C.O.; Borsani, J.; Lombardo, V.A.; Lauxmann, M.A.; Andreo, C.S.; Lara, M.V.; Drincovich, M.F. Heat treatment of peach fruit: Modifications in the extracellular compartment and identification of novel extracellular proteins. *Plant. Physiol. Biochem.* **2012**, *60*, 35–45. [CrossRef]
62. Gholizadeh, A. Pectin methylesterase activity of plant DUF538 protein superfamily. *Physiol. Mol. Biol. Plants* **2020**, *26*, 829–839. [CrossRef] [PubMed]
63. Francoz, E.; Ranocha, P.; Nguyen-Kim, H.; Jamet, E.; Burlat, V.; Dunand, C. Roles of cell wall peroxidases in plant development. *Phytochemistry* **2015**, *112*, 15–21. [CrossRef]
64. Fawal, N.; Li, Q.; Savelli, B.; Brette, M.; Passaia, G.; Fabre, M.; Mathé, C.; Dunand, C. PeroxiBase: A database for large-scale evolutionary analysis of peroxidases. *Nucleic Acids Res.* **2013**, *41*, D441–D444. [CrossRef] [PubMed]
65. Ding, L.-N.; Li, M.; Wang, W.-J.; Cao, J.; Wang, Z.; Zhu, K.-M.; Yang, Y.-H.; Li, Y.-L.; Tan, X.-L. Advances in plant GDSL lipases: From sequences to functional mechanisms. *Acta Physiol. Plant.* **2019**, *41*, 151. [CrossRef]
66. Naranjo, M.A.; Forment, J.; Roldan, M.; Serrano, R.; Vicente, O. Overexpression of *Arabidopsis thaliana* LTL1, a salt-induced gene encoding a GDSL-motif lipase, increases salt tolerance in yeast and transgenic plants. *Plant. Cell Environ.* **2006**, *29*, 1890–1900. [CrossRef] [PubMed]
67. Hayashi, S.; Ishii, T.; Matsunaga, T.; Tominaga, R.; Kuromori, T.; Wada, T.; Shinozaki, K.; Hirayama, T. The glycerophosphoryl diester phosphodiesterase-like proteins SHV3 and its homologs play important roles in cell wall organization. *Plant. Cell Physiol.* **2008**, *49*, 1522–1535. [CrossRef]
68. Gust, A.A.; Willmann, R.; Desaki, Y.; Grabherr, H.M.; Nurnberger, T. Plant LysM proteins: Modules mediating symbiosis and immunity. *Trends Plant. Sci.* **2012**, *17*, 495–502. [CrossRef]
69. Dabravolski, S.A.; Frenkel, Z. Diversity and evolution of pathogenesis-related proteins family 4 beyond plant kingdom. *Plant. Gene* **2021**, *26*, 100279. [CrossRef]
70. Wang, N.; Xiao, B.; Xiong, L. Identification of a cluster of PR4-like genes involved in stress responses in rice. *J. Plant. Physiol.* **2011**, *168*, 2212–2224. [CrossRef]
71. Boiteau, R.M.; Markillie, L.M.; Hoyt, D.W.; Hu, D.; Chu, R.K.; Mitchell, H.D.; Pasa-Tolic, L.; Jansson, J.K.; Jansson, C. Metabolic interactions between *Brachypodium* and *Pseudomonas fluorescens* under controlled iron-limited conditions. *mSystems* **2021**, *6*, e00580-20. [CrossRef]
72. Fraire-Velázquez, S.; Rodríguez-Guerra, R.; Sánchez-Calderón, L. Abiotic and biotic stress response crosstalk in plants. In *Abiotic Stress Response in Plants—Physiological, Biochemical and Genetic Perspectives*; Shanker, A., Venkateswarlu, B., Eds.; IntechOpen: London, UK, 2011; pp. 3–26. [CrossRef]
73. Suzuki, N.; Rivero, R.M.; Shulaev, V.; Blumwald, E.; Mittler, R. Abiotic and biotic stress combinations. *N. Phytol.* **2014**, *203*, 32–43. [CrossRef]
74. Schultz, C.J.; Ferguson, K.L.; Lahnstein, J.; Bacic, A. Post-translational modifications of arabinogalactan-peptides of Arabidopsis thaliana. Endoplasmic reticulum and glycosylphosphatidylinositol-anchor signal cleavage sites and hydroxylation of proline. *J. Biol. Chem.* **2004**, *279*, 45503–45511. [CrossRef] [PubMed]
75. Albenne, C.; Canut, H.; Jamet, E. Plant cell wall proteomics: The leadership of *Arabidopsis thaliana*. *Front. Plant. Sci.* **2013**, *4*, 111. [CrossRef]
76. Feiz, L.; Irshad, M.; Pont-Lezica, R.F.; Canut, H.; Jamet, E. Evaluation of cell wall preparations for proteomics: A new procedure for purifying cell walls from Arabidopsis hypocotyls. *Plant. Methods* **2006**, *2*, 10. [CrossRef] [PubMed]
77. Douché, T.; San Clemente, H.; Burlat, V.; Roujol, D.; Valot, B.; Zivy, M.; Pont-Lezica, R.; Jamet, E. *Brachypodium distachyon* as a model plant toward improved biofuel crops: Search for secreted proteins involved in biogenesis and disassembly of cell wall polymers. *Proteomics* **2013**, *13*, 2438–2454. [CrossRef]
78. Laemmli, U. Denaturing (SDS) discontinuous gel electrophoresis. *Nature* **1970**, *277*, 680–685. [CrossRef] [PubMed]
79. Wisniewski, J.R.; Zougman, A.; Nagaraj, N.; Mann, M. Universal sample preparation method for proteome analysis. *Nat. Methods* **2009**, *6*, 359–362. [CrossRef]

80. Wisniewski, J.R.; Zougman, A.; Mann, M. Combination of FASP and StageTip-based fractionation allows in-depth analysis of the hippocampal membrane proteome. *J. Prot. Res.* **2009**, *8*, 5674–5678. [CrossRef]
81. Chiva, C.; Olivella, R.; Borras, E.; Espadas, G.; Pastor, O.; Sole, A.; Sabido, E. QCloud: A cloud-based quality control system for mass spectrometry-based proteomics laboratories. *PLoS ONE* **2018**, *13*, e0189209. [CrossRef]
82. Tyanova, S.; Temu, T.; Cox, J. The MaxQuant computational platform for mass spectrometry-based shotgun proteomics. *Nat. Protoc.* **2016**, *11*, 2301–2319. [CrossRef]
83. Cox, J.; Neuhauser, N.; Michalski, A.; Scheltema, R.A.; Olsen, J.V.; Mann, M. Andromeda: A peptide search engine integrated into the MaxQuant environment. *J. Proteome Res.* **2011**, *10*, 1794–1805. [CrossRef] [PubMed]
84. Tyanova, S.; Temu, T.; Sinitcyn, P.; Carlson, A.; Hein, M.Y.; Geiger, T.; Mann, M.; Cox, J. The Perseus computational platform for comprehensive analysis of (prote)omics data. *Nat. Methods* **2016**, *13*, 731–740. [CrossRef] [PubMed]
85. Vizcaino, J.A.; Deutsch, E.W.; Wang, R.; Csordas, A.; Reisinger, F.; Rios, D.; Dianes, J.A.; Sun, Z.; Farrah, T.; Bandeira, N.; et al. ProteomeXchange provides globally coordinated proteomics data submission and dissemination. *Nat. Biotechnol.* **2014**, *32*, 223–236. [CrossRef] [PubMed]

II.3

Hus K, Betekhtin A, Pinski A, Rojek-Jelonek M, Grzebelus E, Nibau C, Gao M, Jaeger K.E, Jenkins G, Doonan J.H, Hasterok R.

A CRISPR/Cas9-based mutagenesis protocol for *Brachypodium distachyon* and its allopolyploid relative, *Brachypodium hybridum*

Frontiers in Plant Science, 2020, 11, 614

IF_{2020} – 5,753; pkt MNiSW – 100

frontiers in Plant Science

METHODS
published: 20 May 2020
doi: 10.3389/fpls.2020.00614

A CRISPR/Cas9-Based Mutagenesis Protocol for *Brachypodium distachyon* and Its Allopolyploid Relative, *Brachypodium hybridum*

Karolina Hus[1†], Alexander Betekhtin[1†], Artur Pinski[1], Magdalena Rojek-Jelonek[1], Ewa Grzebelus[2], Candida Nibau[3], Mingjun Gao[4], Katja E. Jaeger[4,5], Glyn Jenkins[6], John H. Doonan[3] and Robert Hasterok[1]*

[1] Plant Cytogenetics and Molecular Biology Group, Institute of Biology, Biotechnology and Environmental Protection, Faculty of Natural Sciences, University of Silesia in Katowice, Katowice, Poland, [2] Department of Plant Biology and Biotechnology, Faculty of Biotechnology and Horticulture, University of Agriculture in Cracow, Cracow, Poland, [3] National Plant Phenomics Centre, Institute of Biological, Environmental and Rural Sciences, Aberystwyth University, Aberystwyth, United Kingdom, [4] Sainsbury Laboratory, University of Cambridge, Cambridge, United Kingdom, [5] Department for Plant Adaptation, Leibniz Institute of Vegetable and Ornamental Crops, Großbeeren, Germany, [6] Institute of Biological, Environmental and Rural Sciences, Aberystwyth University, Aberystwyth, United Kingdom

OPEN ACCESS

Edited by:
Roger Deal,
Emory University, United States

Reviewed by:
Zhen Chang Liang,
Chinese Academy of Sciences, China
Zhaoqing Chu,
Shanghai Chenshan Plant Science Research Center (CAS), China

***Correspondence:**
Alexander Betekhtin
alexander.betekhtin@us.edu.pl;
abetekht@us.edu.pl

[†] These authors have contributed equally to this work

Specialty section:
This article was submitted to Technical Advances in Plant Science, a section of the journal Frontiers in Plant Science

Received: *20 February 2020*
Accepted: *21 April 2020*
Published: *20 May 2020*

Citation:
Hus K, Betekhtin A, Pinski A, Rojek-Jelonek M, Grzebelus E, Nibau C, Gao M, Jaeger KE, Jenkins G, Doonan JH and Hasterok R (2020) A CRISPR/Cas9-Based Mutagenesis Protocol for Brachypodium distachyon and Its Allopolyploid Relative, Brachypodium hybridum. Front. Plant Sci. 11:614. doi: 10.3389/fpls.2020.00614

The CRISPR/Cas9 system enables precise genome editing and is a useful tool for functional genomic studies. Here we report a detailed protocol for targeted genome editing in the model grass *Brachypodium distachyon* and its allotetraploid relative *B. hybridum*, describing gRNA design, a transient protoplast assay to test gRNA efficiency, *Agrobacterium*-mediated transformation and the selection and analysis of regenerated plants. In *B. distachyon*, we targeted the gene encoding phytoene desaturase (PDS), which is a crucial enzyme in the chlorophyll biosynthesis pathway. The albino phenotype of mutants obtained confirmed the effectiveness of the protocol for functional gene analysis. Additionally, we targeted two genes related to cell wall maintenance, encoding a fasciclin-like arabinogalactan protein (FLA) and a pectin methylesterase (PME), also in *B. distachyon*. Two genes encoding cyclin-dependent kinases (CDKG1 and CDKG2), which may be involved in DNA recombination were targeted in both *B. distachyon* and *B. hybridum*. Cas9 activity induces mainly insertions or deletions, resulting in frameshift mutations that, may lead to premature stop codons. Because of the close phylogenetic relationship between *Brachypodium* species and key temperate cereals and forage grasses, this protocol should be easily adapted to target genes underpinning agronomically important traits.

Keywords: CRISPR/Cas9 system, targeted mutagenesis, *Brachypodium distachyon*, *Brachypodium hybridum*, *Agrobacterium*-mediated transformation, transient protoplast assay

INTRODUCTION

Precise and efficient genome targeting technologies are invaluable for functional genomics. Zinc-finger nucleases (ZFNs) (Miller et al., 2007; Caroll, 2008; Sander et al., 2011) and transcription activator–like effector nucleases (TALENs) (Christian et al., 2010; Miller et al., 2011) have been widely used to edit the genomes of many plant species (Shukla et al., 2009; Townsend et al., 2009;

Zhang et al., 2010, 2013; Li et al., 2012; Wendt et al., 2013), including that of the model grass *Brachypodium distachyon* (Shan et al., 2013). However, the routine use of both ZFNs and TALENs is limited by a number of technically challenging steps including bespoke protein design and the relatively high cost of protein synthesis.

The CRISPR/Cas9 system (Jinek et al., 2012; Cong et al., 2013) revolutionized targeted mutagenesis and enables highly flexible genome editing at low cost. CRISPR/Cas9 technology was developed from the bacterial type II CRISPR/Cas system. The CRISPR-associated protein Cas9 is an endonuclease that uses a 20-nucleotide guide sequence (gRNA) within an RNA duplex, tracrRNA:crRNA to induce site-specific DSBs in DNA. To simplify genome editing, a dual tracrRNA:crRNA was engineered as a single guide RNA (sgRNA). Thus, only two components – Cas9 endonuclease and sgRNA – are required for targeted mutagenesis. Target site recognition by Cas9 is programmed by a sgRNA that encodes a gRNA sequence complementary to a target sequence in the DNA, but also requires recognition of a short neighboring sequence downstream of the 20-nucleotide target, known as the protospacer adjacent motif (PAM). The most commonly used variant of the Cas9 protein is an endonuclease from *Streptococcus pyogenes* (SpCas9) that requires the 20-nucleotide long sequence in the target DNA to be contiguous to a NGG PAM (5′-N_{20}-NGG-3′). The 10–12 base pairs (bp) adjacent to the PAM at the 3′ end of the gRNA, called the "seed sequence," determine Cas9 specificity and are generally more important than the rest of the gRNA sequence. Single mismatches between the target sequence and the gRNA can be tolerated but only in the "non-seed" region. DSBs are always introduced three nucleotides upstream of the PAM, so this method is very predictable and accurate. Notably, the CRISPR/Cas9 system does not rely upon expensive protein design and synthesis since the target sequence is recognized by a gRNA, which can be easily synthesized and incorporated into the sgRNA.

The development of efficient transformation protocols for *Brachypodium* (Draper et al., 2001; Christiansen et al., 2005; Pacurar et al., 2008; Vain et al., 2008; Vogel and Hill, 2008; Alves et al., 2009) has enabled the production of many publicly available T-DNA insertional lines (Bragg et al., 2012; Hsia et al., 2017) that can be useful in plant functional genomic studies. However, the T-DNA is inserted more or less randomly into the genome and may miss the genes of interest, particularly small ones. In contrast, the CRISPR/Cas9 system enables precise mutagenesis of virtually every selected gene. Many plant species have been successfully edited using this technique, such as *Arabidopsis thaliana*, tobacco, sorghum, rice (Jiang et al., 2013), wheat (Upadhyay et al., 2013), tomato (Pan et al., 2016) and watermelon (Tian et al., 2017). Although genome editing of *B. distachyon* has been reported before in several recent studies (O'Connor et al., 2017; Raissig et al., 2017; van der Schuren et al., 2018; Gao et al., 2019; Qin et al., 2019), none has presented a step-by-step protocol sufficiently detailed for use in the laboratory. Moreover, only *B. distachyon* in the genus has been edited to date.

Here we present a detailed step-by-step protocol for CRISPR/Cas9-mediated targeted mutagenesis of both a diploid (*B. distachyon*) and an allotetraploid species (*B. hybridum*). As a simple visual marker to gauge success of the editing, we chose as a target the gene encoding phytoene desaturase (PDS). *PDS* encodes one of the key enzymes involved in the chlorophyll biosynthesis pathway and, if knocked out, produces an albino phenotype (Shan et al., 2014; Pan et al., 2016; Tian et al., 2017; Kaur et al., 2018). To demonstrate that our protocol has general applicability, we also targeted two genes responsible for cell wall maintenance, encoding fasciclin-like arabinogalactan protein (FLA) and pectin methylesterase (PME) and 2 protein kinase genes from the CDKG group. We have previously found that expression of the *FLA* gene is upregulated in *B. distachyon* leaves in response to the temperature stress (Pinski et al., 2019). The inactivation of the second gene, *PME,* in *A. thaliana* led to increased susceptibility to salt stress (Yan et al., 2018). The Arabidopsis CDKG genes are also involved in modulating stress responses (Ma et al., 2015; Chen et al., 2018) and, moreover, are closely related to the CDK-like genes present at the Ph1 locus of *Triticum aestivum*, which is important for the restriction of pairing and recombination to homologous chromosomes only (Al-Kaff et al., 2008). In Arabidopsis, the *CDKG1* gene controls chromosome pairing during meiotic division in this diploid species (Zheng et al., 2014). The role of CDKG in homologous chromosome pairing in a polyploid species is not known, prompting us to target *CDKG* genes in both the diploid *B. distachyon* and its allotetraploid relative *B. hybridum*.

MATERIALS AND METHODS

Plant Material and Growth Conditions

Seeds of *B. distachyon* reference genotype Bd21 and *B. hybridum* reference genotype ABR113 were cultivated in pots filled with 3:1 soil vermiculite mix in a greenhouse at 21 ± 1°C/16h-photoperiod. The 4-week-old plants were vernalised for two weeks at 4°C to induce flowering.

Reagents

- 10xTris-borate-EDTA buffer (TBE; PanReac AppliChem, Cat. No. A0972,1000)
- 2,4-Dichlorophenoxyacetic acid (2,4-D; Sigma, Cat. No. 07299)
- 2-Mercaptoethanol (Sigma, Cat. No. M3148)
- Acetosyringone (Sigma, Cat. No. D134406)
- Agarose (VWR, Cat. No. 443666A)
- Agrobacterium Plasmid Miniprep DNA Purification Kit (EurX, Cat. No. E3535)
- *Agrobacterium tumefaciens* AGL1 strain
- Ampicillin (Duchefa, Cat. No. A01104)
- Biotin (Duchefa, Cat. No. B0603)
- BSA (Sigma, Cat. No. A7030)
- *Bsa*I restriction enzyme (New England BioLabs, Cat. No. R0535S)
- Calcium chloride ($CaCl_2$; POCH, Cat. No. 874870116)
- Calcium hypochlorite ($Ca(ClO)_2$; Sigma, Cat. No. 211389)

- Cefotaxime (Biotaksym, Polpharma)
- Cellulase (Duchefa, Cat. No. C8001)
- Cetyltrimethylammonium bromide (CTAB; Sigma, Cat. No. H6269)
- Chloroform (CHEMPUR, Cat. No. 112344305)
- Color Taq PCR Master Mix (2x) (EurX, Cat. No. E2525-01)
- Copper sulfate pentahydrate ($CuSO_4 \cdot 5H_2O$; POCH, Cat. No. 658310116)
- Cysteine (Duchefa, Cat. No. C0706)
- D-Mannitol (Sigma, Cat. No. M947)
- DNA Electrophoresis Sample Loading Dye (Bio Rad, Cat. No. 1660401EDU)
- DNeasy Plant Mini Kit (Qiagen, Cat. No. 69106)
- Driselase (Sigma, Cat. No. D8037)
- Ethanol (POCH, Cat. No. 396480111)
- Ethylenediaminetetraacetic acid (EDTA; Sigma, Cat. No. T1503)
- Gateway LR Clonase II Enzyme mix (Thermo Fisher Scientific, Cat. No. 11791020)
- Gelrite (Duchefa, Cat. No. G1101)
- Glycine (Sigma, Cat. No. G7403)
- HEPES (Sigma, Cat. No. H3375)
- Hydrogen chloride (HCl; Merck, Cat. No. 1099110001)
- Hygromycin B (Duchefa, Cat. No. H0192)
- IPTG (Thermo Fisher Scientific, Cat. No. R0391)
- Isoamyl alcohol (POCH, Cat. No. 485560111)
- Isopropanol (CHEMPUR, Cat. No. 117515002)
- Kanamycin (Ducherfa, Cat. No. K0126)
- Kinetin (Sigma, Cat. No. K0753)
- L-glutamine (Duchefa, Cat. No. G0708)
- LB Agar (LabEmpire, Cat. No. LBL406.1)
- LB Broth (Sigma, Cat. No. L3022)
- Macerozyme R10 (Duchefa, Cat. No. M8002)
- Magnesium chloride ($MgCl_2$; GLENTHAM, Cat. No. GK5046)
- Magnesium sulfate heptahydrate ($MgSO_4 \cdot 7H_2O$; POCH, Cat. No. 613780111)
- Maxima H Minus First Strand cDNA Synthesis Kit (Thermo Fisher Scientific, Cat. No. K1651)
- MES (Sigma, Cat. No. M2933)
- Micro agar (Duchefa, Cat. No. M1002)
- Murashige and Skoog Basal Salt Mixture (MS; Duchefa, Cat. No. M0221)
- Myo-inositol (Duchefa, Cat. No. 10609)
- Nicotinic acid (Sigma, Cat. No. N-0765)
- NucleoSpin Gel and PCR Clean-up (Macherey-Nagel, Cat. No. 740609.10)
- O'GeneRuler 1 kb DNA Ladder (Thermo Fisher Scientific, Cat. No. SM1163)
- One Shot *ccd*B Survival 2 T1 Competent Cells (Thermo Fisher Scientific, Cat. No. A10460)
- One Shot TOP10 Chemically Competent *E. coli* (Thermo Fisher Scientific, Cat. No. C404003)
- PEG-4000 (Sigma, Cat. No. 81240)
- pGEM-T Vector System I (Promega, Cat. No. A3600)
- Phytagel (Sigma, Cat. No. P8169)
- Platinum™ Taq DNA Polymerase High Fidelity (Thermo Fisher Scientific, Cat. No. 11304011)
- Potassium chloride (KCl; CHEMPUR, Cat. No. 117397402)
- Potassium dihydrogen phosphate (KH_2PO_4; POCH, Cat. No. 742020112)
- Potassium hydroxide (KOH; POCH, Cat. No. 746800113)
- Pyridoxine hydrochloride (Pyridoxine-HCl; Serva, Cat. No. 33990)
- QIAprep Spin Miniprep Kit (Qiagen, Cat. No. 27104)
- Ribonuclease A (RNase A; Sigma, Cat. No. R4875)
- Rifampicin (Bioshop, Cat. No. RIF2221)
- RNA isolation kit (Macherey-Nagel, Cat. No. 40120.50)
- RNase-Free DNase Set (Qiagen, Cat. No. 79254)
- RNeasy Mini Kit (Qiagen, Cat. No. 74104)
- SDS (Sigma, Cat. No. L3771)
- Sodium chloride (NaCl; POCH, Cat. No. A4121116)
- Sodium hydroxide (NaOH; Merck, Cat. No. 1099130001)
- Spectinomycin (Duchefa, Cat. No. S0188)
- Sucrose (CHEMPUR, Cat. No. 11720907)
- T4 DNA Ligase (New England BioLabs, Cat. No. M0202S)
- T7 Endonuclease I (New England BioLabs, Cat. No. M0302S)
- Thiamine hydrochloride (Thiamine-HCl; Sigma, Cat. No. T-3902)
- Timentin (Duchefa, Cat. No. T0190)
- Trizma hydrochloride (Tris–HCl; Sigma, Cat. No. T5941)
- Tryptone (Sigma, Cat. No. T-9410)
- Vectors pENTRsgRNA and pOsCas9 are from Miao et al. (2013)
- Vectors pYPQ131C, pYPQ132C, pYPQ142, pMDC32 and pYPQ167 are from Lowder et al. (2015)
- X-GAL (Thermo Fisher Scientific, Cat. No. R0404)
- Yeast extract (Sigma, Cat. No. 4-1625)

Equipment

- 6-well plates
- Aluminum foil
- Autoclave
- Centrifuge for 5 mL tubes
- Centrifuge for 50 mL round bottom tubes
- Constant temperature (37°C) incubator
- Tissue culture room with controllable temperature and illumination (25 ± 1°C, 16 h/8 h light/dark photoperiod)
- Desiccator
- Disposable sterile plastic syringes
- Disposable sterile syringe filters (0.45 μm)
- DNA gel electrophoresis system
- Electroporator (capacitance 50 mF, load resistance 200 Ω, maximum power 25 W, current 25 mA and voltage 1800 V) with electroporation cuvettes (1 mm PKG 50, Cat. No. 1652089)
- Filter paper (9-cm diameter)
- Fine forceps
- Fridge (4°C) and freezers (−20°C and −80°C)
- Glass beakers (20 mL, 500 mL)
- Glass bottles (100 mL – 1 L)
- Glass Pasteur pipettes (230 mm)
- Glass Petri dishes (9-cm diameter)
- Glass test tubes (12 mL)

- Greenhouse for whole plant culture with controllable temperature and illumination (20 ± 1°C, 16 h/8 h light/dark photoperiod)
- Haemocytometer
- Laboratory microscope with 20x and 40x phase-contrast objectives
- Laminar flow hood with Bunsen burner
- Magnetic stirrer
- Microfuge for 0.2 mL – 2.0 mL tubes
- Microfuge tubes (0.2 mL, 0.5 mL, 1.5 mL and 2.0 mL)
- Micropipettes and corresponding pipette tips (10 μL – 5 mL)
- Microscope slides
- NanoDrop spectrophotometer (A260/280 and A260/230)
- Nylon filter (100 μm)
- Orbital incubator shaker (26 – 37°C; 30 – 250 rpm)
- Parafilm
- PCR thermal cycler
- pH meter
- Pipetting aid (1–50 mL)
- Plastic pestles
- Pots
- Propagator lid
- Scalpels (22 mm)
- Soil
- Spectrophotometer
- Spreaders (L-shaped)
- Stereomicroscope with white light supply unit
- Sterile plastic disposable tubes (20 mL, 50 mL)
- Sterile plastic Pasteur pipettes (10 mL)
- Sterile plastic Petri dishes (9-cm diameter)
- Sterile plastic square Petri dishes (9 × 9 cm)
- Sterile plastic round bottom centrifuge tubes (50 mL)
- Thermomixer
- Trays
- Vacuum pump
- Vermiculite
- Vortex mixer
- Water bath (42°C and 55°C)

Reagent Setup

- 10% SDS [100 mL]: 10 g SDS + up to 100 mL H_2O, store at room temperature (RT)
- 2.4-D 1 mg/mL [50 mL]: 50 mg 2.4-D dissolve in 2 mL of pure ethanol, add 48 mL H_2O; use fresh
- 5% calcium hypochlorite [50 mL] 2.5 g $Ca(ClO)_2$ + up to 50 mL H_2O; mix well, use fresh
- Acetosyringone stock solution 30 mg/mL: 30 mg acetosyringone + 1 mL 70% ethanol, cover with aluminum foil to prevent light exposure, use fresh
- Ampicillin stock solution 100 mg/mL: 500 mg ampicillin + 5 mL H_2O; filter-sterilize, aliquot 1 mL in 1.5 mL microfuge tubes, store at −20°C
- Annealing buffer [100 mL]: 0.292 g NaCl + 1 mL 1M Tris–HCl pH 8.0 + 400 μL 0.25 M EDTA pH 8.0 + up to 100 mL H_2O; filter sterilize, store at 4°C
- Annealing mix [50 μL]: (A) dilute the synthesized oligonucleotides to 100 μM in annealing buffer (B) 2.5 μL 100 μM forward oligonucleotide + 2.5 μl 100 μM reverse oligonucleotide + 45 μL annealing buffer
- B5 Vitamins stock solution [500 mL]: 0.05 g nicotinic acid + 0.5 g thiamine-HCl + 0.05 g pyridoxine-HCl + 5 g myo-inositol + up to 500 mL H_2O; adjust pH to 5.8 with KOH, filter-sterilize, store at 4°C
- BdAGM [250 mL]: (A) 1.075 g MS + 2.5 g sucrose + 2.5 g mannitol + up to 250 mL H_2O, adjust the pH with KOH to 5.5; autoclave, let the medium to cool down, store at RT (B) add 375 μL 30 mg/mL acetosyringone just before the use
- BdCCM [250 mL]: 1.075 g MS + 7.5 g sucrose + up to 250 mL H_2O, adjust the pH with KOH to 5.8, add 0.625 μL 1 mg/mL 2.4-D and 0.5 g phytagel; autoclave, let the medium to cool down, add 2.5 mL M5 Vitamins and 500 μL 30mg/mL acetosyringone, pour ∼25 mL of medium into sterile Petri dishes, store at 4°C
- BdCIM [250 mL]: 1.075 g MS + 7.5 g sucrose + 150 μL 1mg/mL $CuSO_4{\cdot}5H_2O$ + up to 250 mL H_2O, adjust the pH with KOH to 5.8, add 0.625 μL 1 mg/mL 2.4-D and 0.5 g phytagel; autoclave, let the medium to cool down, add 2.5 mL M5 Vitamins, pour ∼25 mL of medium into sterile Petri dishes, store at RT
- BdGM [500 mL]: 0.86 g MS + 5 g sucrose + up to 500 mL H_2O, adjust the pH with KOH to 5.8, add 3 g gelrite; autoclave, let the medium to cool down, add 5 mL B5 Vitamins + 175 μL 320 mg/mL timentin, pour ∼20 mL to sterile 50 mL plastic disposable tubes, store at RT
- BdHygR [500 mL]: 2.15 g MS + 500 mL H_2O, adjust the pH with KOH to 5.8, add 1 g phytagel; autoclave, let the medium to cool down, add 50 μL 500 mg/mL hygromycin B, pour ∼100 mL of medium into sterile square Petri dishes, store at 4°C
- BdRM [500 mL]: 2.15 g MS + 15 g sucrose + up to 500 mL H_2O, adjust the pH with KOH to 5.8, add 1 g phytagel; autoclave, let the medium to cool down, add 5 mL M5 Vitamins + 100 μL 1 mg/mL kinetin + 500 μL 200 mg/mL cefotaxime + 469 μL 320 mg/mL timentin + 20 μL 500 mg/mL hygromycin B, pour ∼25 mL of medium into sterile Petri dishes, store at 4°C
- BdSM30 [500 mL]: 2.15 g MS + 15 g sucrose + 300 μL 1mg/mL $CuSO_4{\cdot}5H_2O$ + up to 500 mL H_2O, adjust the pH with KOH to 5.8, add 1.25 mL 1 mg/mL 2.4-D and 1 g phytagel; autoclave, let the medium to cool down, add 5 mL M5 Vitamins + 500 μL 200 mg/mL cefotaxime + 469 μL 320 mg/mL timentin + 30 μL 500 mg/mL hygromycin B, pour ∼25 mL of medium into sterile Petri dishes, store at 4°C
- BdSM40 [500 mL]: 2.15 g MS + 15 g sucrose + 300 μL 1 mg/mL $CuSO_4{\cdot}5H_2O$ + up to 500 mL H_2O, adjust the pH with KOH to 5.8, add 1.25 mL 1 mg/mL 2.4-D and 1 g phytagel; autoclave, let the medium to cool down, add 5 mL M5 Vitamins + 500 μL 200 mg/mL cefotaxime + 469 μL 320 mg/mL timentin + 40 μL 500 mg/mL hygromycin B, pour ∼25 mL of medium into sterile Petri dishes, store at 4°C
- Biotin stock solution 1 mg/mL: 50 mg biotin dissolve in 1 mL 1M KOH, add 49 mL H_2O; filter sterilize, cover with aluminum foil to prevent light exposure, store at 4°C

- *Bsa*I restriction enzyme digestion of pENTRsgRNA vector [50 μL]: 1 μg pENTRsgRNA + 5 μL of *Bsa*I buffer + 1μL of *Bsa*I restriction enzyme + up to 50 μl H_2O
- Cas9 PCR reaction [20 μL]: 10 μL Master Mix + 0.8 μL 10 μM forward primer + 0.8 μL 10 μM reverse primer + 1 μL isolated DNA + 7.4 μL H_2O
- Cefotaxime stock solution 200 mg/mL: 1 g cefotaxime + 5 mL H_2O; filter-sterilize, aliquot 1 mL in 1.5 mL microfuge tubes, store at −20°C
- CTAB buffer: (A) [100 mL] 2 g CTAB + 10 mL 1 M Tris–HCl pH 8.0 + 4 mL 0.5 M EDTA + 28 mL 5 M NaCl + up to 100 mL H_2O; autoclave and store at RT (B) 5 mL (A) solution + 10 μL 2-Mercaptoethanol; preheat to 60°C, use fresh
- $CuSO_4{\cdot}5H_2O$ 1 mg/mL [50 mL]: 50 mg $CuSO_4{\cdot}5H_2O$ + up to 50 mL H_2O, store at RT
- EDTA 0.25 M [100 mL]: 7.3 g EDTA + up to 100 mL H_2O; add crystals of NaOH till pH 8.0, autoclave, store at 4°C
- EDTA 0.5 M [100 mL]: 14.6 g EDTA + up to 100 mL H_2O; add crystals of NaOH till pH 8.0, autoclave, store at 4°C
- Enzyme solution (for protoplast isolation): (A) [100 mL]: 11.388 g mannitol + 0.15 g KCl + 0.11 g $CaCl_2$ + 0.39 g MES + 0.01 g BSA + up to 100 mL H_2O; adjust pH to 5.7 with KOH

NOTE: Dissolve mannitol thoroughly before adding other ingredients.

- (B) 20 mL (A) solution + 0.08 g macerozyme + 0.04 g cellulase + 0.1 g driselase; mix for 30 min with a magnetic stirrer and transfer to the 50 mL plastic disposable tube. Incubate 10 min in water bath at 55°C and then keep on ice for 10 min. Filter sterilize when adding to cut leaves, use fresh
- Extraction buffer [50 mL]: 10 mL 1 M Tris–HCl pH 8.0 + 12.5 mL 1 M NaCl + 5 mL 0.25 M EDTA pH 8.0 + 2.5 mL 10% SDS + up to 50 mL H_2O, store at RT
- Kanamycin stock solution 50 mg/mL: 250 mg kanamycin + 5 mL H_2O; filter-sterilize, aliquot 1 mL in 1.5 mL microfuge tubes, store at −20°C
- Kinetin stock solution 1 mg/mL [50 mL]: 50 mg kinetin dissolve in 1 mL 1N NaOH, add 49 mL H_2O; filter sterilize, store at 4°C
- KOH 1 M [100 mL]: 5.6 g KOH + up to 100 mL H_2O; store at RT
- KOH solution to adjust pH of culture media and to dissolve components 0.5 M [100 mL]: 2.8 g KOH + up to 100 mL H_2O; store at RT
- LB agar plates + 100 μg/mL ampicillin [250 mL]: 8.75 g LB agar + 250 mL H_2O; autoclave, let the medium to cool down, add 250 μL 100 mg/mL ampicillin, pour ∼25 mL of medium into sterile Petri dishes, store at 4°C
- LB agar plates + 50 μg/mL kanamycin [250 mL]: 8.75 g LB agar + 250 mL H_2O; autoclave, let the medium to cool down, add 250 μL 50 mg/mL kanamycin, pour ∼25 mL of medium into sterile Petri dishes, store at 4°C
- LB agar plates + 50 μg/mL kanamycin + 25 μg/mL rifampicin [250 mL]: 8.75 g LB agar + 250 mL H_2O; autoclave, let the medium to cool down, add 250 μL 50 mg/mL kanamycin and 62.5 μL 100 mg/mL rifampicin, pour ∼25 mL of medium into sterile Petri dishes, store at 4°C
- LB agar plates + 50 μg/mL spectinomycin [250 mL]: 8.75 g LB agar + 250 mL H_2O; autoclave, let the medium to cool down, add 250 μL 50 mg/mL spectinomycin, pour ∼25 mL of medium into sterile Petri dishes, store at 4°C
- LB agar plates + 50 μg/mL spectinomycin + 25 μg/mL rifampicin [250 mL]: 8.75 g LB agar + 250 mL H_2O; autoclave, let the medium to cool down, add 250 μL 50 mg/mL spectinomycin and 62.5 μL 100 mg/mL rifampicin, pour ∼25 mL of medium into sterile Petri dishes, store at 4°C
- LB liquid medium [250 mL]: 5 g LB Broth + 250 mL H_2O; autoclave, store at 4°C
- LB liquid medium + 100 μg/mL ampicillin [250 mL]: add 250 μL 100 mg/mL ampicillin to 250 mL of RT LB liquid medium; store at 4°C
- LB liquid medium + 50 μg/mL kanamycin [250 mL]: add 250 μL 50 mg/mL kanamycin to 250 mL of RT LB liquid medium; store at 4°C
- LB liquid medium + 50 μg/mL kanamycin + 25 μg/mL rifampicin [250 mL]: add 250 μL 50 mg/mL kanamycin and 62.5 μL 100 mg/mL rifampicin to 250 mL of RT LB liquid medium; store at 4°C
- LB liquid medium + 50 μg/mL spectinomycin [250 mL]: add 250 μL 50 mg/mL spectinomycin to 250 mL of RT LB liquid medium; store at 4°C
- LB liquid medium + 50 μg/mL spectinomycin + 25 μg/mL rifampicin [250 mL]: add 250 μL 50 mg/mL spectinomycin and 62.5 μL 100 mg/mL rifampicin to 250 mL of RT LB liquid medium; store at 4°C
- Ligation of cut pENTRsgRNA vector [10 μL]: 1 μL cut pENTRsgRNA + 1 μL ligase buffer + 1 μL annealed oligonucleotides + 0.5 μL ligase + 6.5 μL H_2O
- LR recombination mix [4 μL]: 1 μL pENTRsgRNA with the introduced gRNA sequence (10 ng/μL) + 1 μL pOsCas9 (109 ng/μL) + 2 μL TE buffer
- M5 Vitamins stock solution [500 mL]: 0.02 g nicotinic acid + 0.025 g thiamine-HCl + 2 g cysteine + 0.1 g glycine + 0.02 g pyridoxine-HCl + up to 500 mL H_2O; adjust pH to 5.8 with KOH, filter-sterilize, store at 4°C

NOTE: Do not use the stock solution if you notice any precipitation.

- MGL + S50 + AS30 [500 mL]: 2.5 g tryptone + 1.25 g yeast extract + 2.6 g NaCl + 5 g mannitol + 1.16 g L-glutamine + 0.25 g KH_2PO_4 + 0.1 g $MgSO_4{\cdot}7H_2O$ + up to 500 mL H_2O, adjust the pH with KOH to 7.2, add 5 g micro agar; autoclave, let the medium to cool down, add 1 μL 1 mg/mL biotin + 500 μL 50 mg/mL spectinomycin + 500 μL 30 mg/mL acetosyringone, pour ∼25 mL of medium into sterile Petri dishes, store at 4°C
- MMG solution [100 mL]: 7.29 g mannitol + 0.08 g MES + 0.14 g $MgCl_2$ + up to 100 mL H_2O; adjust pH to 5.7 with KOH, autoclave, store at RT

- NaCl 1 M [100 mL]: 5.84 g NaCl + up to 100 mL H_2O; autoclave, store at 4°C
- NaCl 5 M [100 mL]: 29.22 g NaCl + up to 100 mL H_2O; autoclave, store at 4°C
- NaOH 1 N [100 mL]: 4 g NaOH + up to 100 mL H_2O; store at RT
- PEG-Calcium solution [100 mL]: 40 g PEG-4000 + 3.64 g mannitol + 1.1g $CaCl_2$ + up to 100 mL H_2O; filter sterilize, store at RT
- PSII solution [250 mL]: 22.771 g mannitol + up to 250 mL H_2O; adjust pH to 5.6–5.8, autoclave, store at RT
- Rifampicin stock solution 100 mg/mL: 500 mg rifampicin + 5 mL 100% methanol; filter-sterilize, aliquot 1 mL in 1.5 mL microfuge tubes, store at −20°C
- RNase A solution 100mg/mL: (A) RNase buffer [50 mL]: 0.5 mL 1 M Tris–HCl pH 8.0 + 150 μL 5 M NaCl + up to 50 mL H_2O; filter sterilize (B) 500 mg RNase A + 5 mL RNase buffer; heat to 100°C for 15 min, cool down at RT, store at −20°C
- Spectinomycin stock solution 50 mg/mL: 250 mg spectinomycin + 5 mL H_2O; filter-sterilize, aliquot 1 mL in 1.5 mL microfuge tubes, store at −20°C
- TE buffer [100 mL]: 10 mL 1 M Tris–HCl pH 8.0 + 400 μL EDTA 0.25M + up to 100 mL H_2O, store at 4°C
- Timentin stock solution 320 mg/mL: 1.6 g timentin + 5 mL H_2O; filter-sterilize, aliquot 1 mL in 1.5 mL microfuge tubes, store at −20°C
- Tris–HCl 1 M [100 mL]: 12.1 g Tris + up to 100 mL H_2O; add pure HCl till pH 8.0, autoclave, store at 4°C
- W5 solution [250 mL]: 2.25 g NaCl + 4.6 g $CaCl_2$ + 0.0925 g KCl + 0.1 g MES + up to 250 mL H_2O; adjust pH to 5.7 with KOH, autoclave, store at RT

Autoclaving conditions: (40 min total cycle, including 20 min at 120°C).

Step-by-Step Procedure

The protocol described here consists of six major steps (gene sequence analysis, gRNA design, vector construction, transient protoplast assay, *Agrobacterium*-mediated transformation and analysis of regenerated plants) and is summarized in **Figure 1**. We describe each step in detail in the following sections.

Gene Sequence Analysis (Timing ∼1 Week)

Mismatches within the gRNA sequence can affect the endonucleolytic activity of the Cas9 protein, especially if they occur in the "seed region." For this reason, it is advisable to sequence the target gene in the species or even the genotype to be edited.

(1). Isolate total RNA from leaves of the genotype to be edited using an RNA isolation kit (Macherey-Nagel) and following the manufacturer's protocol. Treat with DNase (Qiagen) and purify the isolated RNA using an RNeasy Mini Kit (Qiagen).
(2). Check the concentration and quality of the isolated RNA using a NanoDrop spectrophotometer. The A260/280 and A260/230 values must be greater than 1.8. The concentration of the purified RNA should not be less than 100 ng/μL. Take 1000 ng of isolated RNA and add RNase-free water to obtain a volume of 10 μL. Add 2 μL of DNA Electrophoresis Sample Loading Dye (Bio Rad) and run on a 1% agarose gel to check for the quality and integrity. Intact total RNA should have two (28S and 18S rRNA) sharp bands. Use 1000 ng of RNA to synthesize cDNA using a Maxima H Minus First Strand cDNA Synthesis Kit according to the manufacturer's instructions with oligo $(dT)_{18}$ primer.
(3). Amplify the whole coding DNA sequence (CDS) of the gene using specific 18-mers corresponding to the beginning and the end of the sequence. Design the primers based on the sequence of CDS available for particular genes in the Phytozome database. Perform PCR using Platinum™ Taq DNA Polymerase High Fidelity (Thermo Fisher Scientific) and following the manufacturer's protocol, and run the products on a 1% agarose gel.

NOTE: The use of cDNA as a template allows analysis of the gene exon/intron structure. However, as an alternative for small genes, the amplification can be also performed using genomic DNA (gDNA) instead of cDNA. This can be particularly useful, if the expression of a target gene is not high enough. Genomic DNA can be isolated using DNeasy Plant Mini Kit (Qiagen).

(4). Extract the desired band from the gel using a NucleoSpin Gel and PCR Clean-up kit and ligate into a pGEM-T vector according to the manufacturer's instructions.
(5). Transform the ligation (2 μL) into One Shot TOP10 Chemically Competent *Escherichia coli*, plate in plates LB with 100 μg/mL ampicillin and grow overnight at 37°C. Select single colonies and inoculate into 5 mL of LB with 100 μg/mL ampicillin, and incubate overnight at 37°C with constant shaking at 250 rpm.
(6). Isolate plasmids using a QIAprep Spin Miniprep Kit and sequence with an M13 primer pair (sequences of all primers used can be found in **Supplementary Table S1**). Compare the sequences obtained to those in an online database (for example in NCBI or Phytozome).

NOTE: Sequence the gene from five colonies.

NOTE: *B. hybridum* is an allotetraploid, resulting from natural hybridisation between *B. distachyon* and *B. stacei*. The alleles of a gene derived from the *B. distachyon* subgenome (Bd) may differ from the alleles derived from the *B. stacei* subgenome (Bs). Thus, if the goal is simultaneous mutagenesis of all copies of the gene in *B. hybridum*, it is important to obtain and compare the gene sequences from both ancestor genomes – Bd and Bs (at least five colonies for each).

gRNA Design (Timing – 1 Day)

Designing gRNA for diploid *B. distachyon* is much simpler than for allotetraploid *B. hybridum*, as the latter requires a target sequence which is conserved in both its Bd and Bs subgenomes. If it is not possible to find such a sequence, consider sequences with one mismatch at least 13 nucleotides away from PAM, i.e., outside of the gRNA "seed" sequence.

In general, a few important factors should be considered when designing gRNA:

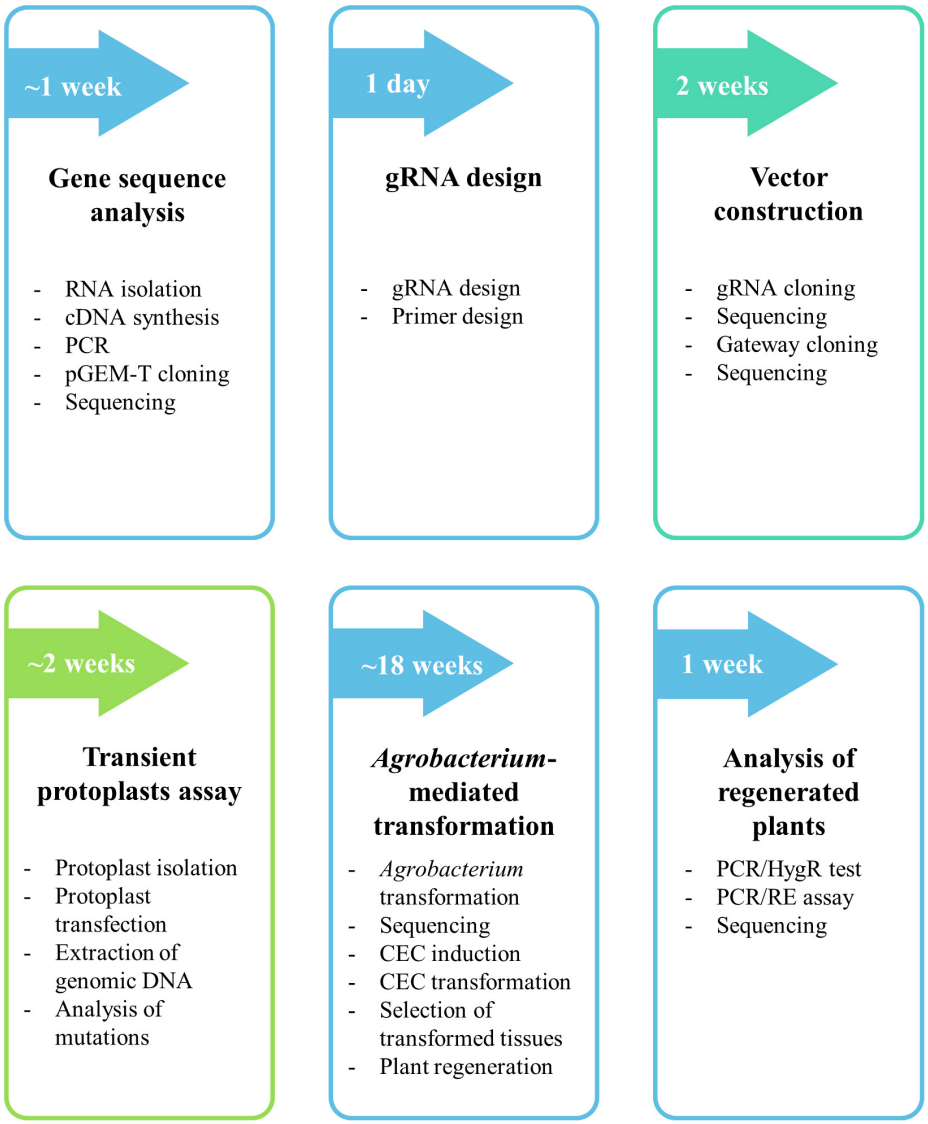

FIGURE 1 | Flow chart of the protocol for targeted mutagenesis of *Brachypodium* species. The detailed procedure is found in the section "MATERIALS AND METHODS."

- If the goal of the experiment is to knock out the gene, the target sequence should be within an exon, preferably the first.

NOTE: It is often not possible to identify a target sequence within the first exon. However, targeting another exon may also prove effective (see the example of *pds* mutants, section "RESULTS AND DISCUSSION").

- The 20-nucleotide target sequence should immediately precede the 5′-NGG PAM. Target either sense (5′-$N_{(20)}$-NGG-3′) or antisense (5′-CCN-$N_{(20)}$-3′) strand of the DNA.
- Off-target sites that could potentially be edited using individual gRNAs should be identified, using the Cas-OFFinder online bioinformatic tool[1] (Bae et al., 2014). Align all the potential gRNA sequences with the *B. distachyon* genome using the following criteria: (1) Mismatch number equal or less than 2 and bulge size equal or less than 1, (2) Mismatch number equal or less than 4 and bulge size 0. Avoid gRNA with potential off-target sites within an exon. Permissible off-target sites include introns, intergenic regions or mismatched sequences in the gRNA "seed" region.
- The target 20-nucleotide sequence should have a restriction site at the Cas9 cutting site (3-bp upstream 5′-NGG). This enables much faster and cheaper analysis of regenerated plants after transformation and allows the analysis of gRNA functionality in transient protoplast assays.

[1]http://www.rgenome.net/cas-offinder/

NOTE: Designing a gRNA with a restriction site is highly recommended. However, if the design of such a gRNA is impossible for a target gene, gRNA without a restriction site can be used. The protoplast test may be omitted and the analysis, whether the sequence is edited or not, can be performed using cloning and sequencing without a PCR/restriction enzyme digestion (PCR/RE) assay.

Optimal gRNA sequences can be selected manually or using bioinformatic tools, as for example https://www.genome.arizona.edu/crispr/CRISPRsearch.html or http://www.e-crisp.org/E-CRISP/. We designed all the gRNAs using the Geneious Prime program, that finds both potential 5′-$N_{(20)}$-NGG-3′ sites and restriction sites.

(7). Design the optimal gRNA sequence with a restriction site at the Cas9 cutting site.
(8). Design primers for amplification of a part of the gene with the gRNA sequence. *B. hybridum* requires primers that are conserved in both Bd and Bs genomes.

NOTE: The restriction site in the gRNA target should be unique within the amplicon, if the intention is to use a PCR/RE assay to detect the mutations. The digestion of the PCR product using a relevant restriction enzyme should produce two smaller fragments of different size in order to be identified by gel electrophoresis.

Vector Construction (Timing ∼2 Weeks)

Vectors with codon-optimized Cas9 and relevant gene promoters were used, as in targeted mutagenesis in rice (Miao et al., 2013). These comprise pENTRsgRNA containing the gRNA cloning site, and pOsCas9 with the gene encoding the Cas9 protein (detailed information about the vector structure can be seen in **Figure 2B**). The pENTRsgRNA vector carries a kanamycin resistance gene, and the pOsCas9 vector carries a spectinomycin resistance gene for antibiotic selection during plasmid cloning. The recommended working concentration for kanamycin and spectinomycin is 50 μg/mL.

NOTE: The pOsCas9 vector contains the *ccd*B gene and cannot be transformed into the One Shot TOP10 Chemically Competent *E. coli*. Consequently, it should be transformed into One Shot *ccd*B Survival 2 T1 Competent Cells.

For the targeted mutagenesis of the *PME* gene, a different set of vectors were prepared according to Lowder et al. (2015). These vectors can carry two different gRNAs and enable simultaneous editing in a single transformation experiment. pYPQ131C and pYPQ132C vectors carrying the U6 promoter from *Oryza sativa*, were used for the introduction of the gRNA. As the detailed protocol for the preparation of these vectors has been reported previously by Lowder et al. (2015), we will focus on the preparation of the mature vector from vectors pENTRsgRNA and pOsCas9.

(9). The pENTRsgRNA vector is linearised by *Bsa*I restriction enzyme digestion (**Figure 2A**). Prepare two *Bsa*I restriction enzyme digestion reactions (see section "Reagent Setup") and incubate overnight in a PCR thermal cycler at 37°C. Inactivate the enzyme at 65°C for 20 min and stop the reaction by adding 10 μL of 6x gel loading dye to both 50 μL reactions. Run the reactions on a 0.7% agarose gel, extract the linearised plasmid, elute in 30 μL of EB and split into 3 aliquots to avoid freeze-thaw cycling.
(10). Once a target site is selected (step 7), forward and reverse oligonucleotides are designed and synthesized, consisting of a 20-nucleotide gRNA sequence (gRNA_F and gRNA_R) with 4-nucleotide adapters (bold) complementary to the overhangs obtained after *Bsa*I digestion of pENTRsgRNA (**Figure 2A**).

5′-**GGCA**-gRNA_F-3′
5′-**AAAC**-gRNA_R-3′

Examples of oligonucleotides used in this study can be found in **Supplementary Table S2**.
(11). Anneal the oligonucleotides. Preheat block to 95°C and prepare the annealing mix (see section "Reagent Setup"). Incubate the reaction for 5 min at 95°C, transfer the tube to RT and let it cool down (∼45 min).

NOTE: Carefully remove the tube from 95°C to avoid opening the tube.

NOTE: Oligonucleotide annealing must be prepared immediately before the ligation.

(12). Prepare the ligation of the linearised pENTRsgRNA vector (from step 9) with an annealed oligonucleotides (from step 11) (see section "Reagent Setup") and run overnight in a PCR thermal cycler using the following program: (10°C for 30 s; 30°C for 30 s) – 300 cycles and 12°C – ∞.
(13). Transform 1 μL of the ligation reaction into 25 μL of One Shot TOP10 Chemically Competent *E. coli* according to the manufacturer's protocol. At the end of the transformation procedure spread 200 μL of transformation mix onto LB agar plates with kanamycin 50 μg/mL and incubate upside down overnight at 37°C. Then inoculate 5 single colonies into 5 mL of LB + kanamycin 50 μg/mL, grow overnight at 37°C with shaking at 250 rpm, isolate plasmids and sequence with the M13For primer to check for the presence and integrity of the sgRNA.
Gateway® Recombination Cloning Technology was used to combine the sgRNA sequence, together with the relevant promoter, to the destination vector containing the gene encoding the Cas9 protein. The LR recombination reaction was carried out between an *att*L-containing pENTRsgRNA with the incorporated gRNA sequence and an *att*R-containing pOsCas9 vector, producing the pOsCas9_sgRNA final vector (**Figure 2B**).
(14). The LR recombination reaction is effected by first diluting the pENTRsgRNA vector to 10 ng/μL, and the pOsCas9 plasmid to 109 ng/μL.

Prepare the LR recombination mix (see section "Reagent Setup"). Thaw on ice the LR Clonase II Enzyme Mix for about 2 min, vortex briefly and add 1 μL to the reaction mixture. Vortex briefly again, centrifuge and incubate at 25°C for 3 h. After incubation, add 0.5 μL of proteinase K solution, vortex briefly and incubate for 10 min at 37°C. Transform 0.5 μL of the LR

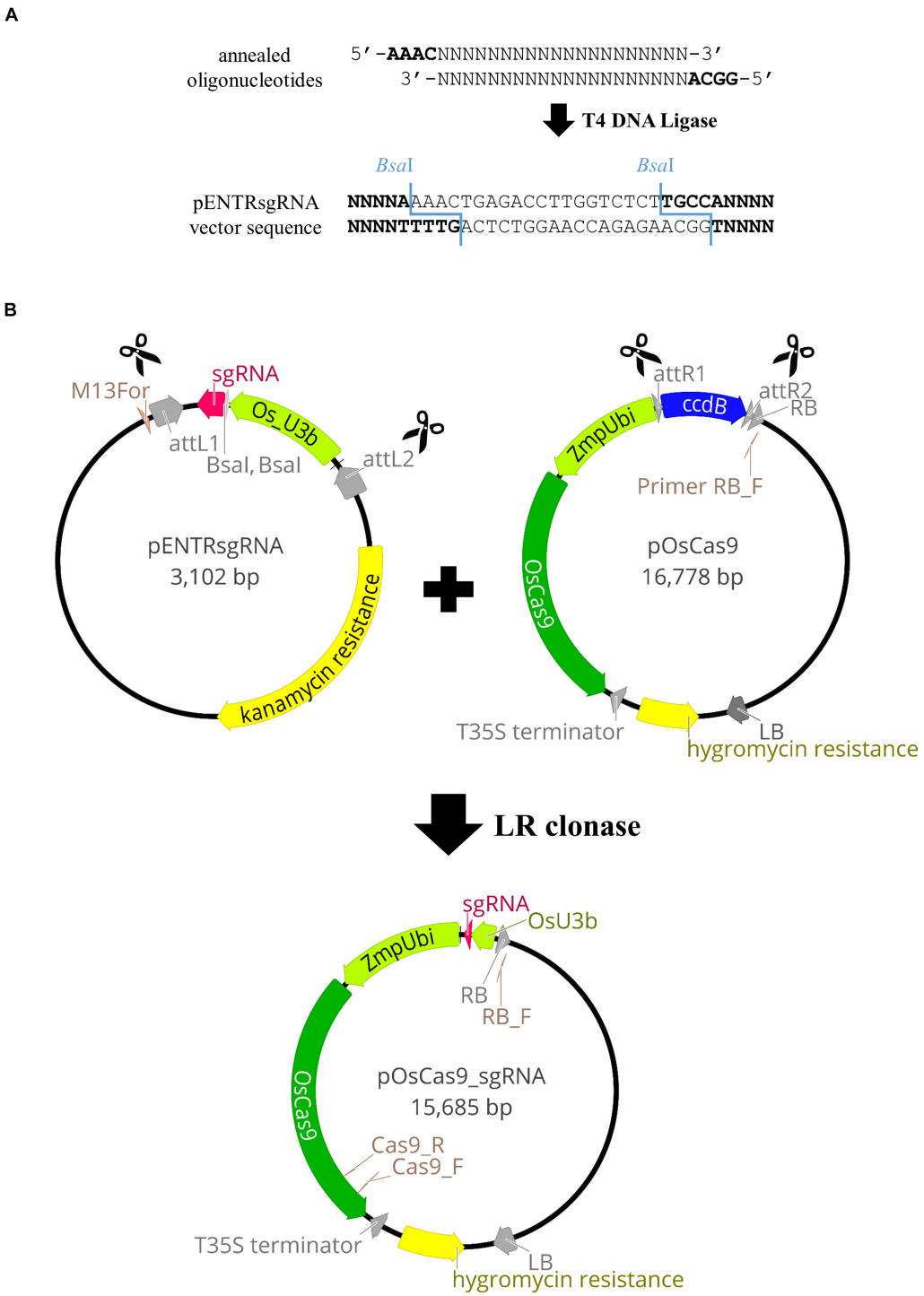

FIGURE 2 | Schematic illustration of the pOsCas9_sgRNA vector construction. **(A)** Cloning of the gRNA sequence into pENTRsgRNA vector. **(B)** Diagrams of the plasmids used for targeted mutagenesis of *Brachypodium* species and the scheme of the LR recombination reaction.

reaction into 25 μL of One Shot TOP10 Chemically Competent *E. coli*, at the end of the transformation procedure spread 200 μL of transformation mix onto LB agar plates with spectinomycin at 50 μg/mL, and incubate upside down overnight at 37°C. Inoculate 5 single colonies into 5 mL of LB + spectinomycin at 50 μg/mL, grow overnight at 37°C with 250 rpm shaking, and isolate plasmids (elute in water instead of EB, as these plasmids will be used later for *Agrobacterium* transformation in step 23).

Sequence isolated plasmids with the RB_F primer to check for the presence of the sgRNA. Plasmids containing the expected pOsCas9_sgRNA sequence are stored at −80°C as glycerol stocks after mixing 500 μL of the overnight liquid bacterial culture with 500 μL of 50% glycerol.

Transient Protoplast Assay (Timing ∼2 Weeks)

Before *Agrobacterium*-mediated transformation, vectors may be tested using a protoplast transient assay. An optimized, short protocol for transient protoplast assay in *Brachypodium* species is presented below. This test might be useful for checking the functionality of individual vectors in *Brachypodium* genome editing (see section "RESULTS AND DISCUSSION"). However, since false negative results can be also obtained, it should be emphasized, that the use of this test (step 15 – 22) is optional and it is also possible to skip it and go directly to *Agrobacterium*-mediated transformation (step 23).

(15). A high concentration of plasmid DNA is required for protoplast transfection (at least 1 μg/μL). Inoculate the glycerol stock of *E. coli* with the pOsCas9_sgRNA vector (prepared in step 14) in 5 mL LB + spectinomycin at 50 μg/mL. Grow overnight at 37°C with 250 rpm shaking and isolate plasmids as follows:

Centrifuge 5 mL of bacterial culture for 5 min at 8000 rpm and discard the supernatant. Use reagents from QIAprep Spin Miniprep Kit. Add 250 μL of P1 buffer and mix to resuspend the bacteria. Add 250 μL of P2 buffer and wait for 4.5 min, before mixing gently by inverting.

NOTE: To avoid contamination with bacterial genomic DNA, do not extend the incubation in P2 buffer.

Add 350 μL N3 buffer, mix by inverting and leave for 5 min on ice. Centrifuge for 10 min at 14 000 rpm. Transfer the clear supernatant to a clean 1.5 mL tube, taking care not to disturb the pellet, add 1 mL of cold (−20°C) isopropanol and mix thoroughly by inverting and centrifuge for 20 min at 14 000 rpm. Discard the supernatant and add 1 mL 70% ethanol, mix by inverting and centrifuge for 3 min at 14 000 rpm. Discard the supernatant and repeat the washing with ethanol. Discard the supernatant, air dry and resuspend in 30 μL of EB buffer. Check the concentration on a NanoDrop spectrophotometer and dilute the plasmid to a concentration of 1 μg/μL. Store at −20°C.

A step-by-step protocol for protoplast isolation from leaf mesophyll cells of the Bd21-3 inbred line has been published by Jung et al. (2015). We present the optimized protocol for the isolation of protoplasts from *B. distachyon* Bd21. This protocol can be completed within one day and uses young leaves from 5–7 week-old Bd21 plants. To avoid contamination of the protoplasts, work under sterile conditions in a laminar flow hood, and use sterilized buffers and sterile Petri dishes, tubes, beakers, filters and Pasteur pipettes. Handle protoplasts with care, as they are easily broken.

(16). Place 0.2 g of young *B. distachyon* leaves in a glass Petri dish and add a small amount of PSII solution. Cut the leaves using two 22 mm scalpels into small (∼2 mm) pieces. Wash the plant material with ∼10 mL of PSII solution. Remove the PSII solution using a Pasteur pipette and add immediately the enzyme solution to avoid drying of the material. Mix gently and vacuum-infiltrate for 30 min at RT by placing the open Petri dish with the plant material in a desiccator under a laminar flow hood, running the vacuum pump up to 500 mBa, turning off the pump and holding the vacuum for 30 min. After 30 min close the Petri dish, seal with Parafilm and wrap in aluminum foil. Transfer the Petri dish to an orbital incubator shaker for 3 h with gentle shaking at 30 rpm at 26°C. After 3 h, increase the shaking speed to 50 rpm and continue the incubation for 30 min. Collect the protoplasts in round bottom centrifuge tubes by filtering through a nylon filter. To increase the protoplast yield, wash the Petri dish with 10 mL of W5 solution and filter it into the same round bottom tube. Centrifuge the protoplasts for 5 min at 1000 rpm and 4°C, remove the supernatant with a pipette (the protoplasts will be collected at the bottom of the tube), and slowly add 30 mL of W5 solution. Centrifuge for 5 min at 1000 rpm and 4°C. Pipette out the W5 solution and resuspend the purified protoplasts in 2 mL of W5 solution. Determine protoplast yield and integrity by cell counting using a haemocytometer. For optimal transformation, the density of protoplasts should be $\sim 10^6$ protoplasts/mL. If the density of the isolated protoplasts is higher, add more W5 solution.

(17). Incubate freshly isolated protoplasts for 30 min on ice, and centrifuge for 5 min at 1000 rpm and 4°C. Pipette out the supernatant and add an equal amount of MMG solution to obtain the required density of protoplasts. Make two transfection reactions for each vector. Prepare two 12 mL sterile glass test tubes and add 10 μL of 1 μg/μL plasmid to the bottom of each. Slowly add 100 μL of isolated protoplasts to each tube and mix gently. Initiate the transfection reaction by addition of 110 μL PEG solution and mix gently. Incubate for 7 min at RT. Terminate the reaction by adding 700 μL W5 solution, mix gently and centrifuge for 2 min at 1000 rpm and 4°C. Pipette out the supernatant to leave ∼50 μL of protoplasts suspension. Meanwhile, prepare plates for protoplast incubation. Use 6-well plates in which reactions can be incubated from three different plasmids (2 wells each). Transfer the protoplasts from each reaction to 1 mL of W5 solution in each well. Cover the plates with Parafilm and incubate for 2 days at 25°C in the dark.

(18). After 2 days of incubation, check the quality of the protoplasts using a light microscope. Most of them should still have a spherical shape (**Figure 3D**). If most protoplasts have broken, it is better to repeat the isolation and transfection experiments (steps 16 and 17). From step 18 onward there is no need to work under sterile conditions. Use the CTAB method to isolate genomic DNA from protoplasts. Mix gently the protoplast solution and transfer the duplicates of transfected protoplasts (2 × 1 mL) to one 5 mL tube. Wash the wells in which the protoplasts were incubated with 1 mL of water and transfer to the same 5 mL tube. Centrifuge for 15 min at 14 000 rpm. Discard the supernatant and add 800 μL of CTAB buffer preheated to 60°C and 3 μL of RNase (100 mg/mL). Vortex to dissolve the protoplasts pellet. Incubate for 1 h at 60°C in a thermomixer (mix by inverting every 15 min). Add 800 μL of chloroform:isoamyl alcohol solution (24:1), mix by inverting, incubate for 3 min

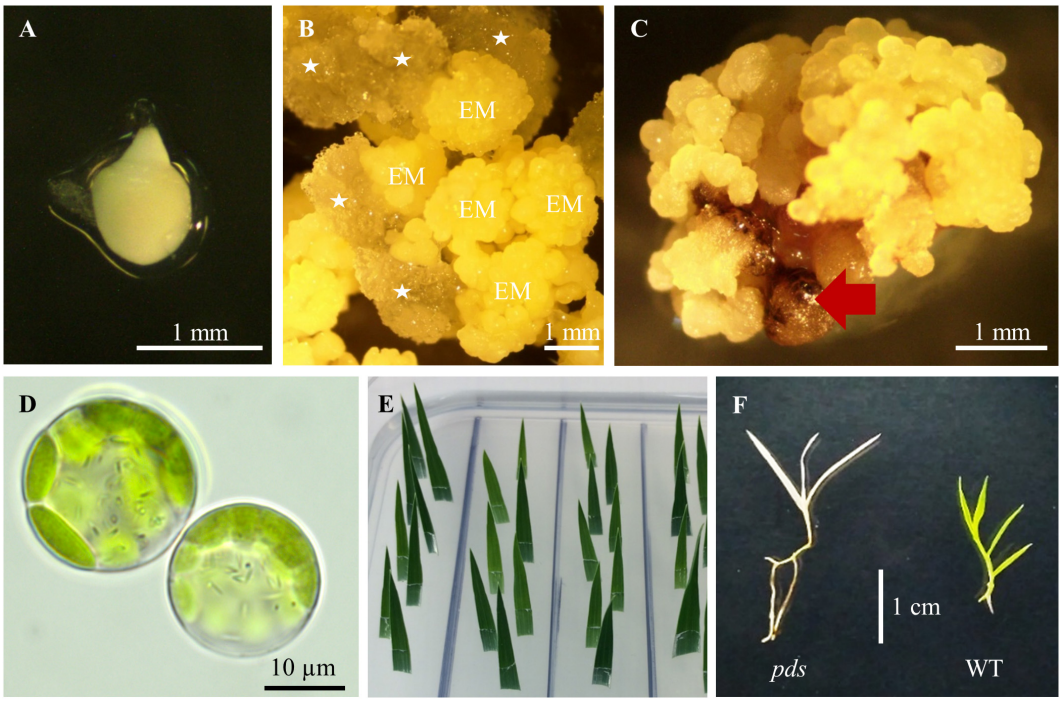

FIGURE 3 | Tissue culture in *B. distachyon*. **(A)** Immature embryo used for callus induction. **(B)** Induced callus: EM – embryogenic masses; parenchymatous cells are marked by white asterisks. **(C)** Embryogenic callus after transformation. Non-transformed calli are indicated by the red arrow. **(D)** Two day-old protoplasts of *B. distachyon*. **(E)** HygR test with *B. distachyon* leaves. **(F)** Albino phenotype of the *B. distachyon*. *pds* mutant in comparison to the green wild-type (WT) plant.

at RT, and centrifuge for 10 min at 14 000 rpm. Transfer the clear, upper phase to a new 1.5 mL tube. Add 600 µL of cold (−20°C) isopropanol and incubate for 1 h at −20°C. Spin for 15 min at 14 000 rpm and 4°C. Discard the supernatant, add 1 mL of cold (−20°C) 70% ethanol and centrifuge for 5 min at 14 000 rpm and 4°C. Discard the supernatant, air dry and dilute in 20 µL TE buffer.

(19). Digest whole genomic DNA from the protoplasts after transfection with the relevant restriction enzyme that recognizes the Cas9 cutting site in a wild-type target sequence. New England BioLabs enzymes were used, and the restriction digestion reaction was prepared following the manufacturer's protocol.

NOTE: If it is possible (i.e., if the restriction enzyme does not show the star activity (which means cleaving sequences which are similar, but not identical, to their defined recognition sequence) during extended digestion), perform the restriction digestion overnight.

(20). Perform PCR using Platinum Taq DNA Polymerase High Fidelity (Thermo Fisher Scientific) and following the manufacturer's protocol. Add 5 µL of digested genomic DNA to 50 µL of PCR reaction containing the primers (step 8) in order to amplify part of the target gene with the gRNA sequence. Run the PCR reaction on the 1% agarose gel. The enrichment PCR reaction, after the restriction digestion of genomic DNA, amplifies exclusively part of the gene from edited protoplasts. Introduced mutations are resistant to restriction enzyme digestion due to the loss of the restriction site, so the PCR products should be derived only from the edited protoplasts.

(21). Cut out the band from the gel and clone into a pGEM-T vector. Transform *E. coli* with the recombinant vector to obtain single colonies carrying one gene copy.

The enrichment PCR reaction is not completely effective, and many colonies may still carry plasmids without the mutation of the target sequence. To circumvent this problem, continue as follows.

(22). Before plasmid isolation and sequencing, prepare a colony PCR reaction to amplify part of the target gene, using a Platinum^{TM} Taq DNA Polymerase High Fidelity (Thermo Fisher Scientific) and following the manufacturer's protocol. Touch the colony with a tip, transfer to the PCR mixture, mix by pipetting, and perform colony PCR. Digest the PCR product with the relevant restriction enzyme and run on the 1% agarose gel. If the PCR product cannot be restricted, it is likely that the target sequence is edited. Isolate plasmids from potentially edited colonies and sequence with M13F primer to determine the nature of the mutation.

NOTE: Some mutations may be present but do not lead to the loss of a restriction site. For example, if a single nucleotide is inserted at the border of the restriction site and shares the same identity as the nucleotide of the wild type sequence the restriction site will be unimpaired. This insertion cannot be detected with the PCR/RE assay but will cause a frameshift mutation and will lead to the production of a non-functional protein.

Agrobacterium tumefaciens-Mediated Transformation (Timing ∼18 Weeks)

Agrobacterium-mediated transformation is the longest part of targeted mutagenesis in *Brachypodium* species. It is advisable, therefore, to test first the efficacy of vectors using the transient protoplast assays described above to save time and resources. *Agrobacterium*-mediated *Brachypodium* transformation is effected by introducing the pOsCas9_sgRNA or pYPQ_Cas9_gRNA vectors to *A. tumefaciens* strain AGL1 using electroporation.

(23). Thaw on ice 40 μL of competent AGL1 cells (see **NOTE** for the *Agrobacterium* electrocompetent cells preparation). Add ∼500 ng of pOsCas9_sgRNA (from step 14) or pYPQ_Cas9_gRNA vector prepared according to the protocol by Lowder et al. (2015) and mix gently. Transfer the bacteria to an electroporation cuvette and apply one pulse of Agr program (capacitance 50 mF, load resistance 200 **Ω**, maximum power 25 W, current 25 mA and voltage 1800 V). Very slowly add 500 μL of LB medium to the cuvette and transfer the bacteria to a 1.5 mL tube and incubate for 3 h at 28°C with horizontal shaking at 125 rpm. Add 500 μL of LB medium to reduce bacterial density, mix gently by inverting the tube and then inoculate 50 μL of the bacterial culture on LB agar plates with spectinomycin at 50 μg/mL and rifampicin at 25 μg/mL for the pOsCas9_sgRNA vector, and on LB agar plates with kanamycin at 50 μg/mL and rifampicin at 25 μg/mL for the pYPQ_Cas9_gRNA vector. Culture upside down for 2 days at 28°C in the dark. From the many colonies produced, pick five and inoculate into 10 mL of LB + spectinomycin at 50 μg/mL and rifampicin at 25 μg/mL for the pOsCas9_sgRNA vector and LB + kanamycin at 50 μg/mL and rifampicin at 25 μg/mL for the pYPQ_Cas9_gRNA vector in a 50 mL plastic disposable tube. Grow for 2 days in the incubator shaker at 28°C with 250 rpm shaking in the dark and isolate plasmids using an Agrobacterium Plasmid Miniprep DNA Purification Kit according to the manufacturer's instructions. Sequence vectors with the RB_F primer for the pOsCas9_sgRNA vector, or with the pTC14-F2 primer for the pYPQ_Cas9_gRNA vector (**Supplementary Table S1**). Prepare a glycerol stock of the *A. tumefaciens* with the pOsCas9_sgRNA or pYPQ_Cas9_gRNA by mixing the 500 μL of the 2 day-old liquid bacterial culture with 500 μL of 50% glycerol. Store at −80°C.

NOTE: To prepare *Agrobacterium* competent cells: (1) Refresh *Agrobacterium* in LB + rifampicin medium and grow at 28°C until you have nice single colonies (1–2 days); (2). Pick a single colony and inoculate in 10 mL LB + rifampicin. Grow at 28°C, shaking for two days; (3). Take 2 ml of the *Agrobacterium* culture and inoculate it into 100 mL of LB + rifampicin. Incubate at 28°C shaking until OD600 reaches 0.5; (4). Chill culture on ice for 10 min. Harvest cells by centrifugation (5000 rpm for 10 min at 4°C); (5). Wash pellet with 10 mL of cold HEPES pH 7 (filter sterilized). Do this gently. Spin down (5000 rpm for 10 min at 4°C). Repeat step above twice; (6). Wash pellet with 10 mL of cold 10% glycerol (filter sterilized). Spin; (7). Gently resuspend pellet in 1 mL of cold 10% glycerol; (8). Divide into 100 μL aliquots into chilled Eppendorf tubes and immediately freeze in liquid nitrogen. Store at −80°C.

(24). Collect green immature seeds from 7–9 week old plants. Remove the top glume from the seeds, and put ∼100 seeds into a 50 mL plastic disposable tube. Sterilize 2 min with 50 mL 70% ethanol, discard ethanol and add 50 mL 5% calcium hypochlorite, incubate for 10 min (mix gently by inverting), and rinse three times with sterile deionised water. Isolate immature embryos (**Figure 3A**) ∼0.3–0.7 mm in length and put them onto BdCIM medium. Cover the plates with Parafilm and incubate for 3 weeks at 25°C in the dark.

NOTE: Only very small immature embryos produce CEC at high frequency.

(25). After three weeks fragment the embryogenic masses (**Figure 3B**) into small pieces and transfer onto fresh BdCIM medium for another two weeks at 25°C in the dark. Discard the vitreous and friable parenchymatous cells.

(26). At week five, split CEC into 4–6 pieces and transfer them onto fresh BdCIM medium for another week at 25°C in the dark. Perform the transformation exactly after 6 weeks of callus induction.

(27). Three days before the planned transformation add 5 μL of *A. tumefaciens* from the glycerol stock (prepared in step 23) to 1 mL of LB + spectinomycin at 50 μg/mL, cover with aluminum foil and grow overnight at 28°C with 200 rpm shaking. Inoculate 200 μL of the overnight culture onto MGL + S50 + AS30 plates. Culture upside down for 2 days at 28°C in the dark.

(28). Scrape the *Agrobacterium* layer with a sterile scalpel and add to 10 mL BdAGM medium in a 50 mL plastic disposable tube. Shake vigorously and incubate for 45 min at 28°C with shaking at 220 rpm. Measure the optical density of the suspension at 600 nm and dilute to an OD600 between 0.9–1.0 with BdAGM medium.

(29). Transfer the CEC to a sterile plastic Petri dish, and cut them into the small pieces using a scalpel. Collect the callus in a 50 mL plastic disposable tube and cover with the *Agrobacterium* suspension. Incubate for 5 min (mixing by inverting), pipette out the bacterial suspension completely from the CEC and transfer them onto dry sterile filter paper in an empty Petri dish.

NOTE: Use three layers of filter paper in each Petri dish to ensure better CEC drying.

NOTE: Thorough drying of the CEC from bacterial suspension is extremely important.

Leave the open Petri dish with CEC under a laminar flow hood for seven min as a desiccation treatment. Transfer the CEC onto BdCCM medium, cover the plates with Parafilm and incubate for 2 days at 25°C in the dark.

(30). Transfer the CEC onto BdSM40 medium and culture for three weeks at 25°C in the dark.

NOTE: Do not transfer CEC overgrown with *Agrobacterium*.

(31). After three weeks split the transformed CEC (**Figure 3C**) into 4–6 pieces and transfer them onto BdSM30 medium

for another three weeks at 25°C in the dark. Discard non-transformed dark brown calli.
(32). Six weeks after transformation, transfer the hygromycin-resistant calli onto BdRM medium and incubate for three weeks at 25°C under 16-h photoperiod.
(33). When shoots appear and reach a length not less than 2 cm, transfer them to plastic disposable tubes with BdGM medium. Culture at 25°C under a 16-photoperiod until the roots appear and the plants are at least a few cm long.

NOTE: Do not transfer smaller plants because they are very vulnerable and prone to dying.

(34). Transfer fully rooted plantlets to pots filled with soil mixed with vermiculite at a ratio of 3:1. Keep seedlings covered with a propagator lid during first two weeks. Grow plants in a greenhouse at 21 ± 1°C/16 h-photoperiod until the seeds are ready to collect. Collect the seeds and store at 4°C.

Analysis of Regenerated Plants (Timing ∼1 Week)

Analyze the regenerated plants for T-DNA insertion and mutation in the target sequence.

(35). Isolate the DNA from the leaves of regenerated plants using a quick protocol. Carry out the whole procedure at RT. Cut a piece of a young leaf around 1 cm^2 and macerate using a plastic pestle in a 1.5 mL tube. Add 400 μL of extraction buffer and continue to grind the leaf until a homogenous solution is attained. Centrifuge for 3 min at 14 000 rpm, and transfer 300 μL of the supernatant to a new 1.5 mL tube. Add 300 μL of isopropanol, vortex briefly and centrifuge for 5 min at 14 000 rpm. Discard the supernatant and wash the pellet with 300 μL 70% ethanol. Centrifuge for 5 min at 14 000 rpm again, discard the supernatant and dry the pellet. Resuspend the pellet in 50 μL TE buffer. Use 1 μL of isolated DNA for 20 μL of PCR reaction.
(36). Assay the transformation of regenerated plants using one of the following options (A or B).

(A) Determination of the presence or absence of the Cas9 gene

Use the primers that amplify part of the gene encoding the Cas9 protein in pOsCas9_sgRNA or pYPQ_Cas9_gRNA vectors (**Supplementary Table S1**). Use the Color Taq PCR Master Mix for the Cas9 PCR reaction (see section "Reagent Setup") and run using following program: 94°C for 3 min; (94°C for 30 s; 58°C for 30 s; 72°C for 30 s) – 30 cycles; 72°C for 7 min; 4°C for ∞. Run the PCR product on a 1% agarose gel. A 382-nucleotide PCR product for the pOsCas9_sgRNA vector and a 357-nucleotide PCR product for pYPQ_Cas9_gRNA indicate successful transformation. Always include a negative control – DNA isolated from the wild-type plant, and a positive control – for example vector DNA (pOsCas9_sgRNA or pYPQ_Cas9_gRNA).

(B) Determination of the presence or absence of the gene conferring resistance to hygromycin (HygR test)

Snip 1 – 1.5 cm from the tips of the youngest, but completely expanded leaves of each regenerated plant. Place the leaf immediately in BdHygR medium with its abaxial side down and slightly angled (**Figure 3E**). Do not damage the leaf and make sure the cut tip of the leaf does not go all the way through the media. 1 leaf/cm^2 is the appropriate density. Cover the plates with Parafilm and culture for 5 days at 25°C under a 16-photoperiod. Hygromycin resistant leaves remain green, whereas susceptible leaves turn white at the cut edge.

To determine the success of editing, follow the PCR/RE assay, cloning and sequencing (steps 37 and 38). Alternatively, skip step 37 and go directly to step 38, as we found that some of the mutations cannot be detected using the PCR/RE assay, and yet most of the transformed plants are edited (see section "RESULTS AND DISCUSSION").

(37). Amplify part of the targeted gene using the primers designed in step 8 and Platinum™ Taq DNA Polymerase High Fidelity (Thermo Fisher Scientific). Prepare a 25 μL reaction according to the manufacturer's protocol. Restrict 15 μL of the PCR product with the relevant restriction enzyme according to the manufacturer's protocol. As a control, a wild-type plant should be included in the analysis. Run the digested PCR product on a 1% agarose gel.

Three outcomes are possible:

- One band of a size corresponding to the part of the gene defined by the primers. This suggests that the restriction site was lost by mutation of all copies of the target gene.
- Two bands that reflect two fragments of the amplified sequence following digestion by the restriction enzyme. This suggests that restriction sites are still present in the target sequence, and that no copies of the target gene have been edited, or an induced mutation did not lead to the loss of a restriction site.
- Three bands suggest that at least one copy of the gene has been successfully edited. The other copies may not be edited or the induced mutation did not lead to the loss of a restriction site.

NOTE: Another possibility for the results of three bands is that the target band was not fully digested due to the incomplete effectiveness of the restriction enzyme activity. Thus, it is necessary to include for each experiment the control reaction with the DNA from wild-type plant.

Select for further analysis only those plants that have at least one edited copy of the gene. Do not include plants from which the PCR product has been completely digested by the restriction enzyme.

NOTE: Alternatively, in *B. distachyon*, the amplified PCR product could be analyzed with the use of T7 Endonuclease 1 (T7E1, New England Biolabs) instead of the digestion using the restriction enzyme. However, this enzyme also has its limitations and may not detect some mutations. For example, it works best at C mismatches and does not recognize all DNA mismatches.

(38). Clone the undigested PCR product into a pGEM-T vector in order to determine the nature of the mutations. Non-digested PCR product is used, in order to include all gene copies, regardless of whether they are edited or not. If the outcome was one band, this band can be directly isolated from the gel and used for cloning. If three bands

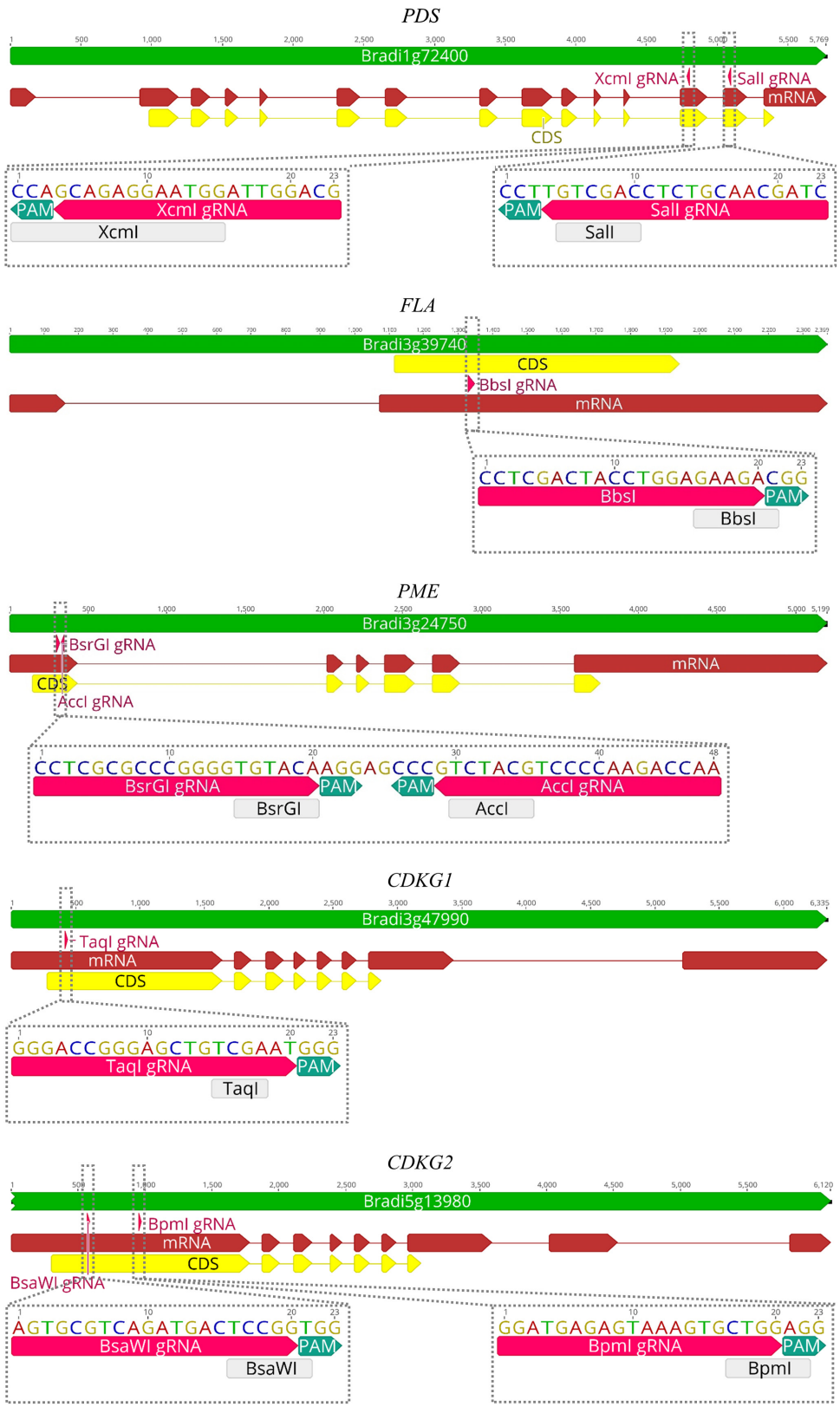

FIGURE 4 | Maps of *PDS*, *FLA*, *PME*, *CDKG1,* and *CDKG2* genes with marked positions of gRNAs (pink arrows) and appropriate restriction sites (light gray rectangles). PAM – protospacer-adjacent motif.

were observed, run the rest of undigested PCR product (10 μL) on a 1% agarose, isolate from the gel and use for cloning. Transform *E. coli* with the recombinant vector, isolate plasmids from individual bacterial colonies, and sequence using a M13For primer. Align the sequence with that of wild-type.

NOTE: Since each individual colony carries only one copy of the gene, five colonies should be sequenced in order to be sure of including both gene copies in *B. distachyon* and 10 colonies to include all gene copies in *B. hybridum*.

If the T1 or subsequent generations are used for phenotypic analysis, it is best to select those plants in which the T-DNA cassette has been lost by segregation.

(39). The presence or absence of the T-DNA cassette is determined by using one of the methods presented in step 36 – PCR reaction (option A) or HygR test (option B).

RESULTS AND DISCUSSION

CRISPR/Cas9 technology enables rapid and efficient targeted mutagenesis. We targeted five different genes (*PDS*, *FLA*, *PME*, *CDKG1* and *CDKG2*) in a model grass species, diploid *B. distachyon*, and two of them (*CDKG1* and *CDKG2*) in its allotetraploid derivative *B. hybridum*. Single gRNA sequences were designed for *FLA* gene (*Bbs*I gRNA) and *CDKG1* gene (*Taq*I gRNA) and two gRNA sequences for *PDS* gene (*Xcm*I gRNA, *Sal*I gRNA), *PME* gene (*Bsr*GI gRNA, *Acc*I gRNA) and *CDKG2* gene (*Bpm*I gRNA and *Bsa*WI gRNA) (**Figure 4**). The efficiency of all designed gRNAs in *Brachypodium* genome editing was tested using a transient protoplast assay. All the gRNA sequences targeted the conserved regions of the genes in both the Bd and Bs genome, with the exception that *Bpm*I gRNA contains one single nucleotide polymorphism (SNP) distal to PAM (**Figure 5A**). The SNP in the region outside the gRNA sequence helps to differentiate between all of the gene copies from the Bd and Bs genomes (**Figure 5B**). The *Bpm*I gRNA is complementary to the Bs *CDKG2* sequence. The transient protoplast assay was conducted on protoplasts of Bd21 leaves and, since the SNP is in the "non-seed" gRNA region, the Cas9 endonuclease was able to introduce DSBs in the target gene. Two different mutations were obtained: deletion of T and substitution of T by C (**Figure 6**). It confirmed that *Bpm*I gRNA, despite the SNP, is functional in editing of Bd *CDKG2* copy. Positive results of the transient protoplast assay were also obtained for *Bsr*GI gRNA (the obtained mutation: deletion of T or G). Although no mutations were detected by the transient protoplast assay for the remaining gRNAs, they proved nevertheless to be effective in editing the *Brachypodium* genome, as demonstrated in the mutants described below. False negative results may arise because some of the mutations do not lead to a loss of the restriction site. On the other hand, depending on the activity of individual restriction enzymes, not all unedited sequences may be successfully digested. Therefore, when analyzing individual colonies, a large number of them may have a copy of the gene that has not been edited. Increasing the number of colonies analyzed, increases the likelihood of detecting mutations in protoplasts. Summarizing the results of the transient protoplast assay, we suggest, that the use of transient protoplast assay is optional and can be omitted, but due to its relatively low cost and speed, it might be useful for selecting the best gRNA among several designed for one gene, in order to save time and resources during the long process of *Agrobacterium*-mediated transformation. Moreover, as the transient protoplast assay can also be used for other purposes than just analysis of gRNA efficiency, for example for study the subcellular protein localisation

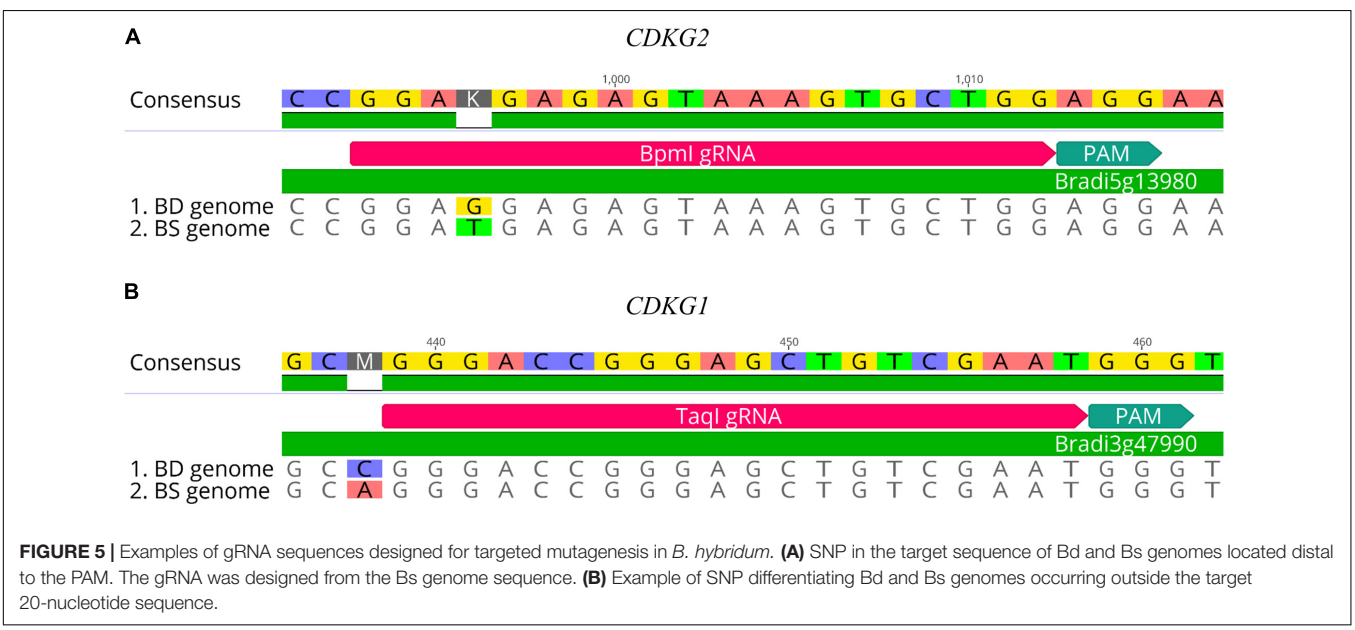

FIGURE 5 | Examples of gRNA sequences designed for targeted mutagenesis in *B. hybridum*. **(A)** SNP in the target sequence of Bd and Bs genomes located distal to the PAM. The gRNA was designed from the Bs genome sequence. **(B)** Example of SNP differentiating Bd and Bs genomes occurring outside the target 20-nucleotide sequence.

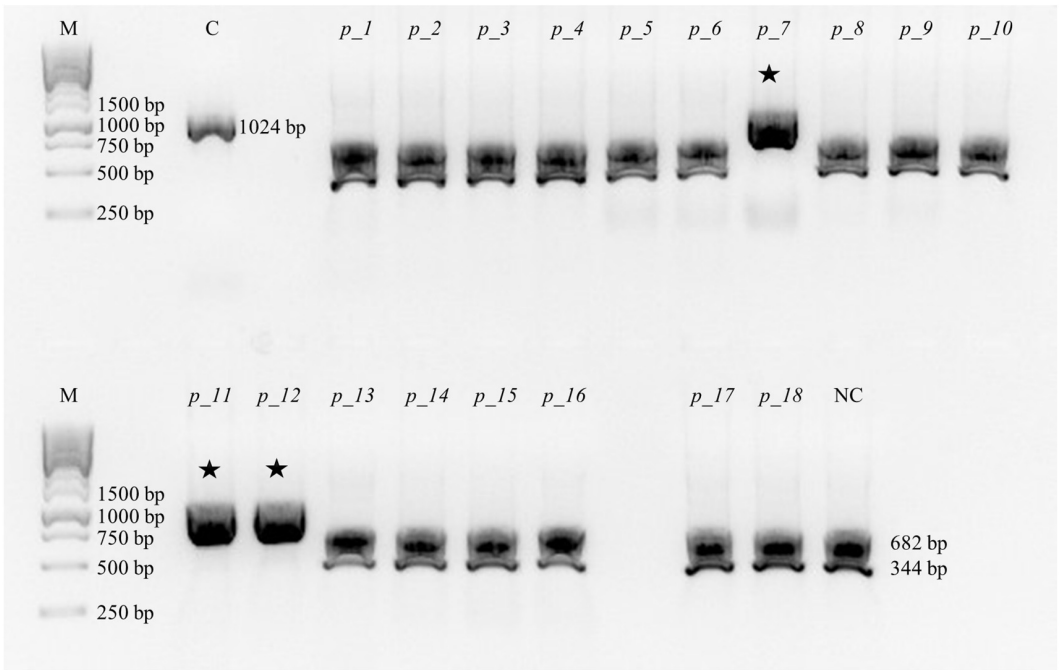

B

***B. distachyon* mutations (from protoplasts)**

CDKG2 gene

WT (*Bpm*I gRNA)	5′-GGATGAGAGTAAAGTGCTGGAGG-3′	
p_7	5′-GGAGGAGAGTAAAGTGC-GGAGG-3′	-1bp
p_11	5′-GGAGGAGAGTAAAGTGC**C**GGAGG-3′	
p_12	5′-GGAGGAGAGTAAAGTGC**C**GGAGG-3′	

FIGURE 6 | Example of the nature of mutations obtained using CRISPR/Cas9 targeted mutagenesis with *Bpm*I gRNA in Bd21 protoplasts. **(A)** Analysis of the obtained colonies using PCR/RE assay and gel electrophoresis. Lane M, molecular weight marker, lane C, control – undigested PCR product, lanes *p_1 – p_18,* analyzed colonies obtained during the transient protoplast assay, lane NC, negative control – the PCR product from the WT plant digested using *Bpm*I restriction enzyme. bp – base pairs. Edited sequences are indicated by asterisks. **(B)** Results of sequencing of plasmids from individual colonies. Deletions are denoted as hyphens (-) and substitutions as bold, underlined red letters. The PAM sequence is shown in blue. SNP in the target sequence of Bd and Bs genomes is shown in green. bp – base pairs.

(Jung et al., 2015), it seems reasonable to include our optimized, shortened protocol here.

All of the plants regenerated after *Agrobacterium*-mediated transformation were assayed for transformation status, and if positive, followed by assays for mutations. Twenty-two out of 24 transformed plants were successfully edited (**Table 1**). **Figure 7** presents the nature of the mutations of *B. distachyon,* and **Figure 8** shows those in *B. hybridum*. Some of the mutants obtained had exactly the same mutations, so they are shown only once in the figure. Our results show that Cas9 activity results mainly in small indels three nucleotides upstream of the PAM (**Figures 7**, **8**), which caused frameshift mutations. Single nucleotide insertions or deletions have been reported previously in other *B. distachyon* mutants (O'Connor et al., 2017; Raissig et al., 2017; Gao et al., 2019). We also observed larger deletions at the target sequence, which involved 21 bp, 17 bp or 13 bp (**Figures 7**, **8**).

We obtained four different *pds* mutants (**Figure 7**), of which three were edited in both gene copies (biallelic mutants) and showed the expected albino phenotype (**Figure 3F**). One of the *PDS* mutants had just one copy of the gene edited (single-allelic mutant) and resembled a wild-type plant, indicating that all copies of the gene must be knocked-out to change the phenotype. Similar results were reported previously by Shan et al. (2013) and Pan et al. (2016).

Four different *fla* biallelic mutants were obtained (**Figure 7**). *PME* was the only gene we targeted simultaneously with two different gRNAs. We expected, that larger deletions, covering the area between both gRNAs, will occur if the DSBs are simultaneously induced at both gRNA sites. We produced four different *pme* mutants (**Figure 7**) and observed that *Bsr*GI gRNA

TABLE 1 | List of all obtained transgenic lines.

	Transgenic line name	Species/Genotype	Target gene	Editing status
1	*Bd21_pds_I*	*B. distachyon*/Bd21	*PDS*	Edited
2	*Bd21_pds_2*	*B. distachyon*/Bd21	*PDS*	Edited
3	*Bd21_pds_3*	*B. distachyon*/Bd21	*PDS*	Edited
4	*Bd21_pds_4*	*B. distachyon*/Bd21	*PDS*	Edited
5	*Bd21_fla_I*	*B. distachyon*/Bd21	*FLA*	Edited
6	*Bd21_fla_2*	*B. distachyon*/Bd21	*FLA*	Edited
7	*Bd21_fla_3*	*B. distachyon*/Bd21	*FLA*	Edited
8	*Bd21_fla_4*	*B. distachyon*/Bd21	*FLA*	Edited
9	*Bd21_fla_4**	*B. distachyon*/Bd21	*FLA*	Edited
10	*Bd21_FLA_I*	*B. distachyon*/Bd21	*FLA*	Not edited
11	*Bd21_FLA_2*	*B. distachyon*/Bd21	*FLA*	Not edited
12	*Bd21_pme_I*	*B. distachyon*/Bd21	*PME*	Edited
13	*Bd21_pme_2*	*B. distachyon*/Bd21	*PME*	Edited
14	*Bd21_pme_3*	*B. distachyon*/Bd21	*PME*	Edited
15	*Bd21_pme_3**	*B. distachyon*/Bd21	*PME*	Edited
16	*Bd21_pme_4*	*B. distachyon*/Bd21	*PME*	Edited
17	*Bd21_cdkg2_I*	*B. distachyon*/Bd21	*CDKG2*	Edited
18	*Bd21_cdkg2_I**	*B. distachyon*/Bd21	*CDKG2*	Edited
19	*Bd21_cdkg2_2*	*B. distachyon*/Bd21	*CDKG2*	Edited
20	*Bd21_cdkg2_2**	*B. distachyon*/Bd21	*CDKG2*	Edited
21	*ABR113_cdkgI_I*	*B. hybridum*/ABR113	*CDKG1*	Edited
22	*ABR113_cdkgI_2*	*B. hybridum*/ABR113	*CDKG1*	Edited
23	*ABR113_cdkg2_I*	*B. hybridum*/ABR113	*CDKG2*	Edited
24	*ABR113_cdkg2_2*	*B. hybridum*/ABR113	*CDKG2*	Edited

The plants with the same name and differing only by the asterisk had exactly the same kind of mutation.

edited both gene copies in all four, whereas *Acc*I gRNA edited both gene copies in only two of the four. This confirmed the better efficiency of the *Bsr*GI gRNA than *Acc*I gRNA in *Brachypodium* editing and may be in part explained by different cleavage efficiencies of various gRNAs (Bruegmann et al., 2019). It is also consistent with the results obtained using the transient protoplast assay, as positive results were obtained for *Bsr*GI gRNA and not for *Acc*I gRNA. Even if both gRNAs worked in the same plant, we did not observe bigger deletions in the region between the gRNAs; instead we observed small lesions at both gRNA target sites. It seems, therefore, that the use of vectors with two different gRNA sequences targeting the same gene increases the likelihood of mutation. Such vectors could also be useful for targeted mutagenesis of two different genes at the same time.

We also targeted the *CDKG1* and *CDKG2* genes in both *B. distachyon* and *B. hybridum*. We obtained two different *cdkg2* biallelic mutants of *B. distachyon* (**Figure 7**), and *B. hybridum cdkg1* mutants and *B. hybridum cdkg2* mutants (**Figure 8**). *B. hybridum cdkg1* mutants carry the mutation in all of their gene copies, whereas the *cdkg2* mutants of *B. hybridum* carried the mutations in three out of four gene copies. As shown by the *pds* mutants, an altered plant phenotype requires all of the gene copies to be knocked-out. Thus, from the T1 generation plants of *cdkg2 B. hybridum* mutants we selected those with four mutated alleles using the PCR/RE assay as well as cloning and sequencing. As the *cdkg1* as well as *cdkg2* mutants were obtained, our next step will be the simultaneous mutagenesis of both genes in the same individual. To the best of our knowledge, this is the first example of the successful use of CRISPR/Cas9 technology in targeted mutagenesis of the allotetraploid species *B. hybridum*. Targeted mutagenesis such as TALENs and CRISPR/Cas9 have been used to edit multiple alleles in another allopolyploid species – allohexaploid wheat (Wang et al., 2014; Singh et al., 2018).

Although sequence analysis provides the definitive identification of lesions, it is useful to design a rapid screening method. We presented two different methods for assaying the success transformation of regenerated plants. The method based on PCR is commonly used in many laboratories, and is very sensitive and accurate. However, as an alternative we presented the HygR test, which is fast and allows the simultaneous analysis of many regenerated plants with little effort and low cost.

For the analysis of transformed plants in terms of mutation, we proposed the PCR/RE assay and method based on cloning and sequencing. It should be noted that one of the three mutations in both of the *B. hybridum cdkg2* mutants was the addition of a C nucleotide (**Figure 8**) which did not lead to the loss of a *Bpm*I restriction site (CTGGAG) and could not be detected by a PCR/RE assay. Nevertheless, the remaining mutations were resistant to restriction digestion and implied the occurrence of mutation and the need for further analysis of all gene copies using cloning and sequencing. The probability is low that the mutations undetectable using a PCR/RE assay will occur in all copies of the gene, thus a PCR/RE assay might be useful for the screening of a large number of transformed plants. As we

***B. distachyon* mutants**

PDS gene

WT (*Xcm*I gRNA)	5′-CGTCCAATCCATTCCTCTGCTGG-3′	
*pds_1*_BD	5′-CGTCCAATCCATTCCT-TGCTGG-3′	-1bp
*pds_1*_BD′	5′-CGTCCAATCCATTCCT--GCTGG-3′	-2bp
*pds_2*_BD	5′-CGTCCAATCCATTCCTCTGCTGG-3′	ne
*pds_2*_BD′	5′-CGTCCAATCCATTCCT-TGCTGG-3′	-1bp
WT (*Sal*I gRNA)	5′-GATCGTTGCAGAGGTCGACAAGG-3	
*pds_3*_BD	5′-GATCGTTGCAGAGGTCG**A**ACAAGG-3′	+1bp
*pds_3*_BD′	5′-GATCGTTGCAGAGG--GACAAGG-3′	-2bp
*pds_4*_BD	5′-GATCGTTGCAGAGGTCG**G**ACAAGG-3′	+1bp
*pds_4*_BD′	5′-GATCGTTGCAGAGG--GACAAGG-3′	-2bp

FLA gene

WT (*Bbs*I gRNA)	5′-CCTCGACTACCTGGAGAAGACGG-3′	
*fla_1*_BD	5′-CCTCGACTACCTGGAGA**A**AGACGG-3′	+1bp
*fla_1*_BD′	5′-CCTCGACTACCTGGAG-AGACGG-3′	-1bp
*fla_2*_BD	5′-CCTCGACTACCTGGAGA**A**AGACGG-3′	+1bp
*fla_2*_BD′	5′-CCTCGACTACCTGGAGA**A**AGACGG-3′	+1bp
*fla_3*_BD	5′-CCTCGACTACCTGGAGA**T**AGACGG-3′	+1bp
*fla_3*_BD′	5′-CCTCGACTACCTGGAGA**C**AGACGG-3′	+1bp
*fla_4*_BD	5′-CCTCGACTACCTGGAGA**A**AGACGG-3′	+1bp
*fla_4*_BD′	5′-CCTCGACTACCTGGAGA**T**AGACGG-3′	+1bp

PME gene

WT (*Bsr*GI, *Acc*I gRNA)	5′-CCTCGCGCCCGGGGTGTACAAGGAGCCCGTCTACGTCCCCAAGACCAA-3′	
*pme_1*_BD	5′-CCTCGCGCCCGGGGTGTT**T**ACAAGGAGCCCGTC**T**TACGTCCCCAAGACCAA-3′	+1bp, +1bp
*pme_1*_BD′	5′-CCTCGCGCCCGGGGTGTT**T**ACAAGGAGCCCGTC**T**TACGTCCCCAAGACCAA-3′	+1bp, +1bp
*pme_2*_BD	5′-CCTCGCGCCCGGGGTGTT**T**ACAAGGAGCCCGTC----TCCCCAAGACCAA-3′	+1bp, -4bp
*pme_2*_BD′	5′-CCTCGCGCCCGGGGTGTT**T**ACAAGGAGCCCGTC**T**TACGTCCCCAAGACCAA-3′	+1bp, +1bp
*pme_3*_BD	5′-CCTCGCGCCCGGGGTGTT**T**ACAAGGAGCCCGTCTACGTCCCCAAGACCAA-3′	+1bp, ne
*pme_3*_BD′	5′-CCTCGCGCCCGGGGTGTT**T**ACAAGGAGCCCGTCTACGTCCCCAAGACCAA-3′	+1bp, ne
*pme_4*_BD	5′-CCTCGCGCCCGGGGTGTT**T**ACAAGGAGCCCGTCTACGTCCCCAAGACCAA-3′	+1bp, ne
*pme_4*_BD′	5′------------------ACAAGGAGCCCGTC**T**TACGTCCCCAAGACCAA-3′	-21bp*, +1bp

CDKG2 gene

WT (*Bsa*WI gRNA)	5′-AGTGCGTCAGATGACTCCGGTGG-3′	
*cdkg2_1*_BD	5′-AGTGCGTCAGATGACT-CGGTGG-3′	-1bp
*cdkg2_1*_BD′	5′-AGTGCGTCAGATG-----GGTGG-3′	-5bp
*cdkg2_2*_BD	5′-AGTGCGTCAGATGA---CGGTGG-3′	-3bp
*cdkg2_2*_BD′	5′-AGTGCGTCAGA-G--TC--GTGG-3′	-5bp

FIGURE 7 | Nature of mutations obtained using CRISPR/Cas9 targeted mutagenesis in T0 plants of *B. distachyon*. Deletions are denoted as hyphens (-) and insertions as bold red letters. The PAM sequence is shown in blue. Individual plants are marked with numbers. The sequences of both alleles are presented and marked as BD, BD'. * - the mutation goes beyond the gRNA sequence. bp – base pairs, ne – not edited sequence.

mentioned before, most of our transformed plants were edited, so it may also be feasible to skip the PCR/RE analysis and perform the cloning and sequencing directly. A T7E1 assay (Xie and Yang, 2013) is an alternative method for detecting mutation and can be especially useful if it is difficult to design the gRNA sequence with a restriction site at the Cas9 cutting site. The T7EI assay is based on a PCR reaction, followed by amplicon denaturation and subsequent reannealing. If a mutation occurs at the target

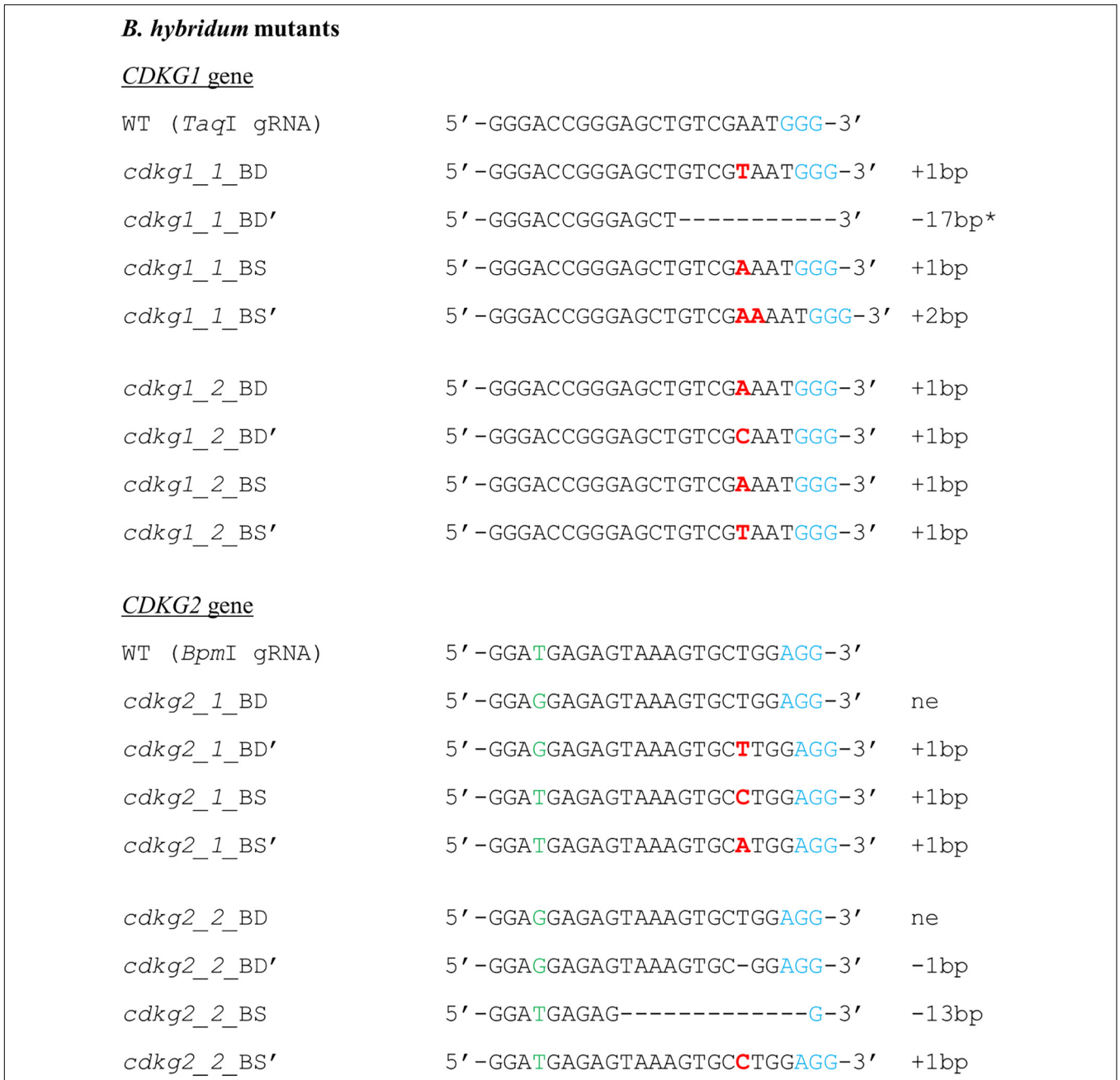

FIGURE 8 | Nature of mutations obtained using CRISPR/Cas9 targeted mutagenesis in T0 plants of *B. hybridum*. Deletions are denoted as hyphens (-) and insertions as bold red letters. The PAM sequence is shown in blue. Individual plants are marked with numbers. The sequences of both alleles are presented and marked as BD, BD' or BS, BS'. SNP in the target sequence of Bd and Bs genomes is shown in green. * - the mutation goes beyond the gRNA sequence. bp – base pairs, ne – not edited sequence.

site, heteroduplexes are formed between the mutant and wild type sequences. Heteroduplexes can be detected by cleaving with the T7EI enzyme. This method might be an alternative way for detecting of mutations in *B. distachyon*. However, applying this method for the detection of mutations in *B. hybridum* is fraught with difficulty, as the Bd and Bs homoeologues are not completely identical. Another method has been proposed recently to analyze mutations identified by a transient protoplast assay, in which double-stranded oligodeoxynucleotide (dsODN) is introduced into the Cas9-induced double stranded break, and PCR with dsODN-specific primers and target gene-specific primers is performed (Nadakuduti et al., 2019). However, the greatest disadvantage of this method is that the addition of dsODNs to the transfection reaction can substantially suppress the frequency of mutation. Taking all of this into account, we recommend analysis based upon restriction enzyme digestion,

cloning and sequencing for the detection of mutations both in protoplasts and regenerated plants.

CONCLUSION

Precise, targeted knock-out by gene editing of diploid *B. distachyon* and allopolyploid *B. hybridum* has been demonstrated using the protocol presented. The method should, therefore, prove useful in functional genomic studies in these model grasses.

DATA AVAILABILITY STATEMENT

All datasets generated for this study are included in the article/supplementary material.

AUTHOR CONTRIBUTIONS

AB, EG, KJ, CN, JD, and RH conceived the experiments. KH, AB, AP, MR-J, and MG conducted the study and processed the data. KH and AB wrote the manuscript. EG, CN, MG, KJ, GJ, JD and RH discussed the results and contributed to manuscript writing. All authors have read and approved the final manuscript.

FUNDING

This research was funded by the National Science Centre Poland (grant nos. DEC-2014/14/M/NZ2/00519 and DEC-2018/31/N/NZ1/01418). JD, GJ, and CN were supported by BBSRC grant BB/M009459/1.

ACKNOWLEDGMENTS

We wish to express our appreciation to Lukasz Kubica (University of Silesia in Katowice) for his excellent technical assistance.

SUPPLEMENTARY MATERIAL

The Supplementary Material for this article can be found online at: https://www.frontiersin.org/articles/10.3389/fpls.2020.00614/full#supplementary-material

REFERENCES

Al-Kaff, N., Knight, E., Bertin, I., Foote, T., Hart, N., Griffiths, S., et al. (2008). Detailed dissection of the chromosomal region containing the Ph1 locus in wheat *Triticum aestivum*: with deletion mutants and expression profiling. *Ann. Bot.* 101, 863–872. doi: 10.1093/aob/mcm252

Alves, S. C., Worland, B., Thole, V., Snape, J. W., Bevan, M. W., and Vain, P. (2009). A protocol for *Agrobacterium*-mediated transformation of *Brachypodium distachyon* community standard line Bd21. *Nat. Protoc.* 4, 638–649. doi: 10.1038/nprot.2009.30

Bae, S., Park, J., and Kim, J. S. (2014). Cas-OFFinder: a fast and versatile algorithm that searches for potential off-target sites of Cas9 RNA-guided endonucleases. *Bioinformatics* 30, 1473–1475. doi: 10.1093/bioinformatics/btu048

Bragg, J. N., Wu, J., Gordon, S. P., Guttman, M. E., Thilmony, R., Lazo, G. R., et al. (2012). Generation and characterization of the Western Regional Research Center *Brachypodium* T-DNA insertional mutant collection. *PLoS One* 7:e41916. doi: 10.1371/journal.pone.0041916

Bruegmann, T., Deecke, K., and Fladung, M. (2019). Evaluating the efficiency of gRNAs in CRISPR/Cas9 mediated genome editing in poplars. *Int. J. Mol. Sci.* 20:E3623. doi: 10.3390/ijms20153623

Caroll, D. (2008). Progress and prospects: zinc-finger nucleasesas gene therapy agents. *Gene Ther.* 15, 1463–1468. doi: 10.1038/gt.2008.145

Chen, Y., Fokar, M., Kang, M., Chen, N., Allen, R. D., and Chen, Y. (2018). Phosphorylation of *Arabidopsis* SINA2 by CDKG1 affects its ubiquitin ligase activity. *BMC Plant Biol.* 18:147. doi: 10.1186/s12870-018-1364-8

Christian, M., Cermak, T., Doyle, E. L., Schmidt, C., Zhang, F., Hummel, A., et al. (2010). Targeting DNA double-strand breaks with TAL effector nucleases. *Genetics* 186, 757–761. doi: 10.1534/genetics.110.120717

Christiansen, P., Andersen, C. H., Didion, T., Folling, M., and Nielsen, K. K. (2005). A rapid and efficient transformation protocol for the grass *Brachypodium distachyon*. *Plant Cell Rep.* 23, 751–758. doi: 10.1007/s00299-004-0889-5

Cong, L., Ran, F. A., Cox, D., Lin, S., Barretto, R., Habib, N., et al. (2013). Multiplex genome engineering using CRISPR/Cas systems. *Science* 339, 819–823. doi: 10.1126/science.1231143

Draper, J., Mur, L. A., Jenkins, G., Ghosh-Biswas, G. C., Bablak, P., Hasterok, R., et al. (2001). *Brachypodium distachyon* a new model system for functional genomics in grasses. *Plant Physiol.* 127, 1539–1555.

Gao, M., Geng, F., Klose, C., Staudt, A.-M., Huang, H., Nguyen, D., et al. (2019). Phytochromes measure photoperiod in *Brachypodium*. *bioRxiv*[Preprint]. doi: 10.1101/697169

Hsia, M. M., O'malley, R., Cartwright, A., Nieu, R., Gordon, S. P., Kelly, S., et al. (2017). Sequencing and functional validation of the JGI *Brachypodium distachyon* T-DNA collection. *Plant J.* 91, 361–370. doi: 10.1111/tpj.13582

Jiang, W., Zhou, H., Bi, H., Fromm, M., Yang, B., and Weeks, D. P. (2013). Demonstration of CRISPR/Cas9/sgRNA-mediated targeted gene modification in *Arabidopsis*, tobacco, sorghum and rice. *Nucleic Acids Res.* 41:e188. doi: 10.1093/nar/gkt780

Jinek, M., Chylinski, K., Fonfara, I., Hauer, M., Doudna, J. A., and Charpentier, E. (2012). A programmable dual-RNA-guided DNA endonuclease in adaptive bacterial immunity. *Science* 337, 816–821. doi: 10.1126/science.1225829

Jung, H., Yan, J., Zhai, Z., and Vatamaniuk, O. K. (2015). "Gene functional analysis using protoplast transient assays," in *Plant Functional Genomics: Methods in Molecular Biology*, eds J. Alonso and A. Stepanova (New York, NY: Humana Press). doi: 10.1007/978-1-4939-2444-8_22

Kaur, N., Alok, A., Shivani, K. N., Pandey, P., Awasthi, P., and Tiwari, S. (2018). CRISPR/Cas9-mediated efficient editing in phytoene desaturase (PDS) demonstrates precise manipulation in banana cv, Rasthali genome. *Funct. Integr. Genomics* 18, 89–99. doi: 10.1007/s10142-017-0577-5

Li, T., Liu, B., Spalding, M. H., Weeks, D. P., and Yang, B. (2012). High-efficiency TALEN-based gene editing produces disease-resistant rice. *Nat. Biotechnol.* 30, 390–392. doi: 10.1038/nbt.2199

Lowder, L. G., Zhang, D., Baltes, N. J., Paul, J. W. III, Tang, X., Zheng, X., et al. (2015). A CRISPR/Cas9 toolbox for multiplexed plant genome editing and transcriptional regulation. *Plant Physiol.* 169, 971–985. doi: 10.1104/pp.15.00636

Ma, X., Qiao, Z., Chen, D., Yang, W., Zhou, R., Zhang, W., et al. (2015). CYCLIN-DEPENDENT KINASE G2 regulates salinity stress response and salt mediated flowering in *Arabidopsis thaliana*. *Plant Mol. Biol.* 88, 287–299. doi: 10.1007/s11103-015-0324-z

Miao, J., Guo, D., Zhang, J., Huang, Q., Qin, G., Zhang, X., et al. (2013). Targeted mutagenesis in rice using CRISPR-Cas system. *Cell Res.* 23, 1233–1236. doi: 10.1038/cr.2013.123

Miller, J. C., Holmes, M. C., Wang, J., Guschin, D. Y., Lee, Y. L., Rupniewski, I., et al. (2007). An improved zinc-finger nuclease architecture for highly

specific genome editing. *Nat. Biotechnol.* 25, 778–785. doi: 10.1038/nbt1319

Miller, J. C., Tan, S., Qiao, G., Barlow, K. A., Wang, J., Xia, D. F., et al. (2011). A TALE nuclease architecture for efficient genome editing. *Nat. Biotechnol.* 29, 143–148. doi: 10.1038/nbt.1755

Nadakuduti, S. S., Starker, C. G., Ko, D. K., Jayakody, T. B., Buell, C. R., Voytas, D. F., et al. (2019). Evaluation of methods to assess in vivo activity of engineered genome-editing nucleases in protoplasts. *Front. Plant Sci.* 10:110. doi: 10.3389/fpls.2019.00110

O'Connor, D. L., Elton, S., Ticchiarelli, F., Hsia, M. M., Vogel, J. P., and Leyser, O. (2017). Cross-species functional diversity within the PIN auxin efflux protein family. *Elife* 6:e31804. doi: 10.7554/eLife.31804

Pacurar, D. I., Thordal-Christensen, H., Nielsen, K. K., and Lenk, I. (2008). A high-throughput *Agrobacterium*-mediated transformation system for the grass model species *Brachypodium distachyon* L. *Transgenic Res.* 17, 965–975. doi: 10.1007/s11248-007-9159-y

Pan, C., Ye, L., Qin, L., Liu, X., He, Y., Wang, J., et al. (2016). CRISPR/Cas9-mediated efficient and heritable targeted mutagenesis in tomato plants in the first and later generations. *Sci. Rep.* 6:24765. doi: 10.1038/srep46916

Pinski, A., Betekhtin, A., Sala, K., Godel-Jedrychowska, K., Kurczynska, E., and Hasterok, R. (2019). Hydroxyproline-rich glycoproteins as markers of temperature stress in the leaves of *Brachypodium distachyon*. *Int. J. Mol. Sci.* 20:E2571. doi: 10.3390/ijms20102571

Qin, Z., Bai, Y., Muhammad, S., Wu, X., Deng, P., Wu, J., et al. (2019). Divergent roles of FT-like 9 in flowering transition under different day lengths in *Brachypodium distachyon*. *Nat. Commun.* 10:812. doi: 10.1038/s41467-019-08785-y

Raissig, M. T., Matos, J. L., Anleu Gil, M. X., Kornfeld, A., Bettadapur, A., Abrash, E., et al. (2017). Mobile MUTE specifies subsidiary cells to build physiologically improved grass stomata. *Science* 355, 1215–1218. doi: 10.1126/science.aan3164

Sander, J. D., Dahlborg, E. J., Goodwin, M. J., Cade, L., Zhang, F., Cifuentes, D., et al. (2011). Selection-free zinc-finger-nuclease engineering by context-dependent assembly (CoDA). *Nat. Methods* 8, 67–69. doi: 10.1038/nmeth.1542

Shan, Q., Wang, Y., Li, J., and Gao, C. (2014). Genome editing in rice and wheat using the CRISPR/Cas system. *Nat. Protoc.* 9, 2395–2410. doi: 10.1038/nprot.2014.157

Shan, Q., Wanga, Y., Chena, K., Lianga, Z., Lia, J., Zhanga, Y., et al. (2013). Rapid and efficient gene modification in rice and *Brachypodium* using TALENs. *Mol. Plant* 6, 1365–1368. doi: 10.1093/mp/sss162

Shukla, V. K., Doyon, Y., Miller, J. C., Dekelver, R. C., Moehle, E., Worden, S. E., et al. (2009). Precise genome modification in the crop species Zea mays using zinc-finger nucleases. *Nature* 459, 437–441. doi: 10.1038/nature07992

Singh, M., Kumar, M., Albertsen, M. C., Young, J. K., and Cigan, A. M. (2018). Concurrent modifications in the three homeologs of Ms45 gene with CRISPR-Cas9 lead to rapid generation of male sterile bread wheat (*Triticum aestivum* L.). *Plant Mol. Biol.* 97, 371–383. doi: 10.1007/s11103-018-0749-2

Tian, S., Jiang, L., Gao, Q., Zhang, J., Zong, M., Zhang, H., et al. (2017). Efficient CRISPR/Cas9-based gene knockout in watermelon. *Plant Cell Rep.* 36, 399–406. doi: 10.1007/s00299-016-2089-5

Townsend, J. A., Wright, D. A., Winfrey, R. J., Fu, F., Maeder, M. L., Joung, J. K., et al. (2009). High-frequency modification of plant genes using engineered zinc-finger nucleases. *Nature* 459, 442–445. doi: 10.1038/nature07845

Upadhyay, S. K., Kumar, J., Alok, A., and Tuli, R. (2013). RNA-guided genome editing for target gene mutations in wheat. *G3 (Bethesda)* 3, 2233–2238. doi: 10.1534/g3.113.008847

Vain, P., Worland, B., Thole, V., Mckenzie, N., Alves, S. C., Opanowicz, M., et al. (2008). *Agrobacterium*-mediated transformation of the temperate grass *Brachypodium distachyon* (genotype Bd21) for T-DNA insertional mutagenesis. *Plant Biotechnol. J.* 6, 236–245. doi: 10.1111/j.1467-7652.2007.00308.x

van der Schuren, A., Voiniciuc, C., Bragg, J., Ljung, K., Vogel, J., Pauly, M., et al. (2018). Broad spectrum developmental role of *Brachypodium* AUX1. *New Phytol.* 219, 1216–1223. doi: 10.1111/nph.15332

Vogel, J., and Hill, T. (2008). High-efficiency *Agrobacterium*-mediated transformation of *Brachypodium distachyon* inbred line Bd21-3. *Plant Cell Rep.* 27, 471–478. doi: 10.1007/s00299-007-0472-y

Wang, Y., Cheng, X., Shan, Q., Zhang, Y., Liu, J., Gao, C., et al. (2014). Simultaneous editing of three homoeoalleles in hexaploid bread wheat confers heritable resistance to powdery mildew. *Nat. Biotechnol.* 32, 947–951. doi: 10.1038/nbt.2969

Wendt, T., Holm, P. B., Starker, C. G., Christian, M., Voytas, D. F., Brinch-Pedersen, H., et al. (2013). TAL effector nucleases induce mutations at a pre-selected location in the genome of primary barley transformants. *Plant Mol. Biol.* 83, 279–285. doi: 10.1007/s11103-013-0078-4

Xie, K., and Yang, Y. (2013). RNA-guided genome editing in plants using a CRISPR-Cas system. *Mol. Plant* 6, 1975–1983. doi: 10.1093/mp/sst119

Yan, J., He, H., Fang, L., and Zhang, A. (2018). Pectin methylesterase31 positively regulates salt stress tolerance in Arabidopsis. *Biochem. Biophys. Res. Commun.* 496, 497–501. doi: 10.1016/j.bbrc.2018.01.025

Zhang, F., Maeder, M. L., Unger-Wallace, E., Hoshaw, J. P., Reyon, D., Christian, M., et al. (2010). High frequency targeted mutagenesis in *Arabidopsis thaliana* using zinc finger nucleases. *Proc. Natl. Acad. Sci. U.S.A.* 107, 12028–12033. doi: 10.1073/pnas.0914991107

Zhang, Y., Zhang, F., Li, X., Baller, J. A., Qi, Y., Starker, C. G., et al. (2013). Transcription activator-like effector nucleases enable efficient plant genome engineering. *Plant Physiol.* 161, 20–27. doi: 10.1104/pp.112.205179

Zheng, T., Nibau, C., Phillips, D. W., Jenkins, G., Armstrong, S. J., and Doonan, J. H. (2014). CDKG1 protein kinase is essential for synapsis and male meiosis at high ambient temperature in *Arabidopsis thaliana*. *Proc. Natl. Acad. Sci. U.S.A.* 111, 2182–2187. doi: 10.1073/pnas.1318460111

Conflict of Interest: The authors declare that the research was conducted in the absence of any commercial or financial relationships that could be construed as a potential conflict of interest.

ROZDZIAŁ III Podsumowanie i wnioski

1. *Brachypodium distachyon* stanowi cenny model do badań nad wpływem stresu temperaturowego na białka ściany komórkowej.

2. Stres temperaturowy indukuje zmiany w składzie białek ściany komórkowej w liściach. Zmiany te są bardziej intensywne w przypadku odpowiedzi na wysoką temperaturę (40 °C) niż niską temperaturę (4 °C).

3. Stres temperaturowy skutkuje zmianami intensywności i rozmieszczenia epitopów AGP, szczególnie w wiązce przewodzącej, ale nie ma wpływu na epitopy ekstensyn.

4. Stres temperaturowy skutkował podniesionym poziomem ekspresji genów kodujących AGP i ekstensyny. Wzrost ekspresji był większy w przypadku wysokiej temperatury niż niskiej temperatury.

5. Analiza proteomiczna białek ściany komórkowej w odpowiedzi na wysoką temperaturę pozwoliła na identyfikację białek o zróżnicowanej obecności w porównaniu do kontroli. Zmiany te sugerują niższą aktywność proteaz, lignifikację, ekspansję ściany komórkowej i zmiany w architekturze polimerów ściany komórkowej, zwłaszcza pektyn.

6. Uzyskane mutanty w genie kodującym białko arabinogalaktanowe typu Fasciclin (*Bradi3g39740*) i w genie metyloesterazy pektynowej (*Bradi3g24750*) z wykorzystaniem systemu CRISPR/Cas9 pozwolą na analizę wpływu ich inaktywacji w kontekście odpowiedzi na warunki stresowe.

ROZDZIAŁ IV Streszczenie

Nasilające się zmiany klimatyczne skutkują wzrostem średniej temperatury powierzchni Ziemi, a także zwiększającą się częstością występowania ekstremalnych zjawisk pogodowych, które są zagrożeniem dla produkcji żywności. Biorąc pod uwagę powiększającą się populację ludzi i spadającą powierzchnię gruntów uprawnych istnieje pilna potrzeba opracowania nowych upraw, lepiej przystosowanych do zmieniających się warunków klimatycznych. Rozwój takich upraw możliwy jest dzięki opracowywaniu nowych odmian roślin. Możliwe jest to z wykorzystaniem klasycznych metod hodowli lub dzięki zastosowaniu inżynierii genetycznej. To drugie podejście wymaga szczegółowej wiedzy na temat mechanizmów molekularnych leżących u podstaw różnych reakcji na stresy, w szczególności stres temperaturowy, który indukowany jest zarówno przez niskie, jak i wysokie temperatury. Stres temperaturowy prowadzi do zmian w wydajności fotosyntezy i zaburzenia potencjału redoks, rearanżacji cytoszkieletu i przebudowy ścian komórkowych, które są stosunkowo słabo poznane. Dlatego też skupiono się na odpowiedzi na stres temperaturowy liści modelowego gatunku dla traw strefy klimatu umiarkowanego, jakim jest *Brachypodium distachyon*.

Celem niniejszej pracy była analiza odpowiedzi białek ściany komórkowej liści *Brachypodium distachyon* na niską (4 °C) i wysoką temperaturę (40 °C), jak też uzyskanie mutantów z inaktywowanymi genami kodującymi białko arabinogalaktanowe typu Fasciclin (*Bradi3g39740*) i metyloesterazę pektynową (*Bradi3g24750*). W celu charakteryzacji wpływu stresu komórkowego na białka ściany komórkowej wykorzystano techniki immunocytochemii z przeciwciałami wiążącymi się specyficznie z epitopami białek arabinogalaktanowych i ekstensyn, analizy profilu ekspresji genów kodujących białka arabinogalaktanowe i ekstensyny, jak też analizę proteomu ściany komórkowej. By uzyskać mutanty z inaktywowanymi genami wykorzystano mutagenezę ukierunkowaną opartą na systemie CRISPR/Cas9. Transformację kalusa embriogennego wyindukowanego z niedojrzałych zarodków przeprowadzono wykorzystując komórki bakteryjne *Agrobacterium tumefaciens.*

Badania rozmieszczenia epitopów AGP w liściach *B. distachyon* ujawniły ich obecność głównie w wiązce przewodzącej, a ekstensyn w mezofilu. Wykazano różnice w rozmieszczeniu i intensywności sygnałów dla czterech przeciwciał rozpoznających AGP: JIM8, JIM16, LM2 i LM6. Jednocześnie nie zaobserwowano różnic w rozmieszczeniu i intensywności sygnałów dla

przeciwciał rozpoznających epitopy ekstensyn. Analiza profilu ekspresji genów kodujących AGP i ekstensyny ujawniła głównie wzrost poziomu ekspresji, który był znacznie większy w przypadku roślin inkubowanych w wysokiej temperaturze. Z kolei, analiza proteomiczna ściany komórkowej pozwoliła na identyfikację 46 białek o zróżnicowanej obecności w wysokiej temperaturze w porównaniu do kontroli. Zmiany te sugerują niższą aktywność proteaz, lignifikację i ekspansję ściany komórkowej oraz zmiany w architekturze polimerów ściany komórkowej, zwłaszcza pektyn. Wykorzystując system CRISPR/Cas9 uzyskano po cztery mutanty z inaktywowanymi genami kodującymi białko arabinogalaktanowe typu Fasciclin i metyloesterazę pektynową. Choć uzyskane mutanty cechują się brakiem zmian w odpowiedzi na stres temperaturowy, to wykazują słabszy wzrost w odpowiedzi na stres solny.

ROZDZIAŁ V Summary

Increasing climate changes increase the average temperature of the Earth's surface and a higher frequency of extreme weather phenomena, which are a threat to food production. Given the growing human population and declining farmland, there is an urgent need to develop new crops adapted to changing climate. It is possible by developing new plant varieties, either with the use of classical breeding methods or through the use of genetic engineering. The latter approach requires a detailed understanding of the molecular mechanisms underlying various stress responses, particularly temperature stress induced by low and high temperatures. Temperature stress changes photosynthetic efficiency and disturbs redox potential. It also leads to rearrangement of the cell wall cytoskeleton and cell wall remodelling. All these processes are relatively poorly understood. Therefore, this work focused on the response to the temperature stress of leaves of a model species for grasses in the temperate climate zone, *Brachypodium distachyon*.

This study aimed to analyse the response of *Brachypodium distachyon* cell wall proteins in leaves subjected to low (4 °C) and high (40 °C) temperature. Another objective was to obtain mutants with inactivated genes encoding the Fasciclin arabinogalactan protein (*Bradi3g39740*) and pectin methylesterase (*Bradi3g24750*). To characterize the effect of cellular stress on the cell wall proteins, immunocytochemistry with antibodies binding specifically to arabinogalactan proteins and extensins epitopes, analysis of the expression profile of genes encoding arabinogalactan and extensin proteins, as well as analysis of the cell wall proteome were applied. In order to obtain mutants with inactivated genes, site-directed mutagenesis based on CRISPR/Cas9 system was used. In addition, the transformation of the embryogenic callus induced from immature embryos was performed using *Agrobacterium tumefaciens* bacterial cells.

Studies on the distribution of AGP epitopes in leaves of *B. distachyon* revealed their presence mainly in the vascular bundle and extensins in the mesophyll. Differences in the distribution and intensity of signals were demonstrated for the four antibodies recognizing AGP: JIM8, JIM16, LM2, and LM6. At the same time, no differences in the distribution and intensity of signals were observed for antibodies recognizing extensin epitopes. Analysis of the expression profile of the genes encoding AGP and extensin revealed an increase in the expression level, significantly greater in the plants incubated at high temperatures. In turn, proteomic analysis of the

cell wall allowed the identification of 46 proteins with the differentiated presence at high temperature compared to the control. These changes suggest lower protease activity, cell wall lignification and expansion, and changes in the architecture of cell wall polymers, especially pectins. Using the CRISPR/Cas9 system, four mutants with inactivated genes encoding the Fasciclin arabinogalactan protein and pectin methylesterase were obtained. Although the obtained mutants show no change in response to temperature stress, they show slower growth in response to salt stress.

Rozdział VI Oświadczenia autorów

UNIWERSYTET ŚLĄSKI
W KATOWICACH

Katowice, dn. 29 czerwca 2021 r.

Mgr Artur Piński

Zespół Cytogenetyki i Biologii Molekularnej Roślin

Instytut Biologii, Biotechnologii i Ochrony Środowiska

Wydział Nauk Przyrodniczych

Uniwersytet Śląski w Katowicach

Oświadczenie

W związku z wykorzystaniem poniższych prac, jako rozprawy doktorskiej, oświadczam, iż mój współudział obejmował:

1. „Hydroxyproline-rich glycoproteins as markers of temperature stress in the leaves of *Brachypodium distachyon*" opublikowanej w *International Journal of Molecular Sciences* (2019, 20(10), 2571) – projektowanie doświadczeń, analiza wyników, opracowanie manuskryptu; traktowanie materiału roślinnego, analiza profilu ekspresji genów, wykonanie zdjęć preparatów po immunobarwieniu;
2. „Changes in the cell wall proteome of leaves in response to high temperature stress in *Brachypodium distachyon*" opublikowanej w *International Journal of Molecular Sciences* (2021, 22(13), 6750) – projektowanie doświadczeń, przeprowadzanie eksperymentów, analiza wyników; izolacja białek ściany komórkowej, analiza profile ekspresji wybranych genów, autor korespondencyjny;
3. „A CRISPR/Cas9-based mutagenesis protocol for *Brachypodium distachyon* and its allopolyploid relative, *Brachypodium hybridum*" opublikowanej w *Frontiers in Plant Science* (2020, 11, 614) – projektowanie doświadczeń, przeprowadzanie eksperymentów, analiza wyników; uzyskanie mutantów z inaktywowanymi genami *Bradi3g39740* i *Bradi3g24750*.

Artur Piński

Uniwersytet Śląski w Katowicach
Wydział Nauk Przyrodniczych
Instytut Biologii, Biotechnologii i Ochrony Środowiska
ul. Jagiellońska 28, 40-032 Katowice
tel.: 32 255 58 73, e-mail: ibbios.wnp@us.edu.pl

Katowice, dn. 23 czerwca 2021 r.

Prof. dr hab. Robert Hasterok

Zespół Cytogenetyki i Biologii Molekularnej Roślin

Instytut Biologii, Biotechnologii i Ochrony Środowiska

Wydział Nauk Przyrodniczych

Uniwersytet Śląski w Katowicach

Oświadczenie

W związku z wykorzystaniem poniższych prac przez mgr Artura Pińskiego, jako rozprawy doktorskiej, oświadczam, iż mój współudział obejmował:

1. „Hydroxyproline-rich glycoproteins as markers of temperature stress in the leaves of *Brachypodium distachyon*" opublikowanej w *International Journal of Molecular Sciences* (2019, 20(10), 2571) – opracowanie manuskryptu i finansowanie;
2. „Changes in the cell wall proteome of leaves in response to temperature stress in *Brachypodium distachyon*" opublikowanej w *International Journal of Molecular Sciences* (2021, 22(13), 6750) – opracowanie manuskryptu i finansowanie;
3. „A CRISPR/Cas9-based mutagenesis protocol for *Brachypodium distachyon* and its allopolyploid relative, *Brachypodium hybridum*" opublikowanej w *Frontiers in Plant Science* (2020, 11, 614) - opracowanie manuskryptu i finansowanie.

.....

Prof. dr hab. Robert Hasterok

Uniwersytet Śląski w Katowicach
Wydział Nauk Przyrodniczych
Instytut Biologii, Biotechnologii i Ochrony Środowiska
ul. Jagiellońska 28, 40-032 Katowice
tel.: 32 255 58 73, e-mail: ibbios.wnp@us.edu.pl

www.us.edu.pl

UNIWERSYTET ŚLĄSKI
W KATOWICACH

Katowice, dn. 29 czerwca 2021 r.

Dr hab. Alexander Betekhtin, Prof. UŚ
Zespół Cytogenetyki i Biologii Molekularnej Roślin
Instytut Biologii, Biotechnologii i Ochrony Środowiska
Wydział Nauk Przyrodniczych
Uniwersytet Śląski w Katowicach

Oświadczenie

W związku z wykorzystaniem poniższych prac przez mgr Artura Pińskiego, jako rozprawy doktorskiej, oświadczam, iż mój współudział obejmował:

1. „Hydroxyproline-rich glycoproteins as markers of temperature stress in the leaves of *Brachypodium distachyon*" opublikowanej w *International Journal of Molecular Sciences* (2019, 20(10), 2571) – projektowanie doświadczeń, analiza wyników, opracowanie manuskryptu;
2. „Changes in the cell wall proteome of leaves in response to high temperature stress in *Brachypodium distachyon*" opublikowanej w *International Journal of Molecular Sciences* (2021, 22(13), 6750) – projektowanie doświadczeń, opracowanie manuskryptu;
3. „A CRISPR/Cas9-based mutagenesis protocol for *Brachypodium distachyon* and its allopolyploid relative, *Brachypodium hybridum*" opublikowanej w *Frontiers in Plant Science* (2020, 11, 614) – projektowanie doświadczeń, przeprowadzanie eksperymentów, analiza wyników, opracowanie manuskryptu.

Alexander Betekhtin

Dr hab. Alexander Betekhtin Prof. UŚ

Uniwersytet Śląski w Katowicach
Wydział Nauk Przyrodniczych
Instytut Biologii, Biotechnologii i Ochrony Środowiska
ul. Jagiellońska 28, 40-032 Katowice
tel.: 32 255 58 73, e-mail: ibbios.wnp@us.edu.pl

UNIWERSYTET ŚLĄSKI
W KATOWICACH

Katowice, dn. 28 maja 2021 r.

Prof. dr hab. Ewa Kurczyńska
Instytut Biologii, Biotechnologii i Ochrony Środowiska
Wydział Nauk Przyrodniczych
Uniwersytet Śląski w Katowicach

Oświadczenie

W związku z wykorzystaniem poniższych prac przez mgr Artura Pińskiego, jako rozprawy doktorskiej, oświadczam, iż mój współudział obejmował:

1. „Hydroxyproline-rich glycoproteins as markers of temperature stress in the leaves of *Brachypodium distachyon*" opublikowanej w *International Journal of Molecular Sciences* (2019, 20(10), 2571) – projektowanie doświadczeń, analiza wyników, opracowanie manuskryptu i finansowanie.

Ewa Kurczyńska
.....

Prof. dr hab. Ewa Kurczyńska

Uniwersytet Śląski w Katowicach
Wydział Nauk Przyrodniczych
Instytut Biologii, Biotechnologii i Ochrony Środowiska
ul. Jagiellońska 28, 40-032 Katowice
tel.: 32 255 58 73, e-mail: ibbios.wnp@us.edu.pl

www.us.edu.pl

HR EXCELLENCE IN RESEARCH

UNIWERSYTET ŚLĄSKI
W KATOWICACH

Katowice, dn. 28 maja 2021 r.

Mgr Kamila Godel-Jedrychowska
Instytut Biologii, Biotechnologii i Ochrony Środowiska
Wydział Nauk Przyrodniczych
Uniwersytet Śląski w Katowicach

Oświadczenie

W związku z wykorzystaniem poniższych prac przez mgr Artura Pińskiego, jako rozprawy doktorskiej, oświadczam, iż mój współudział obejmował:

1. „Hydroxyproline-rich glycoproteins as markers of temperature stress in the leaves of *Brachypodium distachyon*" opublikowanej w *International Journal of Molecular Sciences* (2019, 20(10), 2571) – przeprowadzanie eksperymentów, opracowanie manuskryptu; immunobarwienie.

Kamila Godel-Jedrychowska

Mgr Kamila Godel-Jedrychowska

Uniwersytet Śląski w Katowicach
Wydział Nauk Przyrodniczych
Instytut Biologii, Biotechnologii i Ochrony Środowiska
ul. Jagiellońska 28, 40-032 Katowice
tel.: 32 255 58 73, e-mail: ibbios.wnp@us.edu.pl

www.us.edu.pl

HR EXCELLENCE IN RESEARCH

UNIWERSYTET ŚLĄSKI
W KATOWICACH

Katowice, dn. 28 maja 2021 r.

Dr Katarzyna Sala

Instytut Biologii, Biotechnologii i Ochrony Środowiska

Wydział Nauk Przyrodniczych

Uniwersytet Śląski w Katowicach

Oświadczenie

W związku z wykorzystaniem poniższych prac przez mgr Artura Pińskiego, jako rozprawy doktorskiej, oświadczam, iż mój współudział obejmował:

1. „Hydroxyproline-rich glycoproteins as markers of temperature stress in the leaves of *Brachypodium distachyon*" opublikowanej w *International Journal of Molecular Sciences* (2019, 20(10), 2571) – projektowanie doświadczeń, przeprowadzanie eksperymentów, analiza wyników, opracowanie manuskryptu; przygotowanie preparatów i immunobarwienie.

Katarzyna Sala
.....

Dr Katarzyna Sala

Uniwersytet Śląski w Katowicach
Wydział Nauk Przyrodniczych
Instytut Biologii, Biotechnologii i Ochrony Środowiska
ul. Jagiellońska 28, 40-032 Katowice
tel.: 32 255 58 73, e-mail: ibbios.wnp@us.edu.pl

www.us.edu.pl

HR EXCELLENCE IN RESEARCH

UNIWERSYTET ŚLĄSKI
W KATOWICACH

Kraków, dn. 23 czerwca 2021 r.

Dr Urszula Jankowska

Pracownia Proteomiki i Spektrometrii Mas

Małopolskie Centrum Biotechnologii

Uniwersytet Jagielloński

Oświadczenie

W związku z wykorzystaniem poniższych prac przez mgr Artura Pińskiego, jako rozprawy doktorskiej, oświadczam, iż mój współudział obejmował:

1. „Changes in the cell wall proteome of leaves in response to high temperature stress in *Brachypodium distachyon*" opublikowanej w *International Journal of Molecular Sciences* (2021, 22(13), 6750) – przeprowadzanie eksperymentu i analiza wyników proteomicznych, opracowanie manuskryptu.

Urszula Jankowska

Dr Urszula Jankowska

Uniwersytet Śląski w Katowicach
Wydział Nauk Przyrodniczych
Instytut Biologii, Biotechnologii i Ochrony Środowiska
ul. Jagiellońska 28, 40-032 Katowice
tel.: 32 255 58 73, e-mail: ibbios.wnp@us.edu.pl

www.us.edu.pl

UNIWERSYTET ŚLĄSKI
W KATOWICACH

Kraków, dn. 23 czerwca 2021 r.

Mgr Bożena Skupień-Rabian

Pracownia Proteomiki i Spektrometrii Mas

Małopolskie Centrum Biotechnologii

Uniwersytet Jagielloński

Oświadczenie

W związku z wykorzystaniem poniższych prac przez mgr Artura Pińskiego, jako rozprawy doktorskiej, oświadczam, iż mój współudział obejmował:

1. „Changes in the cell wall proteome of leaves in response to high temperature stress in *Brachypodium distachyon*" opublikowanej w *International Journal of Molecular Sciences* (2021, 22(13), 6750) – przeprowadzanie eksperymentu i analiza wyników proteomicznych, opracowanie manuskryptu.

Bożena Skupień-Rabian

Uniwersytet Śląski w Katowicach
Wydział Nauk Przyrodniczych
Instytut Biologii, Biotechnologii i Ochrony Środowiska
ul. Jagiellońska 28, 40-032 Katowice
tel.: 32 255 58 73, e-mail: ibbios.wnp@us.edu.pl

www.us.edu.pl

HR EXCELLENCE IN RESEARCH

UNIWERSYTET ROLNICZY
im. Hugona Kołłątaja w Krakowie

Kraków, dnia 8 czerwca 2021

dr hab. inż. Ewa Grzebelus prof. UR
Katedra Biologii Roślin i Biotechnologii
Wydział Biotechnologii i Ogrodnictwa
e-mail: ewa.grzebelus@urk.edu.pl

Oświadczenie

W związku z wykorzystaniem poniższej pracy przez mgr Artura Pińskiego, jako rozprawy doktorskiej, oświadczam, iż mój współudział obejmował:

1. „A CRISPR/Cas9-based mutagenesis protocol for *Brachypodium distachyon* and its allopolyploid relative, *Brachypodium hybridum*" opublikowanej w czasopiśmie *Frontiers in Plant Science* (2020, 11, 614) – projektowanie doświadczeń, opracowanie protokołu izolacji protoplastów, korekta manuskryptu.

.....

dr hab. inż. Ewa Grzebelus prof. UR

PL 31-425 Kraków, Al. 29 Listopada 54
tel. +48 (12) 662 51 87, e-mail: kbrib@urk.edu.pl

UNIWERSYTET ŚLĄSKI
W KATOWICACH

Katowice, dn. 8 czerwca 2021 r.

Dr Magdalena Rojek-Jelonek

Zespół Cytogenetyki i Biologii Molekularnej Roślin

Instytut Biologii, Biotechnologii i Ochrony Środowiska

Wydział Nauk Przyrodniczych

Uniwersytet Śląski w Katowicach

Oświadczenie

W związku z wykorzystaniem poniższych prac przez mgr Artura Pińskiego, jako rozprawy doktorskiej, oświadczam, iż mój współudział obejmował:

1. „A CRISPR/Cas9-based mutagenesis protocol for *Brachypodium distachyon* and its allopolyploid relative, *Brachypodium hybridum*" opublikowanej w *Frontiers in Plant Science* (2020, 11, 614) – projektowanie doświadczeń, przeprowadzanie eksperymentów, analiza wyników; indukcja kalusa i transformacja.

Magdalena Rojek-Jelonek

Dr Magdalena Rojek-Jelonek

Uniwersytet Śląski w Katowicach
Wydział Nauk Przyrodniczych
Instytut Biologii, Biotechnologii i Ochrony Środowiska
ul. Jagiellońska 28, 40-032 Katowice
tel.: 32 255 58 73, e-mail: ibbios.wnp@us.edu.pl

www.us.edu.pl